Using Data Science for Mechanistic Insights and Selectivity Predictions in a Non-Natural Biocatalytic Reaction

Hanna D. Clements[1], Autumn R. Flynn[1], Bryce T. Nicholls[2], Daria Grosheva[2], Sarah J. Lefave[1], Morgan T. Merriman[1], Todd K. Hyster[2]* and Matthew S. Sigman[1*]

[1]Department of Chemistry, University of Utah, 315 South 1400 East, Salt Lake City, Utah 84112, United States
[2]Department of Chemistry and Chemical Biology, Cornell University, 122 Baker Laboratory, Ithaca, New York 14853

Supplementary Information

Table of Contents

1. General Information

Reagents and Analytical. Unless otherwise noted, all chemicals and reagents for chemical reactions were obtained from commercial suppliers and used as received (Sigma-Aldrich, Oakwood Chemical, Combi-Blocks, Chem-Impex, and Acros Chemicals). GDH-105 was purchased from Codexis as cell free lysate and used as received. Polymerases and restriction enzymes were purchased from New England BioLabs (NEB) and used as received. Silica gel chromatography purifications were carried out using AMD Silica Gel 60. ^{1}H- and ^{13}C- NMR spectra were recorded on a Bruker UltraShield Plus (500 and 125 MHz, respectively) instrument, and are internally referenced to residual proton signals in $CDCl_3$ (7.26 ppm). Data for ^{1}H-NMR are reported as follows: chemical shift (δ ppm), multiplicity (s = singlet, brs = broad singlet, d = doublet, t = triplet, q = quartet, m = multiplet, dd = doublet of doublet, dt = doublet of triplet, ddd = doublet of doublet of doublet), coupling constant (Hz), and integration. Data for ^{13}C NMR are reported in terms of chemical shift relative to $CDCl_3$ (77 ppm).

Chromatography. Analytical high-performance liquid chromatography (HPLC) was carried out using an Agilent 1260 Infinity LCMS System. Analytical chiral SFC was carried out using a JASCO SFC-4000 (SFC).

Cloning. pET22b(+) were used as cloning and expression vectors for all enzymes described in this study. Genes for the 'ene' reductase enzymes GluER were purchased as gBlocks from IDT and cloned using Gibson Cloning.[1] Cloning was carried out using BL21 *E. coli.* DH5-*α* cells for storage and *E. coli.* BL21 (DE3) for expression.

Site Directed Mutagenesis. Site directed mutagenesis primers were designed using the PCR protocol from Kille *et al*.[2] The PCR products were digested with DpnI, repaired using Gibson Mix™, and were directly transformed into *E. coli* strain BL21(DE3). The colonies were selected on agar plates containing ampicillin (100 µg/mL). Primers used for mutagenesis are listed along with gene sequences for each protein. Site directed mutagenesis was performed individually for all mutants in the library.

Protein Expression and Purification. The 'ene'-reductase GluER used in purified protein experiments were expressed in BL21(DE3) *E. coli* cultures transformed with plasmid encoding GluER variants. Transformed glycerol stocks were used to initiate 10 mL overnight cultures (37 ºC, 250 rpm). Expression cultures (500 mL of Turbo Broth with ampicillin (100 µg/ml final concentration) in a 2L flask) were inoculated with 1-2 ml of the overnight culture (37 ºC, 250 rpm). GluER variants were expressed using the addition of 4% (v/v) auto inducing mix (sterile filtered mixture of 1.25% glucose, 5% lactose and 15% glycerol). The pellets were kept at -80 °C for at least 24 hrs before thawing for purification. For purification, frozen cells were thawed in ice-cold water and resuspended in buffer A (for GluER: 50 mM TEOA 25 mM imidazole pH 7.0). Lysozyme (1 mg/mL), DNAse (0.1 mg/mL), FMN (1 mg/mL), and PMSF (1 mg/mL, added as a 35 mg/mL solution in absolute ethanol) were added to the resuspended cells, followed by shaking at room temperature for 30 minutes. The resuspended cells were disrupted by sonication (2 x 4 min, output control 5, 35% duty cycle; Sonicator QSonica Q500 Ultra Sonicator). To pellet insoluble material, lysates were centrifuged at 14,000 x g for 1.5 h at 4 °C. Proteins were purified using a nickel NTA column (5 mL HisTrap HP, GE Healthcare, Piscataway, NJ) using an AKTAStart purifier FPLC system (GE healthcare). The protein was eluted with 100 % buffer B (50 mM triethanolamine (TEOA), 250 mM imidazole pH 7.0) over 5 column volumes. Fractions containing enzyme were pooled, concentrated, and subjected to three exchanges with no-imidazole Buffer C (50 mM triethanolamine (TEOA), pH=7.0, for all other ERED) to remove excess salt and imidazole. Concentrated (1.0-1.5 mM) proteins were aliquoted, flash-frozen in liquid N_2, and stored at -80 °C until later use. Protein concentration was determined by A_{464} with calculated extinction coefficients. (GluER: 11.4×10^{-3} $M^{-1}cm^{-1}$ at 464 nm).

2. Dataset Design

Sequence Information for GluER WT and GluER-T36A

'Ene'-reductase from *Gluconobacter Oxydans* (GluER)
(GenBank Accession Code: WP_011252080.1)

GluER WT

GluER WT DNA sequence

ATGCCGACCCTTTTCGACCCCATCGATTTCGGACCTATCCACGCCAAGAATCGTATCGTCATGTCC
CCCCTGACTCGCGGTCGCGCTGACAAAGAGGCGGTTCCAACCCCCATTATGGCTGAATACTACGC
CCAACGCGCTTCGGCGGGTTTAATTATCACTGAAGCGACGGGGATTTCACGCGAAGGCTTAGGTT
GGCCGTTTGCGCCGGGAATTTGGTCCGATGCACAGGTTGAGGCGTGGAAACCTATCGTCGCGGGT
GTCCATGCAAAGGGCGGCAAGATCGTATGTCAGCTTTGGCATATGGGCCGTATGGTACATTCTTCA
GTTACAGGGACGCAGCCCGTAAGCAGTTCCGCCACTACTGCTCCAGGTGAGGTTCACACCTATGA
GGGCAAGAAGCCCTTCGAACAAGCGCGTGCAATCGATGCTGCAGACATCTCCCGCATCCTTAACG
ATTACGAAAATGCAGCACGTAATGCAATCCGCGCGGGTTTCGATGGAGTGCAGATCCACGCAGCC
AATGGCTACCTTATCGATGAGTTTTTGCGTAACGGAACCAATCATCGCACCGATGAGTATGGGGG
GGTGCCGGAGAACCGTATTCGTTTCTTGAAAGAGGTAACAGAACGCGTCATCGCGGCGATTGGCG
CTGACCGTACGGGTGTGCGTCTGAGTCCAAACGGTGACACACAGGGTTGTATCGACAGTGCTCCC
GAAACCGTTTTTGTTCCTGCCGCAAAGCTTTTGCAAGATTTAGGGGTAGCGTGGCTTGAGCTGCGT
GAACCTGGTCCGAATGGTACGTTTGGAAAGACGGATCAACCAAAATTATCTCCACAAATCCGTAA
GGTATTCCTTCGTCCATTGGTCTTAAATCAAGACTATACTTTTGAGGCGGCACAGACGGCCCTGGC
TGAGGGCAAGGCGGACGCTATTGCGTTTGGCCGTAAGTTCATTTCAAATCCAGACTTGCCTGAGCG
CTTTGCCCGTGGCATCGCACTGCAACCAGACGATATGAAAACATGGTACTCCCAAGGCCCAGAGG
GTTACACAGACTATCCATCCGCAACTTCTGGGCCGAACTGA

GluER WT amino acid sequence

MPTLFDPIDFGPIHAKNRIVMSPLTRGRADKEAVPTPIMAEYYAQRASAGLIIT
EATGISREGLGWPFAPGIWSDAQVEAWKPIVAGVHAKGGKIVCQLWHMGRMVHSSVT
GTQPVSSSATTAPGEVHTYEGKKPFEQARAIDAADISRILNDYENAARNAIRAGFDGVQI
HAANGYLIDEFLRNGTNHRTDEYGGVPENRIRFLKEVTERVIAAIGADRTGVRLSPNGD
TQGCIDSAPETVFVPAAKLLQDLGVAWLELREPGPNGTFGKTDQPKLSPQIRKVFLRPL
VLNQDYTFEAAQTALAEGKADAIAFGRKFISNPDLPERFARGIALQPDDMKTWYSQGP
EGYTDYPSATSGPN

GluER T36A DNA sequence

ATGCCGACCCTTTTCGACCCCATCGATTTCGGACCTATCCACGCCAAGAATCGTATCGTCATGTCC
CCCCTGACTCGCGGTCGCGCTGACAAAGAGGCGGTTCCAGCTCCCATTATGGCTGAATACTACGCC
CAACGCGCTTCGGCGGGTTTAATTATCACTGAAGCGACGGGGATTTCACGCGAAGGCTTAGGTTG
GCCGTTTGCGCCGGGAATTTGGTCCGATGCACAGGTTGAGGCGTGGAAACCTATCGTCGCGGGTG
TCCATGCAAAGGGCGGCAAGATCGTATGTCAGCTTTGGCATATGGGCCGTATGGTACATTCTTCAG
TTACAGGGACGCAGCCCGTAAGCAGTTCCGCCACTACTGCTCCAGGTGAGGTTCACACCTATGAG
GGCAAGAAGCCCTTCGAACAAGCGCGTGCAATCGATGCTGCAGACATCTCCCGCATCCTTAACGA
TTACGAAAATGCAGCACGTAATGCAATCCGCGCGGGTTTCGATGGAGTGCAGATCCACGCAGCCA
ATGGCTACCTTATCGATGAGTTTTTGCGTAACGGAACCAATCATCGCACCGATGAGTATGGGGGG
GTGCCGGAGAACCGTATTCGTTTCTTGAAAGAGGTAACAGAACGCGTCATCGCGGCGATTGGCGC
TGACCGTACGGGTGTGCGTCTGAGTCCAAACGGTGACACACAGGGTTGTATCGACAGTGCTCCCG
AAACCGTTTTTGTTCCTGCCGCAAAGCTTTTGCAAGATTTAGGGGTAGCGTGGCTTGAGCTGCGTG

AACCTGGTCCGAATGGTACGTTTGGAAAGACGGATCAACCAAAATTATCTCCACAAATCCGTAAG
GTATTCCTTCGTCCATTGGTCTTAAATCAAGACTATACTTTTGAGGCGGCACAGACGGCCCTGGCT
GAGGGCAAGGCGGACGCTATTGCGTTTGGCCGTAAGTTCATTTCAAATCCAGACTTGCCTGAGCGC
TTTGCCCGTGGCATCGCACTGCAACCAGACGATATGAAAACATGGTACTCCCAAGGCCCAGAGGG
TTACACAGACTATCCATCCGCAACTTCTGGGCCGAACAAT

GluER T36A amino acid sequence
MPTLFDPIDFGPIHAKNRIVMSPLTRGRADKEAVPAPIMAEYYAQRASAGLIITEATGISREGLGWPFAP
GIWSDAQVEAWKPIVAGVHAKGGKIVCQLWHMGRMVHSSVTGTQPVSSSATTAPGEVHTYEGKKPF
EQARAIDAADISRILNDYENAARNAIRAGFDGVQIHAANGYLIDEFLRNGTNHRTDEYGGVPENRIRFL
KEVTERVIAAIGADRTGVRLSPNGDTQGCIDSAPETVFVPAAKLLQDLGVAWLELREPGPNGTFGKTD
QPKLSPQIRKVFLRPLVLNQDYTFEAAQTALAEGKADAIAFGRKFISNPDLPERFARGIALQPDDMKTW
YSQGPEGYTDYPSATSGPNN

Supplementary Figure S1. Site-Directed Mutagenesis Library

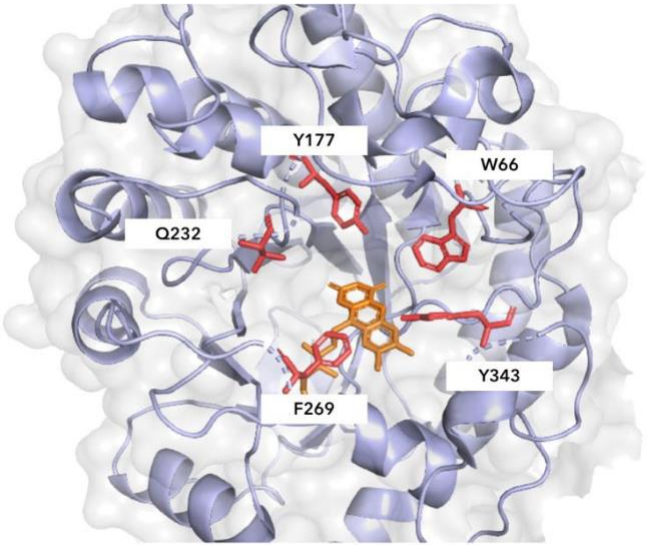

GluER - T36A				
W66A	Y177A	Q232A	F269A	Y343A
W66D	Y177D	Q232D	F269D	Y343D
W66F	Y177F	Q232F	F269L	Y343F
W66L	Y177L	Q232L	F269L	Y343L
	Y177W	Q232W	F269W	Y343W

Figure S1. Left: The crystal structure of the parent enzyme GluER-T36A (PDB ID: 6MYW), highlighting the residues chosen for targeted mutagenesis (W66, Y177, Q232, F269, and Y343) and the redox-active cofactor, FMN. Right: Mutants targeted.

Primers for Site-Directed Mutagenesis Library

GluER-W66
W66A Forward primer:
5’- TTTCACGCGAAGGCTTAGGTGCCCCGTTTGCGCCGGGAATTTG -3’
W66D Forward primer:
5’- TTTCACGCGAAGGCTTAGGTGATCCGTTTGCGCCGGGAATTTG 3’
W66F Forward primer:
5’- TTTCACGCGAAGGCTTAGGTTTTCCGTTTGCGCCGGGAATTTG -3’
W66L Forward primer:
5’- TTTCACGCGAAGGCTTAGGTCTGCCGTTTGCGCCGGGAATTTG -3’
Reverse primer:

5’- ACCTAAGCCTTCGCGTGAAATCCCCGTCGCTTCAGTGATAA-3’

GluER-Y177
Y177A Forward primer:
5’- AGATCCACGCAGCCAATGGCGCCCTTATCGATGAGTTTTTGCG 3’
Y177D Forward primer:
5’- AGATCCACGCAGCCAATGGCGATCTTATCGATGAGTTTTTGCG -3’
Y177F Forward primer:
5’- AGATCCACGCAGCCAATGGCTTTCTTATCGATGAGTTTTTGCG -3’
Y177L Forward primer:
5’- AGATCCACGCAGCCAATGGCCTGCTTATCGATGAGTTTTTGCG -3’
Y177W Forward primer:
5’- AGATCCACGCAGCCAATGGCTGGCTTATCGATGAGTTTTTGCG -3’
Reverse primer:
5’- GCCATTGGCTGCGTGGATCTGCACTCCATCGAAACCCGCGC-3’

GluER-Q232
Q232A Forward primer:
5’- TGAGTCCAAACGGTGACACAGCCGGTTGTATCGACAGTGCTCC -3’
Q232D Forward primer:
5’- TGAGTCCAAACGGTGACACAGATGGTTGTATCGACAGTGCTCC -3’
Q232F Forward primer:
5’- TGAGTCCAAACGGTGACACATTTGGTTGTATCGACAGTGCTCC -3’
Q232L Forward primer:
5’- TGAGTCCAAACGGTGACACACTGGGTTGTATCGACAGTGCTCC -3’
Q232W Forward primer:
5’- TGAGTCCAAACGGTGACACATGGGGTTGTATCGACAGTGCTCC -3’
Reverse primer:
5’- TGTGTCACCGTTTGGACTCAGACGCACACCCGTACGGTCA-3’

GluER-F269
F269A Forward primer:
5’- AACCTGGTCCGAATGGTACGGCCGGAAAGACGGATCAACCAAA -3’
F269D Forward primer:
5’- AACCTGGTCCGAATGGTACGGATGGAAAGACGGATCAACCAAA -3’
F269L Forward primer:
5’- AACCTGGTCCGAATGGTACGCTGGGAAAGACGGATCAACCAAA -3’
F269W Forward primer:
5’- AACCTGGTCCGAATGGTACGTGGGGAAAGACGGATCAACCAAA-3’
Reverse primer:
5’- CGTACCATTCGGACCAGGTTCACGCAGCTCAAGCCACGCTA-3’

GluER-Y343
Y343A Forward primer:
5’- CAGACGATATGAAAACATGGGCCTCCCAAGGCCCAGAGGGTTA -3’
Y343D Forward primer:
5’- CAGACGATATGAAAACATGGGATTCCCAAGGCCCAGAGGGTTA -3’
Y343F Forward primer:
5’- CAGACGATATGAAAACATGGTTTTCCCAAGGCCCAGAGGGTTA -3’
Y343L Forward primer:
5’- CAGACGATATGAAAACATGGCTGTCCCAAGGCCCAGAGGGTTA-3’

Y343W Forward primer:
5’- CAGACGATATGAAAACATGGTGGTCCCAAGGCCCAGAGGGTTA-3’
Reverse primer:
5’- CCATGTTTTCATATCGTCTGGTTGCAGTGCGATGCCACGGG-3’

Supplementary Table S1. Experimental Data Used for Model Training

GluER Variant	Product 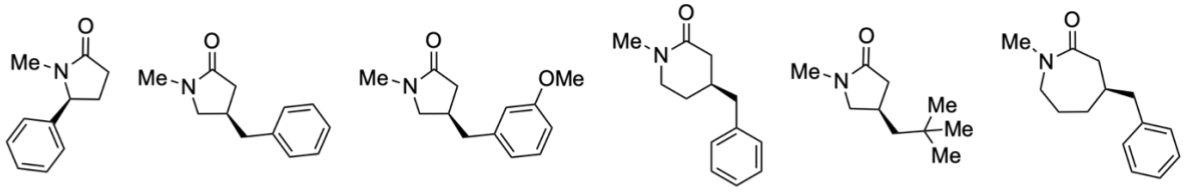					
	1b	**2b**	**3b**	**4b**	**5b**	**6b**
T36A	80.2	83.1	85.2	30.0	70.0	80.0
T36A W66A	13.7	38.6	n.d.	26.1		
T36A W66D	47.0	58.5	n.d.	28.9		
T36A W66F	52.1	81.8	n.d.	39.2		
T36A W66L	n.d.	45.2	53.1	29.7		
T36A Y177A	21.3	n.d.	n.d.	n.d.		
T36A Y177D	n.d.	n.d.	n.d.	n.d.		
T36A Y177F	36.5	62.8	61.5	14.5		
T36A Y177L	n.d.	n.d.	n.d.	n.d.		
T36A Y177W	33.7	81.0	77.0	n.d.		
T36A Q232F	23.4	74.5	80.7	47.6		
T36A F269A	10.9	79.0	70.4	n.d.		
T36A F269D	n.d.	74.3	60.8	n.d.		
T36A F269L	n.d.	70.6	74.9	n.d.		
T36A F269W	n.d.	88.5	89.9	50.0		
T36A Y343A	n.d.	56.3	70.9	43.9		
T36A Y343D	n.d.	65.5	76.7	31.3		
T36A Y343F	n.d.	90.9	89.4	n.d.		
T36A Y343L	n.d.	59.2	79.3	n.d.		
T36A Y343W	n.d.	90.7	87.8	n.d.		

each cell contains the %ee for the major enantiomer of the resultant products. Substrate/Variant combinations that did not result in a detectable level of product are labeled n.d.

Supplementary Table S2. Additional Experimental Data Used in Updated Model

Entry	GluER-T36A Variant	Substrate	ΔΔG‡ Measured
1	W66E	1a	-1.182
2	W66R	1a	-0.824
3	W66Y	1a	-1.031
4	W66C	2a	-0.587
5	W66E	2a	-0.751
6	W66G	2a	-0.862
7	W66R	2a	-1.519
8	W66Y	2a	-1.239
9	W66C	5a	-0.331
10	W66E	5a	-0.717
11	W66G	5a	-0.331
12	W66R	5a	-0.469
13	Q232F_Y343L	5a	0.000
14	W66D-Y343W	5a	0.000
15	W66F-Y177F-Y343F	5a	-0.136
16	F269A-Y343W	6a	-1.031
17	W66D-F269W-Y343L	6a	-0.304
18	F269W-Y343F	6a	-0.252

3. Enzymatic Ensemble Generation

Induced Fit Docking (IFD)

Protein Structure Preparation using Schrodinger's Protein Preparation Wizard and Pymol's Mutagenesis Wizard

GluER-T36A (PDB ID: 6MYW) was loaded into Schrodinger's Maestro.[3] Within the Protein Preparation Wizard, the structure was reduced to a monomer unit, and all sulfate ions, glycerols, acetate ions, sodium ions, and water molecules were removed (no waters found in the active site are known to be conserved in this mode of reactivity). To introduce mutations, a mutation was introduced to the preprocessed structure using Pymol's Mutation wizard and the lowest energy rotamer was selected.[4] This structure was imported back into Schrodinger. Within the Protein Preparation Wizard, hydrogen bonds and protonation states were optimized using propka with a pH of 8.0. A restrained minimization was submitted where heavy atoms were converged to an RMSD of 0.3 Å with the OPLS3e forcefield. Each resultant enzyme file that was used for IFD can be found in the included supplementary files.

Ligand Preparation using Schrodinger's LigPrep

Ligands were imported by their SMILES strings and prepared using LigPrep with the OPLS3e forcefield. Only the specified chirality of the major observed enantiomer was investigated.

Induced Fit Docking with the Schrodinger Suite

The Standard docking protocol was utilized using the OPLS3e forcefield. The receptor was prepared by defining the Box Center for docking as the centroid of selected residues 027, 058, 066, 098, 100, 133, 174, 175, 177, 224, 231, 232, 261, 269, 316, 342, 343, and FMN (401). Some structures used have FMN numbered as residue 001. In these cases, the Box Center for docking was defined by the centroid of selected residues 028, 059, 067, 101, 134, 175, 156, 178, 225, 232, 233, 262, 270, 317, 343, and 344. The box size was set to "Dock ligands similar in size to Workspace ligand," which the program identifies as FMN. This allows for all synthetic ligands investigated in this study to be docked. Docking was constrained to maintain a ligand-enzyme hydrogen bond to N175 during both initial and re-docking. Ligands were allowed to be flexible, ring conformations within 2.5 kcal/mol were sampled, and nonplanar conformations of amide bonds were penalized. For Glide Docking, both receptor and ligand van der Waals scaling was set to 0.5 with a maximum number of poses set to 20. During Prime refinement, residues within 5.0Å of ligand poses were refined, and side chains were optimized. Redocking was performed into structures within 30.0 kcal/mol of the best structure, and within the top 20 structures overall with SP precision.

Singlepoint Energy Calculations for Ligands

Singlepoint calculations of each ligand conformer were run with M06-def2TZVP. NBO charges were calculated using NBO 6.0 at the M06-def2TZVP level. Parameters were acquired from these ground state structures by a semi-automated process similarly to previous reports from the Sigman lab. Sterimol values were calculated using a modified version of Paton's Python script to accommodate non-terminal reference atoms. Dynamic parameters were calculated in UCSF's ChimeraX (v1.1).[4]

Accelerated Molecular Dynamics (aMD)

System Preparation and Molecular Dynamics Simulations

Molecular dynamics simulations were performed using the GPU code (*pmemd*) of the Amber18 package. The crystal structure of the parent enzyme, the Gluconobacter Ene-Reductase (GluER) variant GluER-T36A (PDB code: 6MYW, resolution = 1.16 Å) was used to initiate aMD conformational searches. After removal of crystallographic waters and sulfate ions, glycerols, acetate ions, and sodium ions, the appropriate mutations were introduced *in silico* to the GluER-T36A crystal structure using the Pymol Mutagenesis Wizard;[5] the protonation state of residues were assigned based on the computed pKa values at pH 8.0 from the PROPKA software, executed with the PDB2PQR web interface.[6,7] Structures of pKa adjusted enzyme structures can be found in the included

supplementary files. The enzyme mutant constructs were situated in a box of TIP3P water, extending a minimum of 8 Å from the protein surface (~8,700 solvent atoms), and sodium cations were added to neutralize the charge of the system. The updated general amber force field (GAFF2) was used to parameterize the trianionic flavin mononucleotide (FMN) cofactor, and additional parameters were constructed in Leap using the AM1-BCC charge calculation method, while the Amber ff14SB force-field was applied to the protein residues.

The solvated enzymes were minimized, heated, and relaxed prior to the production run. Throughout, the bonds in water molecules and all bonds involving hydrogen atoms were constrained with the SHAKE algorithm and a 2 fs timestep was used. Minimization was performed over three steps using a combination of the steepest descent and conjugate gradient methods, and minimization proceeded in a constant volume periodic box. A 9 Å potential cutoff distance was applied to the minimizations and a 10 Å potential cutoff was used in all other simulations. The velocity of the atoms in the minimized systems was slowly increased through incremental heating to 300 K, and then the systems were relaxed over a series of steps, where the Langevin thermostat and isotropic position scaling were implemented to regulate the temperature and pressure of each system to mimic reaction conditions.

Accelerated Molecular Dynamics Simulations

The equilibrated systems were subjected to aMD simulation to scan possible configurations of the enzyme. The parameters needed to apply the biasing potential for the aMD simulations were calculated from NPT simulations according to the procedure reported by Pierce, *et al.*[8] The aMD simulation invoked a 10 Å potential cutoff distance with a 2 fs timestep, and proceeded for a total of 20 ns of simulated time. The root mean squared fluctuation (RMSF) of key residues was compared between the 20 ns simulation and simulations of 10 ns and 30 ns. This comparison revealed that 20 ns provided acceptable convergence (Table S3).

The resultant aMD trajectories were subjected to clustering analysis in order to select a manageable number of representative enzyme conformations with the density-based algorithm, DBSCAN procedure.[9] Clustering analysis resulted in ~3-15 clusters per enzyme; the centroid of each cluster was identified and subjected to parameterization.

Supplementary Table S3. Comparison of aMD Simulation Timescales

Residue	RMSF (Å) 10 ns Trajectory	RMSF (Å), 20ns Trajectory	RMSF (Å), 30 ns Trajectory
27	4.4522	6.4693	6.0353
58	4.7663	5.84	6.7108
66	4.5352	6.6992	5.2405
100	4.5619	5.4963	5.4683
133	4.9901	8.6194	8.0143
174	4.7168	4.8802	5.8599
178	4.6576	5.6093	4.6989
231	4.8449	5.4761	5.5568
232	5.0231	6.3259	6.1565
261	4.9725	4.3125	8.4315
269	5.3073	5.3006	8.5893
343	5.5742	6.8445	7.619

Free Ligand Search

Conformational searches of truncated ligands were performed using MacroModel version 11.8 and the OPLS3e forcefield in implicit water.[10] Substrate and product input structures can be found in the included supplementary files. Conformers up to 5.0 kcal/mol higher than the lowest energy structure were considered for each ligand. All ligand structures were optimized in the gas phase with B3LYPGD3BJ/6-31G(d,p) as implemented in Gaussian 09 (RevC.01).[11] The optimized geometries were verified by frequency computations as minima (zero imaginary

frequencies). Single point calculations of each ligand were run with M06-def2TZVP. NBO charges were calculated using NBO 6.0 at the M06-def2TZVP level. Parameters were acquired from these ground state structures by a semi-automated process similarly to previous reports from the Sigman lab. Sterimol values were calculated using a modified version of Paton's Python script to accommodate non-terminal reference atoms. Dynamic parameters were calculated in UCSF's ChimeraX (v1.1).[4]

4. Parameterization

A full set of parameters and their unscaled values is available on the Sigman Group GitHub: https://github.com/SigmanGroup/enzyme-MLR-GluER.

Residues: Sterimol parameters L, B1, and B5, respectively, represent the length, minimum and maximum widths of the considered substituent and are calculated using the Bondi radii. Plane angles were collected as a description of the tilt of conjugated residues relative to their backbone atoms. Angles of the residue trajectory off the backbone were also collected. Intramolecular distances between atoms within the residue and its backbone atoms were collected to represent the degree of compactness within a residue. Dynamic parameters (surface area and volume) for each ligand were formulated by enclosing the conformational ensemble of a ligand in a fictitious surface at 2.8Å resolution and computing topographical properties of the surface.

All residue parameters were collected as averages across the residue ensemble. In the IFD protocol, residue parameters were also weighted by Schrodinger's G-Score for each conformer, where parameter values of well-docked poses contribute to the representative value more heavily (GS). In the aMD protocol, parameters were also weighted by the number of trajectory frames a particular cluster centroid represented. Max-Min values are the difference between the numerical extremes of a parameter within each ensemble and were collected for each parameter. Product-Substrate (p-s) values are the difference between the averaged (or G-Score weighted) values for product-docked and substrate-docked parameters.

Ligands: Sterimol parameters L, B1, and B5, respectively, represent the length, minimum and maximum widths of the considered substituent and are calculated using the Bondi radii. NBO charges have been found to be useful descriptors of steric and electronic properties. HOMO, LUMO, mu, eta, and omega were collected as global parameters for all ligands. Dynamic parameters (surface area and volume) for each ligand were formulated by enclosing the conformational ensemble of a ligand in a fictitious surface at 2.8Å resolution and computing topographical properties of the surface. Docking score (Schrodinger's G-Score) values were also collected in the IFD protocol, and Bolzmann averaging based on DFT single point calculations were used in the aMD protocol.

Mechanistically inspired parameters: Inter-residue distacnces (IRDs) and the RMSD of backbone and R-group atoms were computed with the cpptraj trajectory analysis package.[11]

Supplementary Figure S2. Parameters Gathered.

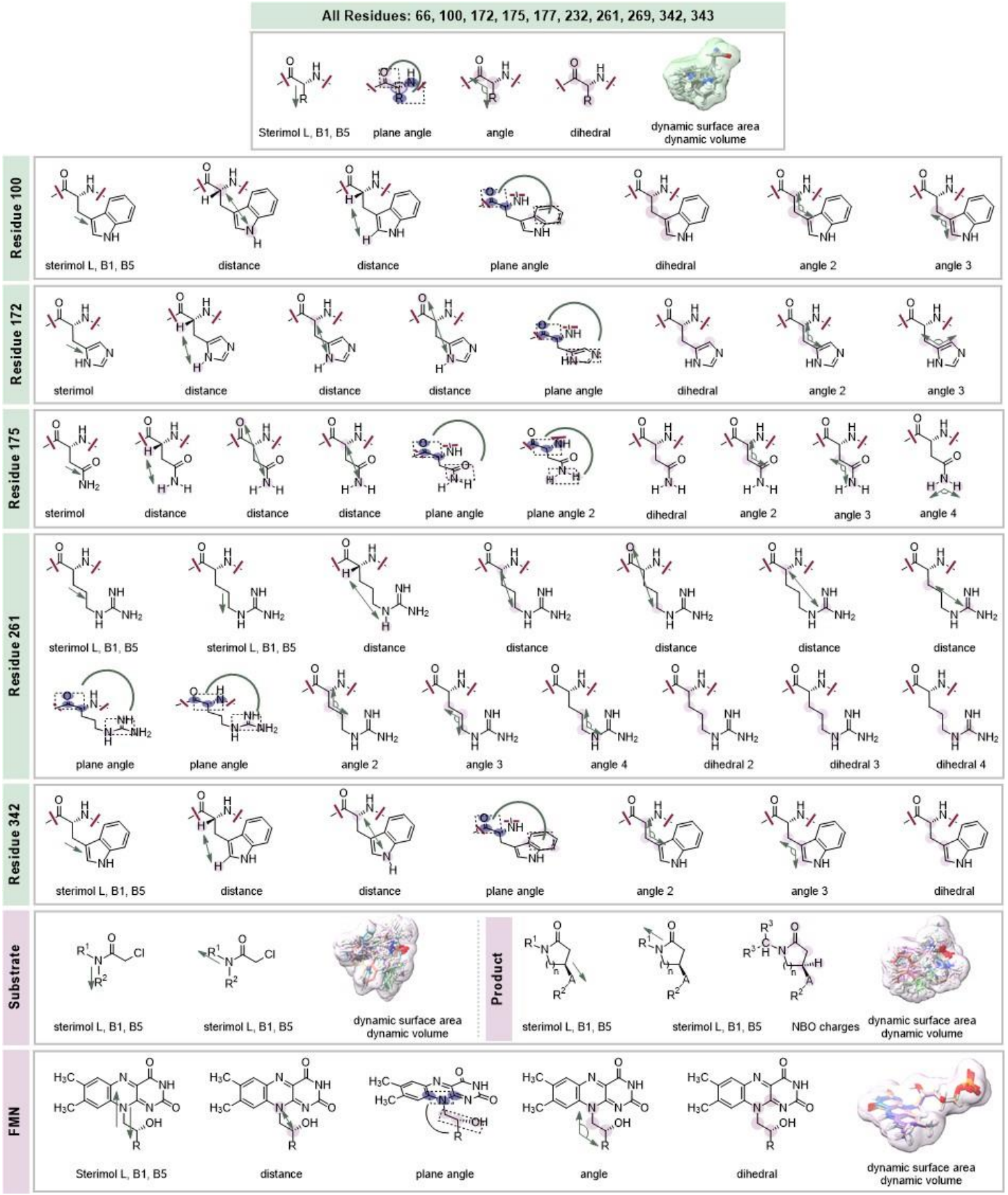

Figure S2. Acquired substrate, product, enzyme, and cofactor parameters.

Supplementary Table S4. Additional Parameters for Updated Model.

Entry	Parameter Name	Residues Measured
1	cDSA and DV (cluster dynamic surface area and volume)	66-100, 100-177, 66-100-177, 172-175, 175-177, 172-175-177, 100-172-177, 342-343
2	IRD: distance between R-group centroids	66-100, 66-177, 100-177,127-175, 172-177, 175-177
3	RMSD: backbone atoms	66, 100, 172, 175, 177, 232, 261, 269, 342,343
4	RMSF: R-group atoms	66, 100, 172, 175, 177, 232, 261, 269, 342,343

5. Model Development and Interpretation

The collection of workflow codes used in this project are available on the Sigman Group GitHub: https://github.com/SigmanGroup/enzyme-MLR-GluER.

IFD Model Generation and Selection Details

In brief, the dataset (Table S1) was partitioned into 70% training set and 30% test set by a y-equidistant algorithm, which selects data points that evenly span the output variable ($\Delta\Delta G^{\ddagger}$). Forward stepwise selection of models was performed, keeping 200 candidates at each step for 10 steps. Collinearity criteria was set to 0.4. The unscaled descriptor values for the resulting selected IFD model are available on the Sigman Group GitHub: https://github.com/SigmanGroup/enzyme-MLR-GluER.

aMD Model Generation and Selection Details

In brief, the dataset (Table S1) was partitioned into 70% training set and 30% test set by a y-equidistant algorithm, which selects data points that evenly span the output variable ($\Delta\Delta G^{\ddagger}$). Forward stepwise selection of models was performed, keeping 100 candidates at each step for 8 steps. Collinearity criteria was set to 0.4. The unscaled descriptor values for the selected aMD models are available on the Sigman Group GitHub: https://github.com/SigmanGroup/enzyme-MLR-GluER.

Supplementary Figure S3: aMD Model 2 Used for 5a Selectivity Predictions

The aMD model described above was selected for its ability to accurately predict the selectivity of reactions forming 6- and 7-membered rings in the training set. Another aMD model with similar parameters and statistics was identified (Fig. S3), and while this model had less accurate predictions for 6- and 7- membered ring forming reactions, it was superior at predicting reactions that formed 5-membered rings in the training set. Therefore, this model was used to predict the selectivity of the transformation of **5a** to **5b**.

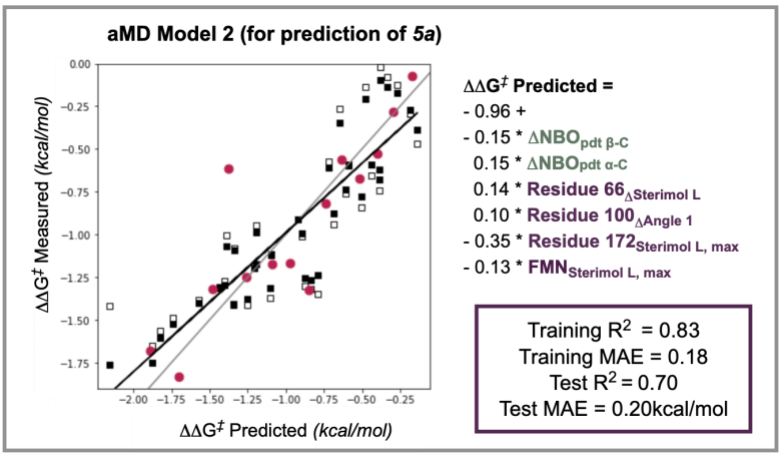

Figure S3: aMD Model 2 has comparable parameters and statistics to Model 1. Although this model had less precise predictions for reactions forming 6- and 7-membered rings, it was more effective in predicting reactions that formed 5-membered rings in the training data. As a result, this model was utilized to forecast the selectivity of the conversion of **5a** to **5b**.

Supplementary Figure S4: Orientation of Substrate 1a from IFD

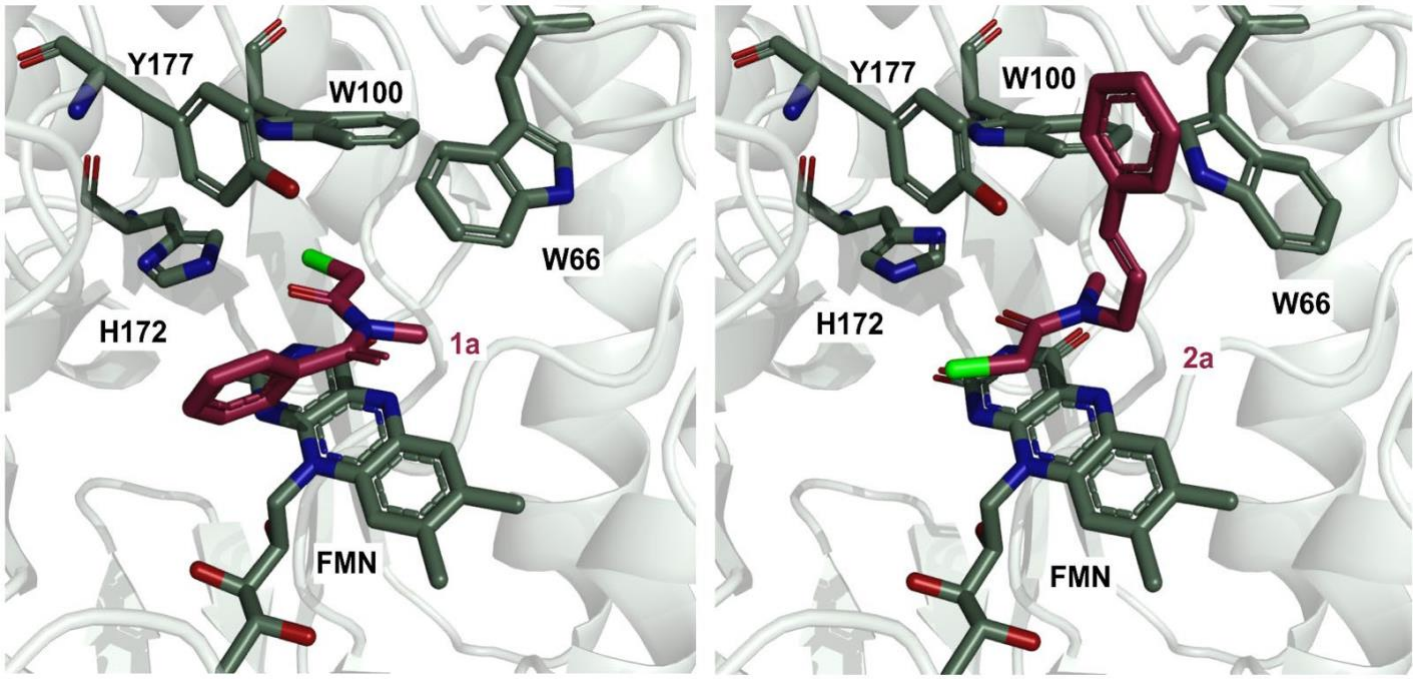

Figure S4: Docked substrate **1a** (left) had a flipped binding mode compared to substrates with internal olefins (**2a**, right), with the substrate alkene and substituent positioned on the opposite side of the active site, away from residue 66. The differential binding mode and steric interactions demonstrated by **1a** may explain why it was the only substrate that resulted in product formation when subjected to GluER-Y177/A/D/L.

Supplementary Figure S5: Simulated Screening with Updated Statistical Model

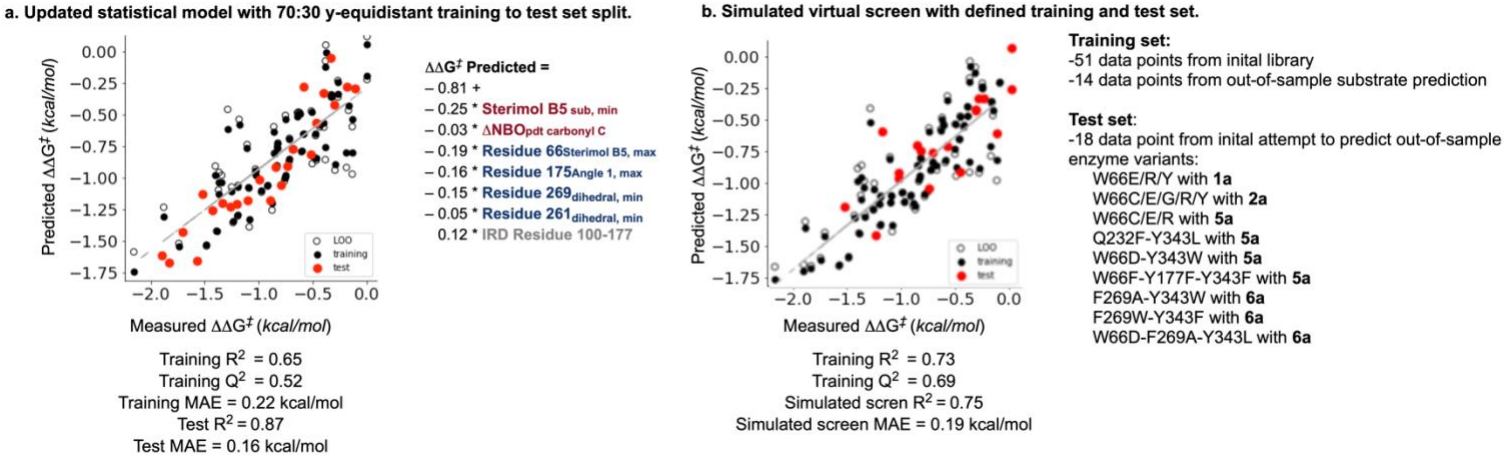

Figure S5: **a.** The updated statistical model was combining the initial experimental data (Table S1) and additional data from the unsuccessful validation of the initial models (Table S2). The experimental data was partitioned into 70% training set and 30% test set by a y-equidistant algorithm, which selects data points that evenly span the output variable ($\Delta\Delta G^{\ddagger}$). Forward stepwise selection of models was performed, keeping 200 candidates at each step for 8 steps. Collinearity criteria was set to 0.4. **b.** A simulated virtual screen was conducted by placing the additional data (Table S2) into the training set, while the initial data set was used to tune the coefficients for each descriptor in the updated statistical model. The model coefficients were only modestly adjusted to fit the defined training set. Unscaled descriptor values for the updated model and virtual screening are available on the Sigman Group GitHub: https://github.com/SigmanGroup/enzyme-MLR-GluER.

HAT Side-Product Model Generation and Selection Details

In brief, the dataset (Table S5) was partitioned into 80% training set and 20% test set by a Kennard-Stone algorithm, which selects data points that evenly span parameter values. Forward stepwise selection of models was performed, keeping 200 candidates at each step for 4 steps. Collinearity criteria was set to 0.4. The unscaled descriptor values for the selected aMD models can be found on the Sigman Group GitHub: https://github.com/SigmanGroup/enzyme-MLR-GluER.

Supplementary Table S5: Experimental Data for HAT Side-Product Model

Product	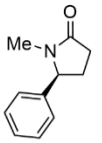	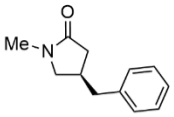	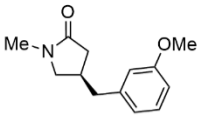	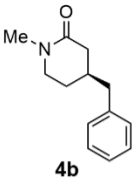	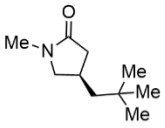	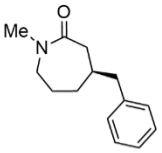
	1b	**2b**	**3b**	**4b**	**5b**	**6b**
HDH	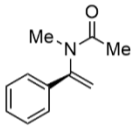	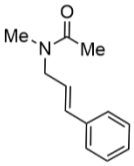	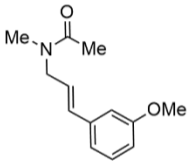	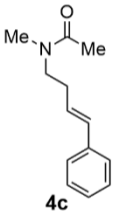	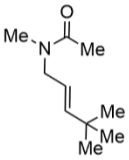	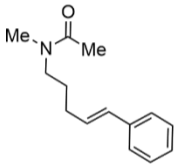
	1c	**2c**	**3c**	**4c**	**5c**	**6c**

GluER Variant	1	2	3	4	5	6
T36A	2.3	20.5	n.d.	8.6	4.8	3.2
T36A W66A	2.0	10.0	n.r.	16.5		
T36A W66D	2.3	41.5	n.d.	n.d.		
T36A W66F	2.0	17.5	n.d.	10.5		
T36A W66L	n.r.	n.d.	n.d.	n.d.		
T36A Y177A	2.4	n.r.	n.r.	n.r.		
T36A Y177F	2.4	5.0	4.0	11.5		
T36A Y177W	1.4	10.5	12.0	n.r.		
T36A Q232F	2.5	34.0	26.5	12.5		
T36A F269A	1.7	10.0	4.5	n.r.		
T36A F269D	n.r.	7.0	2.7	n.r.		
T36A F269L	n.r.	14.5	10.5	n.r.		
T36A F269W	n.r.	30	43.5	5.2		
T36A Y343A	n.r.	30.5	24.0	11.5		
T36A Y343D	n.r.	25	20.0	10.1		
T36A Y343F	n.r.	n.d.	n.d.	n.r.		
T36A Y343L	n.r.	n.d.	n.d.	n.r.		
T36A Y343W	n.r.	17.0	n.d.	n.r.		

each cell contains the **product/HDH (Xb/Xc)** LCMS area integration ratio, detected at 210nm. Substrate/Variant combinations that did not result in a detectable level of HDH are labeled n.d. Substrate/Variant combinations that did not result in a detectable level of product or HDH are labeled n.r.

Comparison of Updated Model to a Regularized Regression Model Over All Features

To compare the updated model used for out-of-sample enzyme predictions to a control model, a regularized regressor was trained on the complete set of aMD descriptors. Hyperparameter scanning was preformed to tune the model for GluER-T36A selectivity; the regularization strength parameter (alpha) was scanned from 0.001 to 1000 on a logarithmic scale. Simultaneously, first, second-, third-, and fourth-degree polynomial fits were scanned, along with linear, polynomial, and radial basis function (RBF) kernel functions. The hyperparameters alpha=1 with a second degree polynomial fit using the RBF kernel lead to the best model based on mean squared error (Fig. S6). The regularized model generally preformed worse than the updated model in predicting both training and test set data points compared to the aMD model.

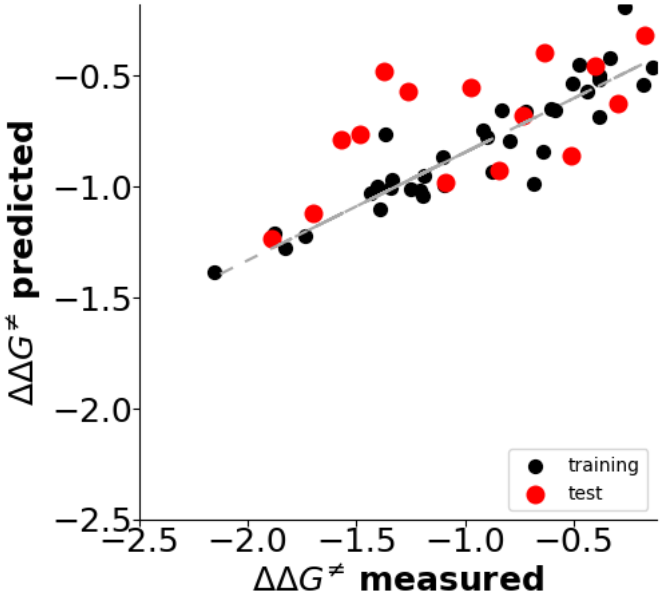

Figure S6: A regularize regression model trained on the entire set of updated aMD parameters. model hyperparameters were scanned to determine the optimal fit (hyperparameters: alpha=1, second degree polynomial, RBF kernel). The model was fit to the same training set used to generate the aMD model, and the out-of-sample GluER-T36A variants with substrates **2a** and **5a** were used as the test set. The resultant model had a training and test set R^2 of 0.63 and 0.10, respectively. The MAE of the test set points was 0.41.

6. Preparation of Substrates

General. All substrates in this publication have been previously reported in *Biegasiewicz et al.*[13] (**1a**, **2a**, **3a**, **4a**, **6a**) as well as *Nicholls et al.*[13] (**5a**). Further synthetic details and characterization can be found therein.

5-*Endo*-Cyclization substrate (**1a**)

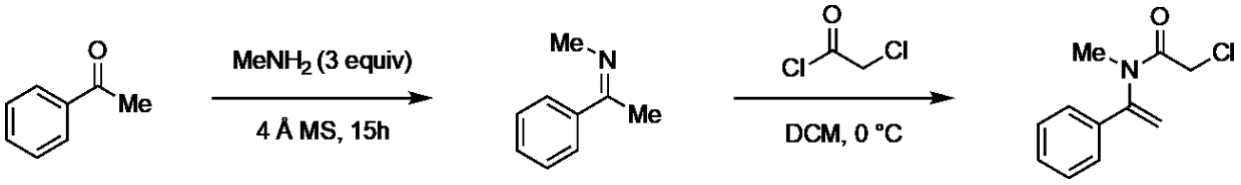

Scheme S1. General Scheme for the 5-*endo* Substrate Synthesis

Procedure from *Biegasiewicz et al*[13] and re-reported here. A round bottom flask was charged with 4 A MS (gram to gram with starting material being used) and teflon stirbar, then flame-dried under an atmosphere of nitrogen. The flask was then charged with methylamine (15 mL, 33 wt % in absolute ethanol, 120 mmol, 6 equiv) and the contents were allowed to stir. To the stirred solution, at room temperature, was added acetophenone (2.3 mL,1 equiv) and the resulting mixture was allowed to stir for 15 h at room temperature. The reaction mixture was filtered through a pad of Celite®, washed with DCM (50 mL), and volatiles were removed to afford a brown oil. The oil was dissolved in dry DCM (30 mL) and cooled to 0 °C and allowed to stir. To the resulting solution was added chloroacetyl chloride (2.3 g, 1.6 mL, 20 mmol, 1 equiv) and the resulting brown solution was allowed to stir for 15 min at the same temperature. The reaction was subsequently quenched by the addition of $NaHCO_3$ (50 mL) and the biphasic 24 mixture was stirred for an additional 30 min, allowing for it to warm to room temperature. The aqueous layer was extracted, and the additional extractions were performed with DCM (3 x 30 mL). The organic fractions were dried over Na_2SO_4 and concentrated in vacuo to afford the crude product. The residue was purified by Biotage (gradient 25 – 100% EtOAc: hexanes) to give 2-chloro-N-methyl-N-(1-phenylvinyl)acetamide.

5-*Exo*-Cyclization substrates (**2a**, **3a**, **5a**)

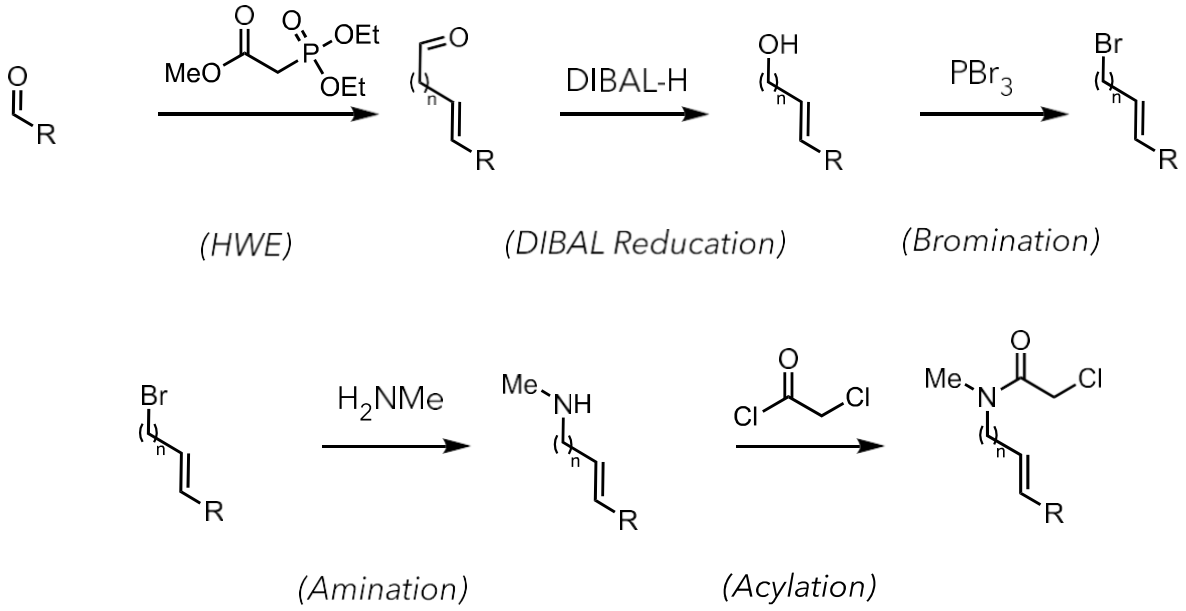

Scheme S2. General Scheme for the 5-*exo* Substrate Synthesis

Horner-Wadsworth-Emmons (HWE) Olefination. Procedure from *Biegasiewicz et al*[13] and re-reported here. Sodium hydride (1.2 equiv) is added to a flame-dried round bottom flask with a magnetic stir bar under nitrogen atmosphere. Dry, degassed THF (0.4 M with respect to ketone/aldehyde) is added, and the suspension cooled to 0 °C. Methyl 2- (diethoxyphosphoryl) acetate (1.3 equiv) is added dropwise followed by an additional hour of stirring at 0 °C. Neat aldehyde is added dropwise and the reaction mixture is stirred overnight at reflux temperature. The reaction mixture is re-cooled to 0 °C and saturated aqueous ammonium chloride solution (2-5 mL) is added. The resultant mixture is transferred to a separatory funnel containing water and ethyl acetate (additional water/saturated ammonium chloride is used to dissolve remaining solids in flask as necessary) and the aqueous layer is extracted with ethyl acetate (3 x 50 mL). Combined organic layers are dried with sodium sulfate and concentrated under reduced pressure. Crude products are purified by silica gel chromatography (mobile phase gradient: 5% ethyl acetate: 95% hexanes – 15% ethyl acetate: 85% hexanes).

DIBAL Reduction. Procedure from *Biegasiewicz et al*[13] and re-reported here. In a flame-dried round bottom flask with a magnetic stir bar under nitrogen atmosphere unsaturated ester is dissolved in dry, degassed THF to create a 0.25 M solution. Cooling to -78 °C is followed by dropwise addition of diisobutylaluminum hydride solution (1M in hexanes, 3 equiv). The mixture is allowed to warm up to room temperature and stirred for ~3 h with monitoring of starting material consumption by TLC. Once complete, the mixture is re-cooled to 0 °C and saturated ammonium chloride solution is added carefully to quench the reaction (3-5 mL). Removal from the ice/water bath and ~6-8 minutes of stirring leads to a gel which is treated with water and ethyl acetate and filtered over a pad of Celite®. The biphasic filtrate is poured into a separatory funnel and the aqueous portion extracted with additional ethyl acetate (2x 50 mL). Combined organics are dried with sodium sulfate and concentrated under reduced pressure to yield essentially pure allylic alcohol, which was carried forward without further manipulation.

Bromination. Procedure from *Biegasiewicz et al*[13] and re-reported here. In a flame-dried round bottom flask with a magnetic stir bar under nitrogen atmosphere, the allylic alcohol obtained from step 1 is dissolved in diethyl ether to create a 0.1 M solution which is cooled to 0 °C. Phosphorus tribromide (1.05 equiv) is added and stirred at 0 °C for 10 minutes (TLC at this time usually revealed clean conversion to a single spot). Upon completion, the reaction mixture is poured directly into a beaker containing ice-cold water. This is poured into a separatory funnel and the aqueous layer is extracted with diethyl ether (3x 50 mL) and the combined organics are washed several times with water before drying with sodium sulfate. Removal of solvent under reduced pressure yields crude allylic bromide, which is taken forward to amination without further manipulation.

Amination. Procedure from *Biegasiewicz et al*[13] and re-reported here. Allylic bromide from Bromination is added neat to a flask with stir bar cooled to 0 °C. Methylamine solution (33 % wt. in ethanol, 10 equiv) is added directly and in one portion (be aware of the exotherm). The reaction flask is allowed to stir overnight at room temperature. A solution of 1 M sodium hydroxide is added and the mixture is transferred to a separatory funnel containing 1 M sodium hydroxide and diethyl ether. Following extraction of the aqueous layer with diethyl ether (2x 20 mL), the combined ethereal extracts are washed with ~35-50 mL of 1 M sodium hydroxide, dried using sodium sulfate and concentrated under reduced pressure to afford amine which is acylated without further purification.

Acylation. Procedure from *Biegasiewicz et al*[13] and re-reported here. The secondary amine (1 equiv.) is added to a flame dried flask under N_2 pressure containing dry DCM and triethylamine (1.5 equiv.) for a final concentration of 0.25 M for the secondary amine. The chloroacetylchloride purchased from Sigma (1.2 equivalents) is added dropwise to the stirred solution at room temperature. The solution is stirred overnight and then poured into a separatory funnel containing a 1:1 solution of 10% HCl and DCM. The aqueous layer is extracted with DCM. The organic layers are collected, washed with brine, dried with anhydrous Na_2SO_4 and concentrated *in vacuo* to yield a crude chloroamide as an oil. The crude oil is purified via silica gel flash chromatography in a gradient of 12 % EtOAc/Hexanes to 60% EtoAC/Hexanes.

<u>6 and 7-*Exo*-Cyclization substrate (**4a** and **6a**)</u>

Procedure adapted from *Biegasiewicz et al*[13] and re-reported here.

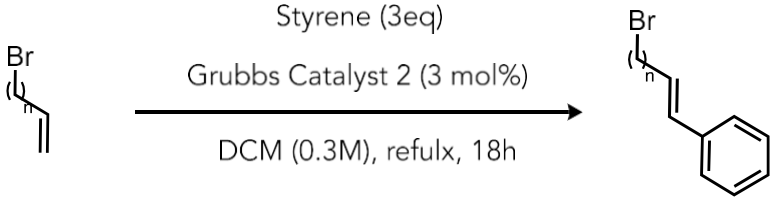

Grubbs Metathesis. Allylic bromide (1 equiv) and styrene (3 equiv) are added to a flame-dried round bottom flask with a magnetic stir bar under nitrogen atmosphere. Dry, degassed DCM (0.3 M) is added with Grubbs Catalyst 2 (0.3 mol%) and heated under reflux for 18h. The reaction is then concentrated under reduced pressure and purified by silica gel chromatography (mobile phase gradient: 100% hexanes).

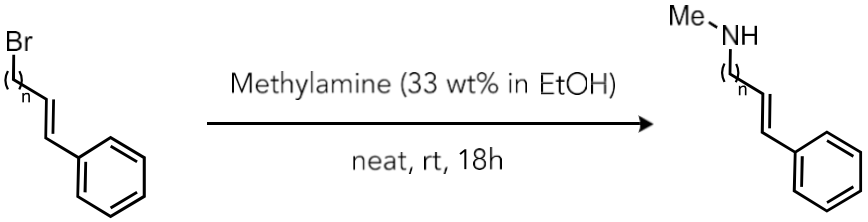

Amination. Allylic bromide from Grubbs Metathesis is added with to a flask with stir bar. Methylamine solution (33 % wt. in ethanol, 10 equiv) is added directly and in one portion. Sodium Iodide (0.1 equiv) is added, and reaction mixture is equid with a reflux condenser and heated to 40 °C and allowed to procced overnight. A solution of 1 M sodium hydroxide is added, and the mixture is transferred to a separatory funnel containing 1 M HCl and diethyl ether. After extraction, the aqueous layer is basified using 1 M sodium hydroxide and the product is extracted of the aqueous layer with diethyl ether. The combined ethereal extracts are dried using sodium sulfate and concentrated under reduced pressure to afford amine which is acylated without further purification.

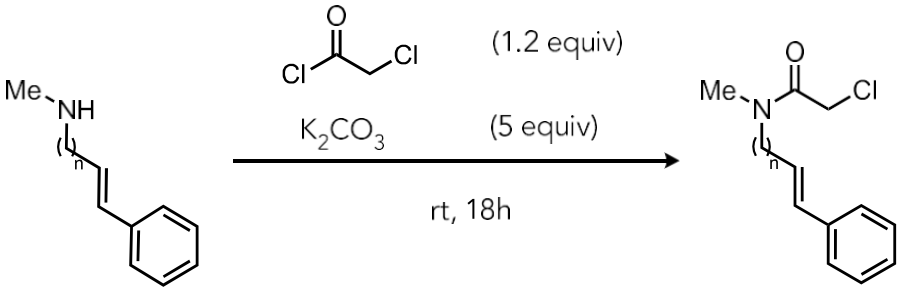

Acylation. The secondary amine (1 equiv.) is added to a flame dried flask under nitrogen pressure containing dry DCM and postassium carbonate (5 equiv.) for a final concentration of 0.25 M for the secondary amine. Chloroacetylchloride (3 equivalents) is added dropwise to the stirred solution at room temperature. The solution is stirred overnight and then poured into a separatory funnel containing a 1:1 solution of 10% HCl and DCM. The aqueous layer is extracted with DCM. The organic layers are collected, washed with brine, dried with anhydrous sodium sulfate and concentrated *in vacuo* to yield a crude amide as an oil. The crude oil is purified via silica gel flash chromatography in a gradient of 12 % EtOAc/Hexanes to 60% EtOAc/Hexanes.

7. Preparation of Products

All racemates in this publication have been previously reported in *Biegasiewicz et al.*[13] (**1b**, **2b**, **3b**, **4b**, **6b**) as well as *Nicholls et al*[14] (**5b**). Further details synthetic details can be seen therein.

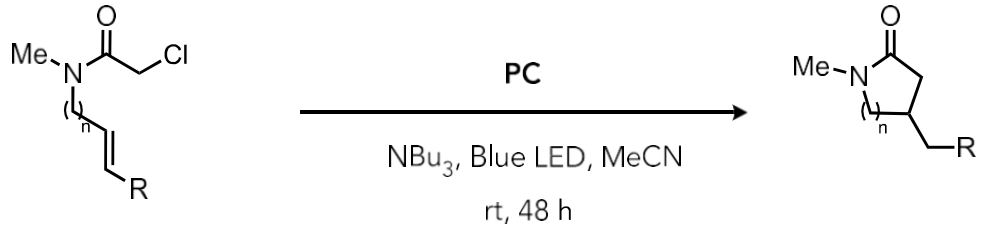

General Method for Racemate Synthesis.

Adapted from Fava *et al*[15] and detailed below**.** An 8 dram vial was charged with chloroamide (0.25 mmol 1 equiv.), $Ir(ppy)_2(dtb\text{-}bpy)PF_6$ (**PC**, 1 mol%) and NBu_3 (2 equiv.) under nitrogen in a glovebox. Degassed acetonitrile (12.5 ml, 0.02M) was added and the reaction sealed. The reaction was then irradiated with a 450 nm Kessil Lamp for 48 hrs. After this period, the mixture was diluted with Et_2O and the organic phase was extracted three times with brine, dried over $MgSO_4$, filtered and evaporated under reduce pressure. The crude residue is purified using automated silica gel chromatography* (SNAP KP-Sil 10 g column) with the following biotage gradient (CV =column volume): equilibration10% EtOAc/90% hexanes → 25% EtOAc/75% hexanes, 5 CV | gradient- 25% EtOAc/75% hexanes, 1 CV | 25% EtOAc/75% hexanes → 100% EtOAc, 4 CV | 100% EtOAc, 18 CV. The product reliably elutes during the 100% ethyl acetate phase of the gradient and can be collected in fractions 8-15. TLC analysis using potassium permanganate stain often may also be used to visualize the product containing fractions, which appear on the plate after heating as temporary white spots, which disappear again over time. LCMS analysis of small aliquots (~15 μL) of suspected product-containing fractions may also be performed. Fractions containing product are combined, concentrated, and subsequently analyzed by HPLC or SFC.

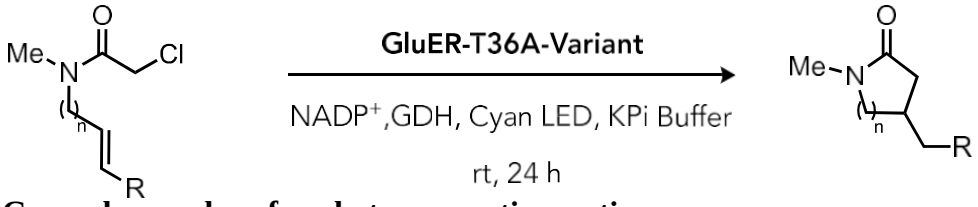

General procedure for photoenzymatic reactions.

Adapted from Page *et al*[16] and detailed below. All reactions for enzyme substrate-matrix were set up in an anerobic chamber and performed in duplicate. Reactions were run with 10 umol of $\alpha\alpha$-chloroamide substrate. In an anerobic chamber, a shell vial with a magnetic cross stir bar was charged with 250 uL of "turnover mix" (GDH-105 (5 mg/mL), glucose (40 mg/mL), and NADP+ (1.5 mg/mL) in KPi 100 mM pH 8, 10% glycerol). Next, 100 nmol of GluER-T36A Variant (1 mol%) was added (between 40-100ul). Additional KPi 100 mM pH 8, 10% glycerol was added such that final reaction volume was 500 ul. Lastly, 15 ul of IPA/ $\alpha\alpha$-chloroamide substrate was added. Vials were sealed with septa, taken out of the anerobic chamber and additionally sealed with black electrical tape. Reactions were irradiated with 1000 W of cyan light for 24 h, stirring at 400 rpm. The reaction was quenched by addition of 3000 uL of MeCN + 200 uL of TBB (2mg/mL in MeCN), kept on a shaker for 60 min, centrifuged at 14000 rpm for 10 min, filtered over KimWipe and subjected to LCMS analysis (MeCN-30-95-8 min-1mL per min; 1 uL injection) calibration curves for conversion. Enantioselectivities determined by HPLC and SFC.

8. References

1. Gibson, D. G. et al. Enzymatic assembly of DNA molecules up to several hundred kilobases. *Nature Methods* **6**, 343–345 (2009).

2. Kille, S. et al. Reducing Codon Redundancy and Screening Effort of Combinatorial Protein Libraries Created by Saturation Mutagenesis. *ACS Syn. Bio.* **2** 83–92 (2012)

3. **Schrödinger Release 2021-4**: Maestro, Schrödinger, LLC, New York, NY, (2021).

4. Pettersen, E. F. *et al.* UCSF Chimera - A visualization system for exploratory research and analysis. *J. Comput. Chem.* **25**, 1605–1612 (2004).

5. The PyMOL Molecular Graphics System, Version 2.0 Schrödinger, LLC.

6. Dolinsky, T. J., Nielsen, J. E., McCammon, J. A. & Baker, N. A. PDB2PQR: An automated pipeline for the setup of Poisson-Boltzmann electrostatics calculations. *Nucleic Acids Res.* **32**, 665–667 (2004).

7. Dolinsky, T. J. *et al.* PDB2PQR: Expanding and upgrading automated preparation of biomolecular structures for molecular simulations. *Nucleic Acids Res.* **35**, 522–525 (2007).

8. Pierce, L.C.T., Salomon-Ferrer, R., de Oliveira, C.A.F., McCammon, J.A, and Walker, R.C. Routine Access to Millisecond Time Scale Events with Accelerated Molecular Dynamics. *J Chem Theory Comput.*, **8**, 2997-3002 (2012).

9. Birant, D. & Kut, A. ST-DBSCAN: An algorithm for clustering spatial-temporal data. *Data Knowl. Eng.* **60**, 208–221 (2007).

10. **Schrödinger Release 2021-4**: MacroModel, Schrödinger, LLC, New York, NY, (2021).

11. Frisch, M. J. et al. Gaussian 09 (2009).

12. Daniel R. Roe and Thomas E. Cheatham, III, "PTRAJ and CPPTRAJ: Software for Processing and Analysis of Molecular Dynamics Trajectory Data". J. Chem. Theory Comput., 2013, 9 (7), pp 3084-309.

13. Biegasiewicz, K. F. et al. Photoexcitation of flavoenzymes enables a stereoselective radical cyclization. *Science* **364**, 1166–1169 (2019).

14. Nicholls, B. T. et al. Engineering a Non-Natural Photoenzyme for Improved Photon Efficiency. *Angew. Chem. Int. Ed.* (2021)

15. Fava, E., Nakajima, M., Tabak, M. B. & Rueping, M. Tin-free visible light photoredox catalysed cyclisation of enamides as a mild procedure for the synthesis of γ-lactams. *Green Chemistry* **18**, 4531–4535 (2016).

16. Page, C. G. et al. Quaternary Charge-Transfer Complex Enables Photoenzymatic Intermolecular Hydroalkylation of Olefins. *J. Am. Chem. Soc.* **143** 97–102 (2020).

9. HPLC Traces

ENZYME-SUBSTRATE MATRIX

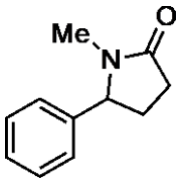

1a

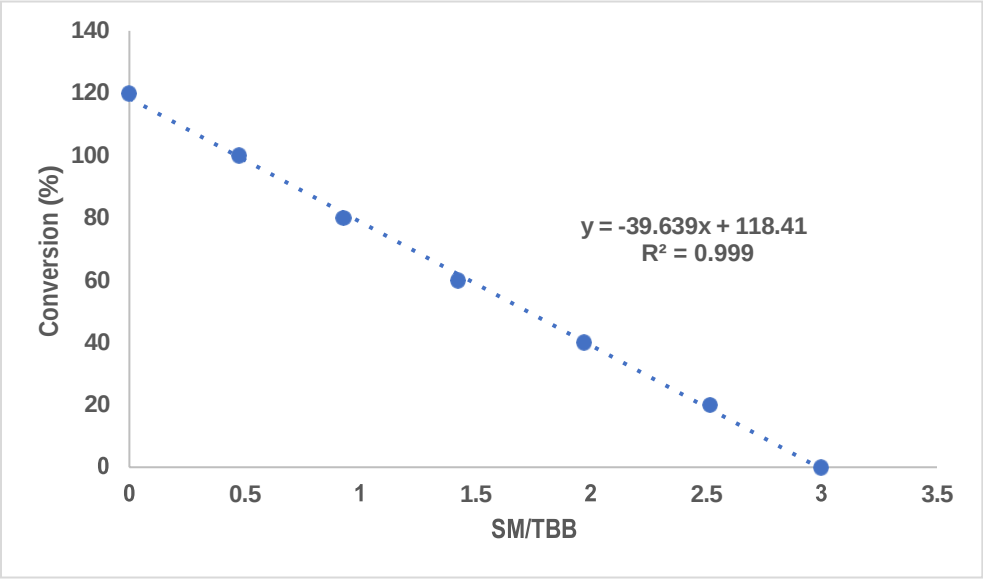

LCMS Method: MeCN-30-95, 8 min-1mL per min; 1 uL injection

	Variant	conversion	er
0-A	T36A	96.7290715	90.2:9.8
0-B		96.3568905	90.0:10.0
1-A	T36A W66A	95.5441235	56.4:43.6
1-B		92.9352239	57.3:42.7
2-A	T36A W66D	96.8021969	73.9:26.1
2-B		81.9244185	73.1:26.9
3-A	T36A W66F	91.3656962	76.2:23.8
3-B		84.923969	75.9:24.1
4-A	T36A W66L	no pdt	nd
4-B		no pdt	nd
5-A	T36A Y177A	87.4221748	60.5:39.5
5-B		78.5810244	60.8:39.2

6-A	T36A Y177D	no pdt	nd
6-B		no pdt	nd
7-A	T36A Y177F	59.7259688	68.1:31.9
7-B		50.8270557	68.4:31.6
8-A	T36A Y177L	no pdt	nd
8-B		no pdt	nd
9-A	T36A Y177W	71.1907536	66.2:33.8
9-B		61.8698195	67.5:32.5
12-A	T36A Q232F	69.1044195	61.3:38.7
12-B		64.0140179	62.1:37.9
15-A	T36A F269A	40.6186952	56.4:43.6
15-B		40.9078646	54.5:45.5
16-A	T36A F269D	43.9719794	nd
16-B		34.7187252	nd
17-A	T36A F269L	54.0872293	nd
17-B		48.6103985	nd
18-A	T36A F269W	no pdt	nd
18-B		no pdt	nd
19-A	T36A Y343A	no pdt	nd
19-B		no pdt	nd
20-A	T36A Y343F	73.7850634	nd
20-B		79.4154267	nd
21-A	T36A Y343D	no pdt	nd
21-B		no pdt	nd
22-A	T36A Y343L	no pdt	nd
22-B		no pdt	nd
23-A	T36A Y343W	no pdt	nd
23-B		no pdt	nd

Racemate 40% IPA-IC-20 Min-1ml/Min

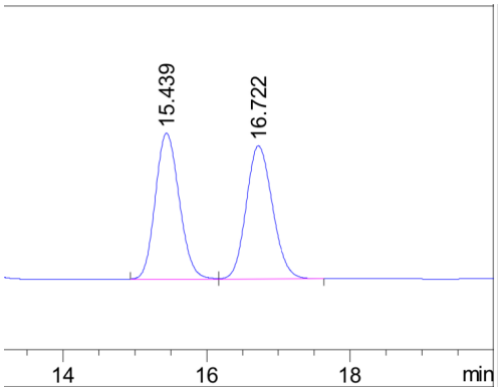

Peak #	RetTime [min]	Type	Width [min]	Area [mAU*s]	Area %
1	15.439	BV	0.3636	2.06257e4	50.0044
2	16.722	VB	0.3999	2.06221e4	49.9956

0A

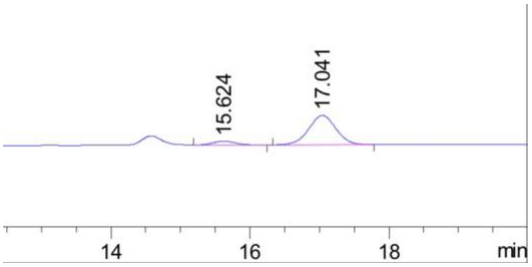

Peak #	RetTime [min]	Type	Width [min]	Area [mAU*s]	Area %
1	15.624	BB	0.3526	427.04327	9.8283
2	17.041	BB	0.4246	3917.99829	90.1717

0B

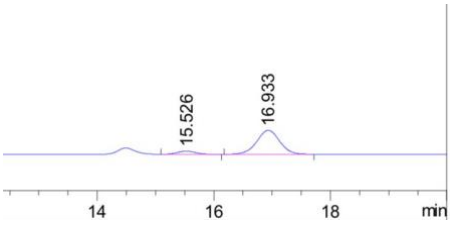

Peak #	RetTime [min]	Type	Width [min]	Area [mAU*s]	Area %
1	15.526	BB	0.3497	514.85693	9.9404
2	16.933	BB	0.4252	4664.55859	90.0596

1A

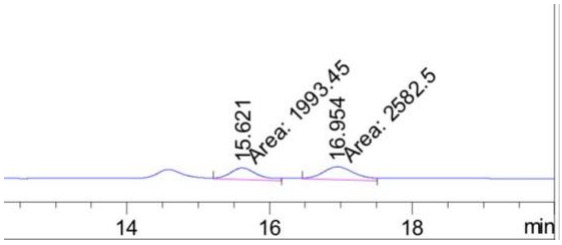

Peak #	RetTime [min]	Type	Width [min]	Area [mAU*s]	Area %
1	15.621	MM	0.4479	1993.44592	43.5636
2	16.954	MM	0.5235	2582.50122	56.4364

1B

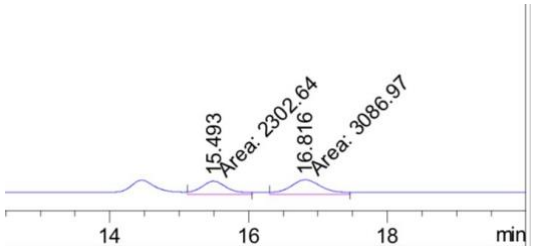

Peak #	RetTime [min]	Type	Width [min]	Area [mAU*s]	Area %
1	15.493	MM	0.4509	2302.64136	42.7237
2	16.816	MM	0.5433	3086.97046	57.2763

2A

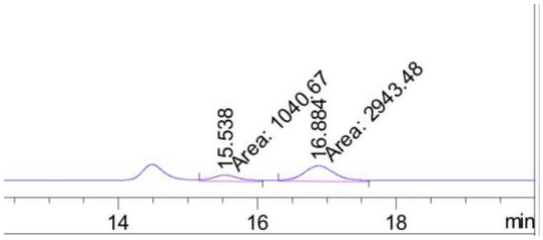

Peak #	RetTime [min]	Type	Width [min]	Area [mAU*s]	Area %
1	15.538	MM	0.4871	1040.66797	26.1202
2	16.884	MM	0.5340	2943.47632	73.8798

2B

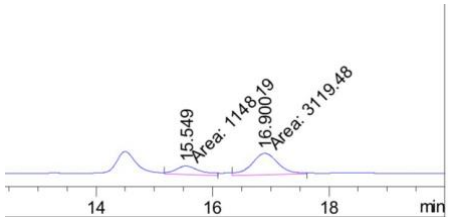

Peak #	RetTime [min]	Type	Width [min]	Area [mAU*s]	Area %
1	15.549	MM	0.4913	1148.18860	26.9043
2	16.900	MM	0.5352	3119.48096	73.0957

3A

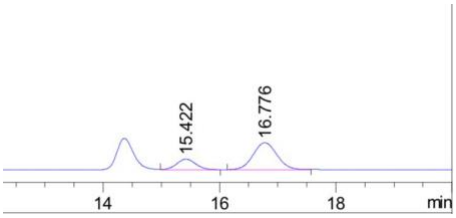

Peak #	RetTime [min]	Type	Width [min]	Area [mAU*s]	Area %
1	15.422	VB	0.3521	1331.47559	23.7719
2	16.776	BB	0.4416	4269.56445	76.2281

3B

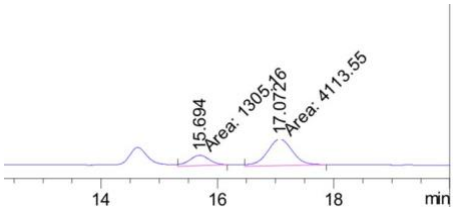

Peak #	RetTime [min]	Type	Width [min]	Area [mAU*s]	Area %
1	15.694	MM	0.4124	1305.16235	24.0862
2	17.072	MM	0.5098	4113.54639	75.9138

5A

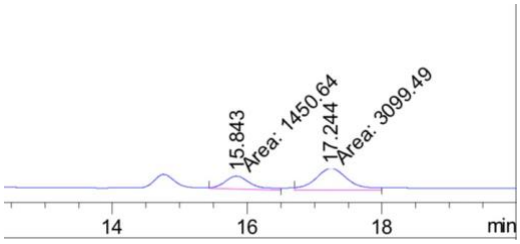

Peak #	RetTime [min]	Type	Width [min]	Area [mAU*s]	Area %
1	15.843	MM	0.4527	1450.64307	31.8813
2	17.244	MM	0.5679	3099.49341	68.1187

5B

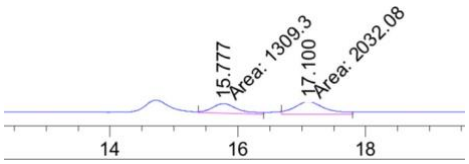

Peak #	RetTime [min]	Type	Width [min]	Area [mAU*s]	Area %
1	15.777	MM	0.4710	1309.29919	39.1844
2	17.100	FM	0.5637	2032.08289	60.8156

7A

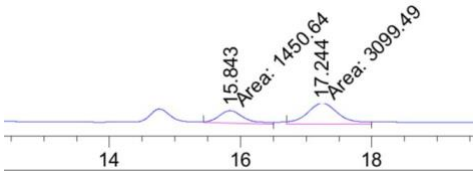

Peak #	RetTime [min]	Type	Width [min]	Area [mAU*s]	Area %
1	15.843	MM	0.4527	1450.64307	31.8813
2	17.244	MM	0.5679	3099.49341	68.1187

7B

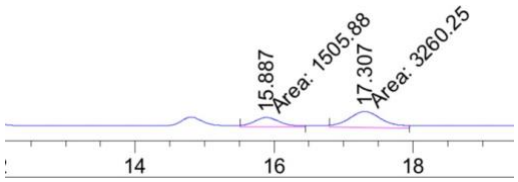

Peak #	RetTime [min]	Type	Width [min]	Area [mAU*s]	Area %
1	15.887	MM	0.4506	1505.87720	31.5954
2	17.307	MM	0.5685	3260.24829	68.4046

9A

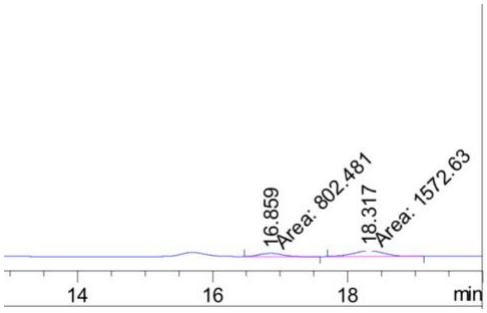

Peak #	RetTime [min]	Type	Width [min]	Area [mAU*s]	Area %
1	16.859	MM	0.4572	802.48114	33.7871
2	18.317	MM	0.5548	1572.62708	66.2129

9B

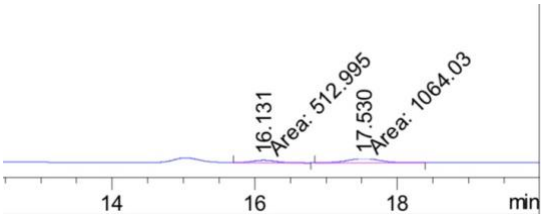

Peak #	RetTime [min]	Type	Width [min]	Area [mAU*s]	Area %
1	16.131	MM	0.4691	512.99493	32.5293
2	17.530	MM	0.5961	1064.03076	67.4707

12A

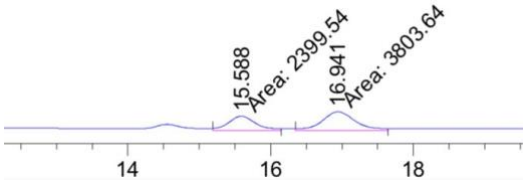

Peak #	RetTime [min]	Type	Width [min]	Area [mAU*s]	Area %
1	15.588	MM	0.4526	2399.53687	38.6824
2	16.941	MM	0.5446	3803.63892	61.3176

12B

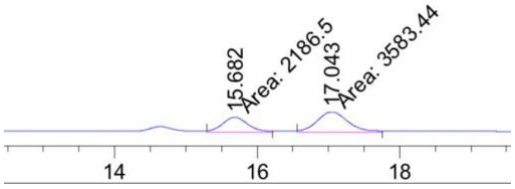

Peak #	RetTime [min]	Type	Width [min]	Area [mAU*s]	Area %
1	15.682	MM	0.4250	2186.50464	37.8947
2	17.043	MM	0.5161	3583.44458	62.1053

15A

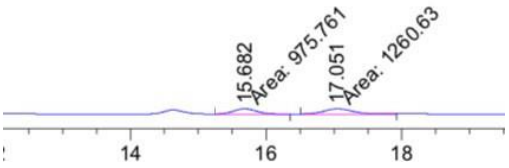

Peak #	RetTime [min]	Type	Width [min]	Area [mAU*s]	Area %
1	15.682	MM	0.4245	975.76074	43.6311
2	17.051	MM	0.5454	1260.62793	56.3689

15B

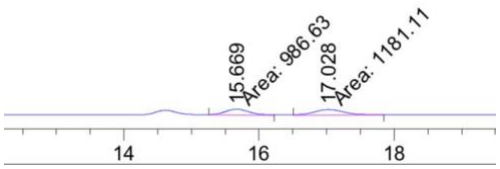

Peak #	RetTime [min]	Type	Width [min]	Area [mAU*s]	Area %
1	15.669	MM	0.4236	986.62982	45.5142
2	17.028	MM	0.5320	1181.11169	54.4858

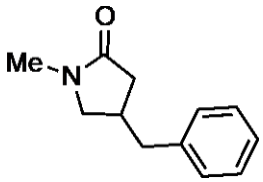

2a

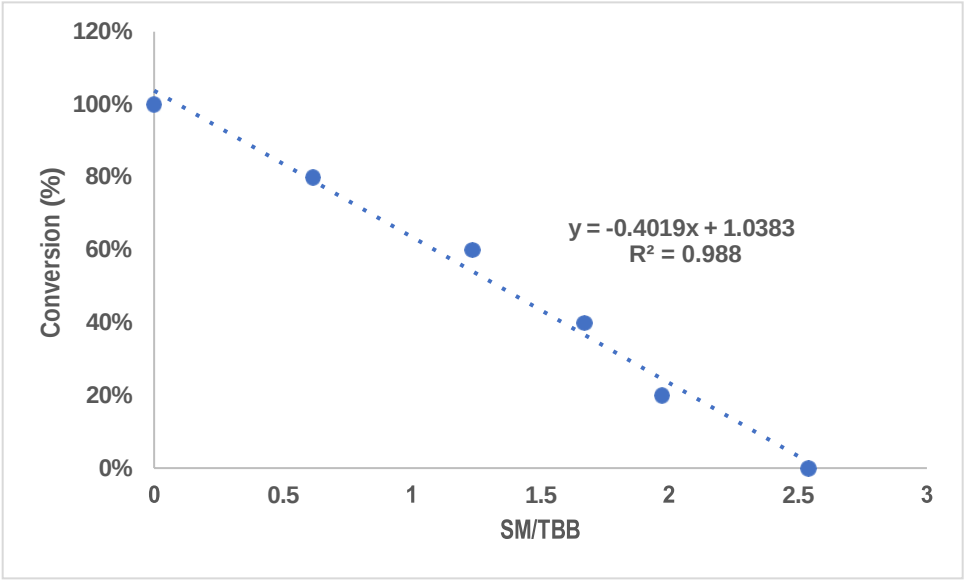

LCMS Method: MeCN-30-95, 8 min-1mL per min; 1 uL injection

	Variant	Conversion	ER
0-A	T36A	102.2940395	91.1:8.9
0-B		101.7949609	92.0:8.0
1-A	T36A W66A	102.1049849	69.3:30.7
1-B		103.1875097	69.3:30.7
2-A	T36A W66D	102.8653324	78.7:21.3
2-B		101.2431343	79.8:20.2
3-A	T36A W66F	99.44276036	90.5:9.5
3-B		98.58797095	91.3:8.7

4-A	T36A W66L	89.8120512	72.8:27.2
4-B		84.43610714	72.4:27.6
5-A	T36A Y177A	30.5516188	nd
5-B		33.19033002	nd
6-A	T36A Y177D	60.29283852	nd
6-B		50.09148052	nd
7-A	T36A Y177F	89.94767591	81.1:18.9
7-B		59.30291441	81.7:18.3
8-A	T36A Y177L	51.87944083	nd
8-B		46.95742411	nd
9-A	T36A Y177W	103.87	90.6:9.4
9-B		97.12724876	90.4:9.6
12-A	T36A Q232F	101.1479927	86.9:13.1
12-B		100.9208121	87.6:12.4
15-A	T36A F269A	93.22615162	88.9:11.1
15-B		94.45492378	90.1:9.9
16-A	T36A F269D	93.71793721	86.8:13.2
16-B		90.39607647	87.5:12.5
17-A	T36A F269L	99.02757931	85.4:14.6
17-B		94.20472265	85.2:14.8
18-A	T36A F269W	101.0400293	94.2:5.8
18-B		103.87	94.3:5.7
19-A	T36A Y343A	103.87	78.0:22.0
19-B		103.87	78.3:21.7
20-A	T36A Y343F	103.87	95.4:4.6
20-B		102.5631034	95.5:4.5
21-A	T36A Y343D	103.87	82.7:17.3
21-B		103.87	82.8:17.2
22-A	T36A Y343L	91.7250586	79.3:20.7
22-B		103.87	79.9:20.1
23-A	T36A Y343W	90.4998094	95.5:4.5
23-B		90.73823085	95.2:4.8

Racemate - 40% IPA in hexanes, 45 min, AS-H, 1.0 mL/min HPLC

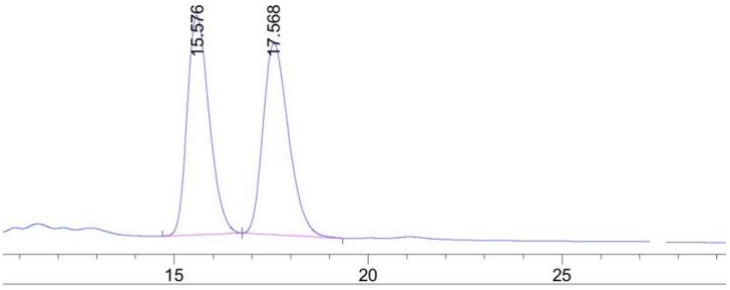

Peak #	RetTime [min]	Type	Width [min]	Area [mAU*s]	Height [mAU]	Area %
1	15.576	BB	0.6125	1186.71753	30.06458	49.7087
2	17.568	BB	0.7045	1200.62695	26.20769	50.2913

0A

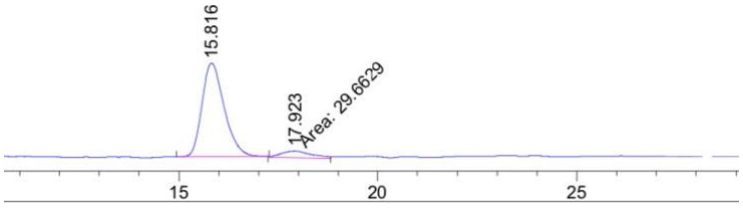

Peak #	RetTime [min]	Type	Width [min]	Area [mAU*s]	Height [mAU]	Area %
1	15.816	BB	0.5986	302.52588	7.79861	91.0705
2	17.923	MM	0.8893	29.66294	5.55929e-1	8.9295

0B

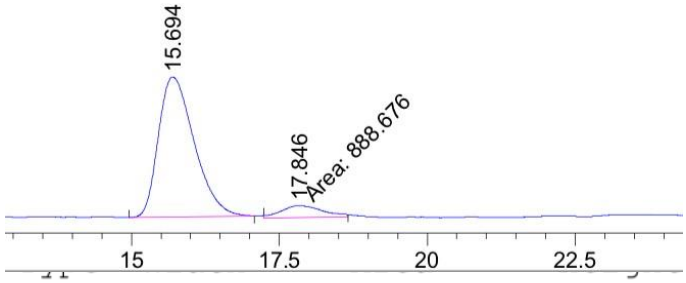

Peak #	RetTime [min]	Type	Width [min]	Area [mAU*s]	Height [mAU]	Area %
1	15.698	MM	0.7212	2332.09692	53.89490	90.5403
2	17.829	MM	0.9459	243.65778	4.29303	9.4597

1A

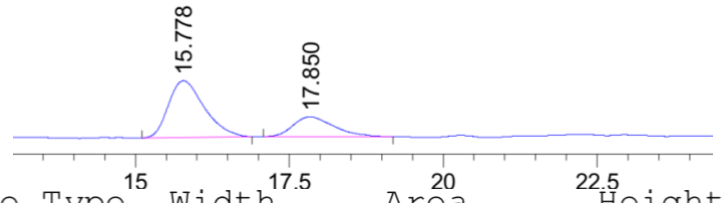

Peak #	RetTime [min]	Type	Width [min]	Area [mAU*s]	Height [mAU]	Area %
1	15.776	MM	0.7560	979.09589	21.58477	69.3489
2	17.835	MM	0.8919	432.74387	8.08613	30.6511

1B

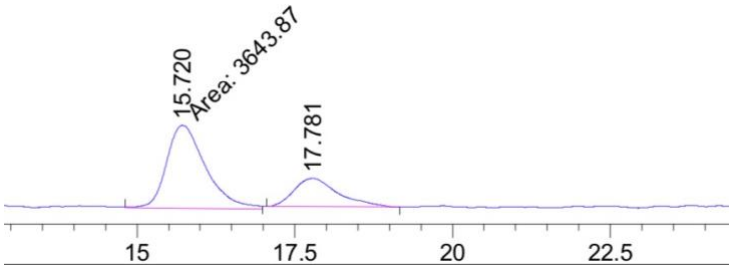

Peak #	RetTime [min]	Type	Width [min]	Area [mAU*s]	Height [mAU]	Area %
1	15.718	MM	0.6879	837.66040	20.29532	69.3292
2	17.762	MM	0.8425	370.57614	7.33056	30.6708

2A

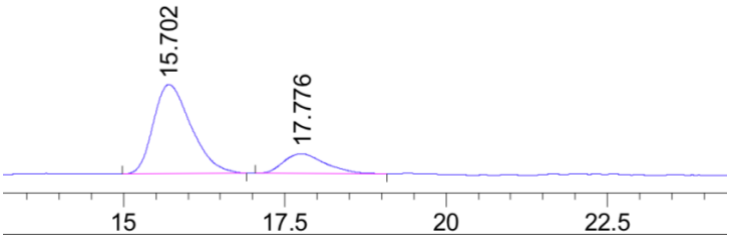

Peak #	RetTime [min]	Type	Width [min]	Area [mAU*s]	Height [mAU]	Area %
1	15.703	MM	0.6921	1024.49438	24.67092	78.6684
2	17.766	MM	0.8055	277.79968	5.74819	21.3316

2B

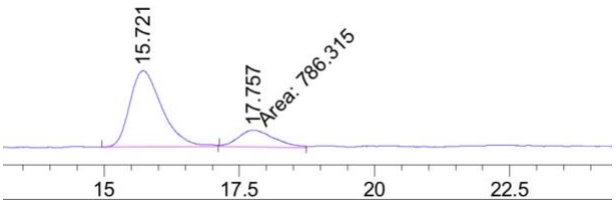

Peak #	RetTime [min]	Type	Width [min]	Area [mAU*s]	Height [mAU]	Area %
1	15.721	BV	0.6130	3254.35889	78.27769	80.5400
2	17.757	MM	0.7730	786.31500	16.95276	19.4600

3A

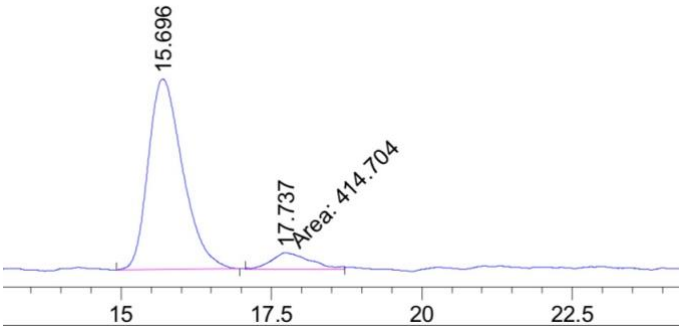

Peak #	RetTime [min]	Type	Width [min]	Area [mAU*s]	Height [mAU]	Area %
1	15.692	BB	0.6125	973.42041	24.44684	90.5442
2	17.753	MM	0.8789	101.65752	1.92784	9.4558

3B

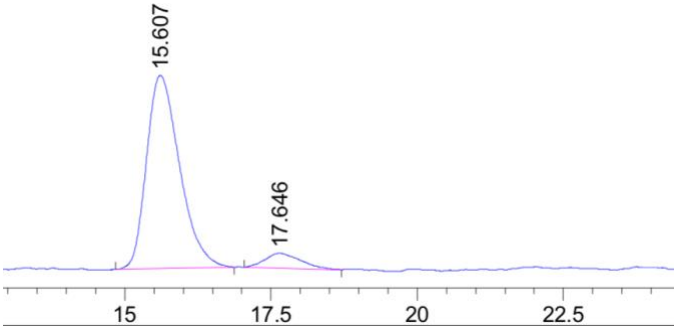

Peak #	RetTime [min]	Type	Width [min]	Area [mAU*s]	Height [mAU]	Area %
1	15.608	BB	0.6013	973.07819	24.82539	91.2639
2	17.664	MM	0.8038	93.14587	1.93144	8.7361

4A

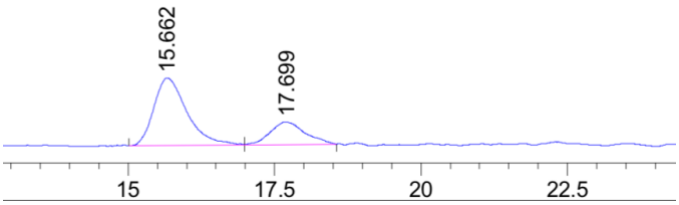

Peak #	RetTime [min]	Type	Width [min]	Area [mAU*s]	Height [mAU]	Area %
1	15.662	BV	0.5316	1501.51270	38.44704	73.9857
2	17.699	VB	0.5004	527.95038	12.76855	26.0143

4B

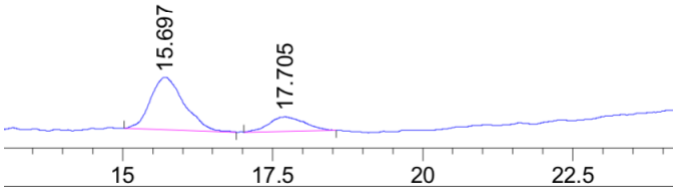

Peak #	RetTime [min]	Type	Width [min]	Area [mAU*s]	Height [mAU]	Area %
1	0.046	BB	0.0997	9.30815	1.29674	0.2410
2	3.284	BB	0.1833	1504.98047	116.05917	38.9715
3	3.956	BB	0.1272	16.55538	1.94665	0.4287
4	6.522	VB	0.2129	19.23965	1.11749	0.4982
5	7.261	BV	0.2239	25.96913	1.44369	0.6725
6	7.747	VB	0.1966	26.32212	1.68202	0.6816
7	9.921	BV	0.3865	1220.06360	45.55566	31.5936
8	15.697	BB	0.4726	802.51837	20.59427	20.7813
9	17.705	BB	0.4927	236.78487	5.77079	6.1316

7A

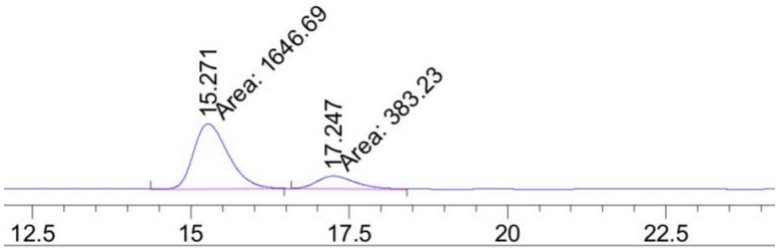

Peak #	RetTime [min]	Type	Width [min]	Area [mAU*s]	Height [mAU]	Area %
1	15.271	MM	0.6476	1646.69299	42.37922	81.1210
2	17.247	MM	0.7487	383.22961	8.53064	18.8790

7B

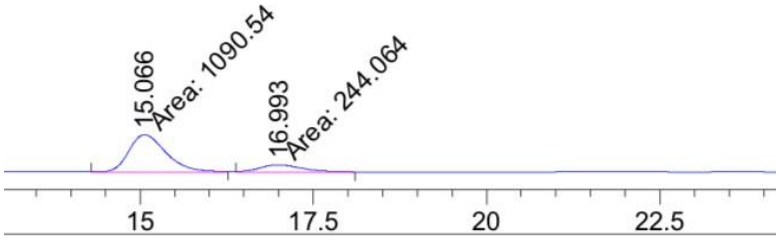

Peak #	RetTime [min]	Type	Width [min]	Area [mAU*s]	Height [mAU]	Area %
1	15.066	MM	0.6443	1090.54016	28.21013	81.7126
2	16.993	MM	0.7441	244.06427	5.46637	18.2874

9A

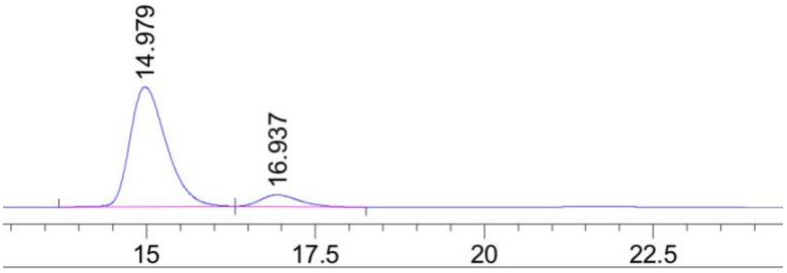

Peak #	RetTime [min]	Type	Width [min]	Area [mAU*s]	Height [mAU]	Area %
1	14.979	BB	0.5767	1970.73608	52.64608	90.6426
2	16.937	BB	0.6013	203.44690	5.12282	9.3574

9B

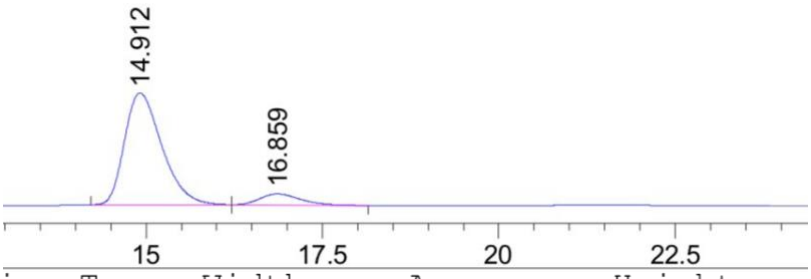

Peak #	RetTime [min]	Type	Width [min]	Area [mAU*s]	Height [mAU]	Area %
1	14.912	BB	0.5685	1980.76880	53.92514	90.4326
2	16.859	BB	0.5959	209.55679	5.31552	9.5674

12A

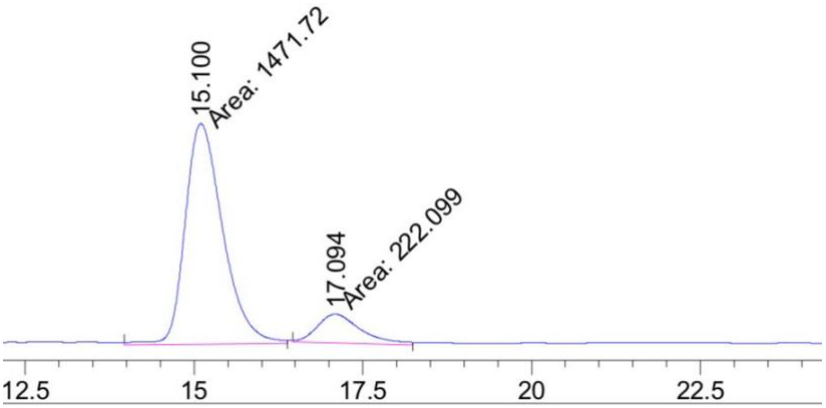

Peak #	RetTime [min]	Type	Width [min]	Area [mAU*s]	Height [mAU]	Area %
1	15.100	MM	0.6488	1471.71680	37.80396	86.8877
2	17.094	MM	0.7506	222.09866	4.93133	13.1123

12B

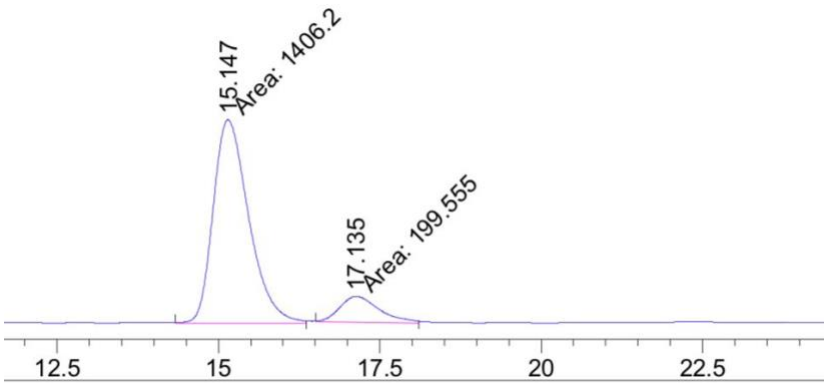

Peak #	RetTime [min]	Type	Width [min]	Area [mAU*s]	Height [mAU]	Area %
1	15.147	MM	0.6403	1406.20227	36.60200	87.5725
2	17.135	MM	0.7135	199.55495	4.66155	12.4275

15A

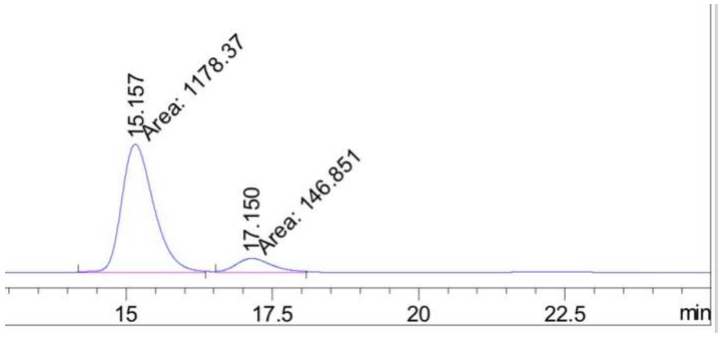

Peak #	RetTime [min]	Type	Width [min]	Area [mAU*s]	Height [mAU]	Area %
1	15.157	MM	0.6376	1178.36511	30.80033	88.9187
2	17.150	MM	0.7211	146.85135	3.39394	11.0813

15B

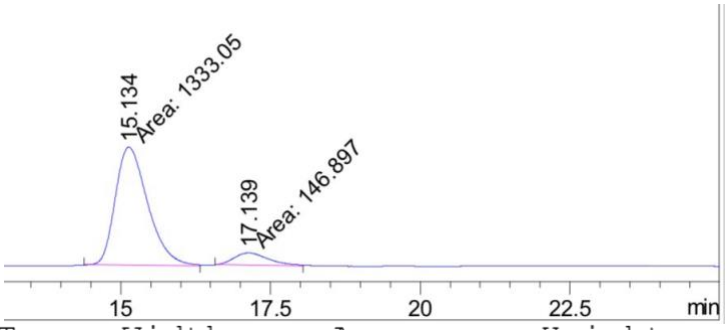

Peak #	RetTime [min]	Type	Width [min]	Area [mAU*s]	Height [mAU]	Area %
1	15.134	MM	0.6288	1333.05005	35.33110	90.0741
2	17.139	MM	0.6689	146.89740	3.66000	9.9259

16A

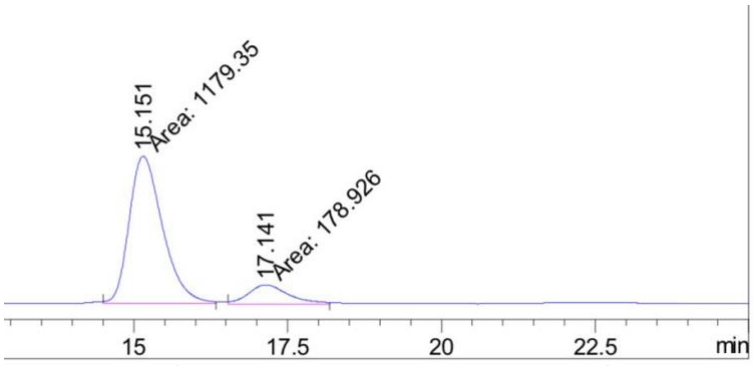

Peak #	RetTime [min]	Type	Width [min]	Area [mAU*s]	Height [mAU]	Area %
1	15.151	MM	0.6301	1179.34729	31.19496	86.8270
2	17.141	MM	0.7432	178.92599	4.01258	13.1730

16B

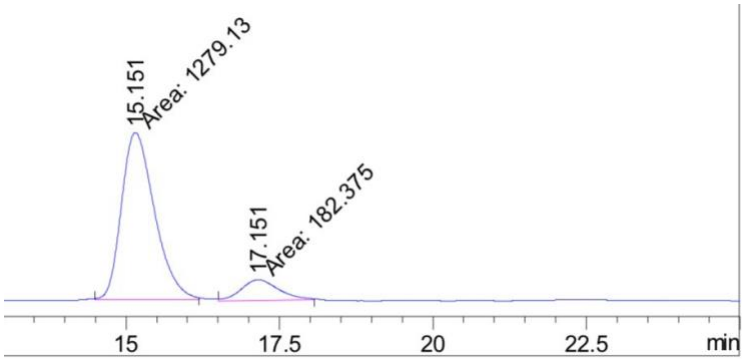

Peak #	RetTime [min]	Type	Width [min]	Area [mAU*s]	Height [mAU]	Area %
1	15.151	MM	0.6264	1279.13416	34.03387	87.5215
2	17.151	MM	0.7151	182.37489	4.25075	12.4785

17A

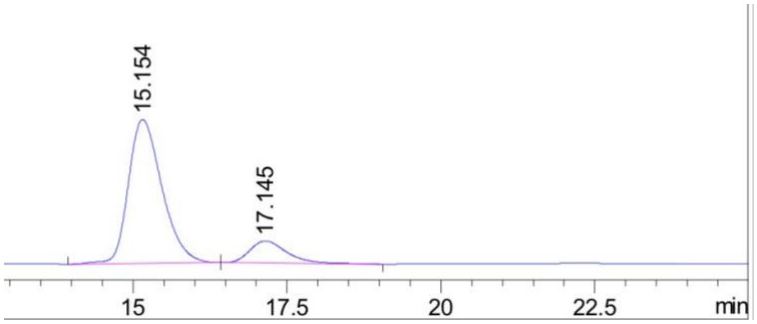

Peak #	RetTime [min]	Type	Width [min]	Area [mAU*s]	Height [mAU]	Area %
1	15.154	BB	0.5853	1319.75598	34.73464	85.4434
2	17.145	BB	0.6303	224.84029	5.32803	14.5566

17B

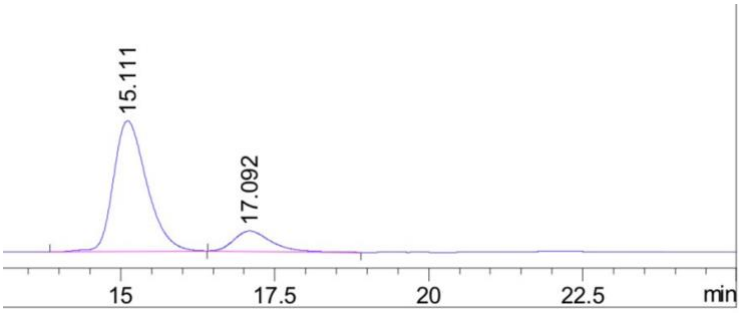

Peak #	RetTime [min]	Type	Width [min]	Area [mAU*s]	Height [mAU]	Area %
1	15.111	BB	0.5800	1197.58801	31.89729	85.1755
2	17.092	BB	0.6346	208.43571	4.95683	14.8245

18A

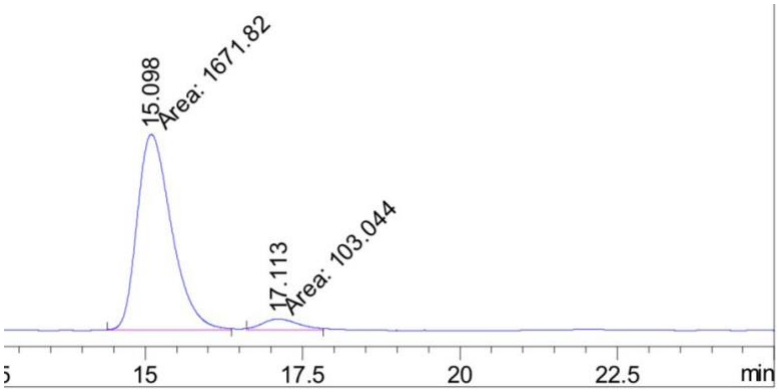

Peak #	RetTime [min]	Type	Width [min]	Area [mAU*s]	Height [mAU]	Area %
1	15.098	MM	0.6346	1671.81860	43.90770	94.1942
2	17.113	MM	0.6854	103.04414	2.50573	5.8058

18B

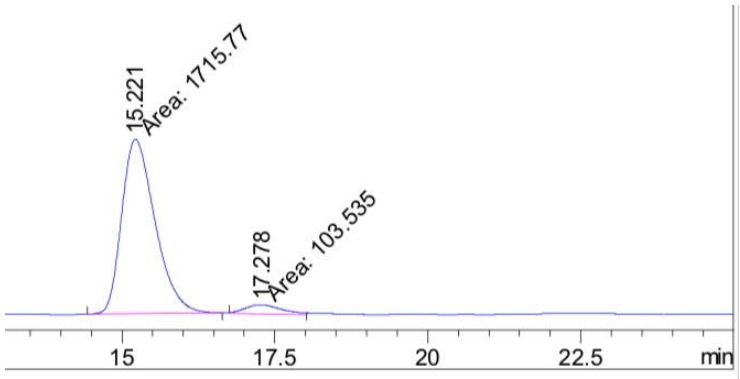

Peak #	RetTime [min]	Type	Width [min]	Area [mAU*s]	Height [mAU]	Area %
1	15.221	FM	0.6391	1715.76880	44.74188	94.3091
2	17.278	MM	0.7142	103.53519	2.41599	5.6909

19A

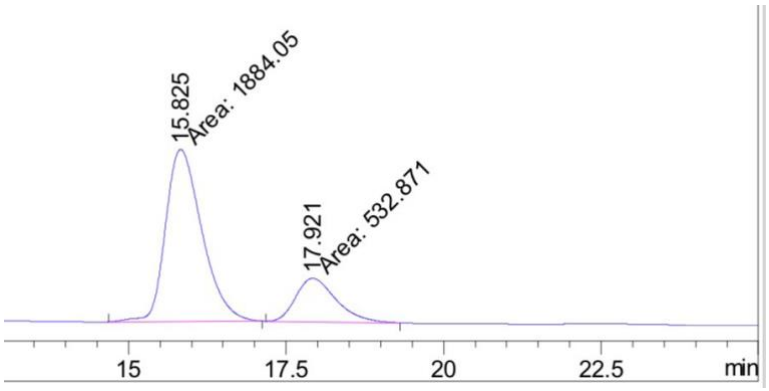

Peak #	RetTime [min]	Type	Width [min]	Area [mAU*s]	Height [mAU]	Area %
1	15.825	MM	0.6711	1884.04663	46.79004	77.9525
2	17.921	MF	0.7497	532.87091	11.84621	22.0475

19B

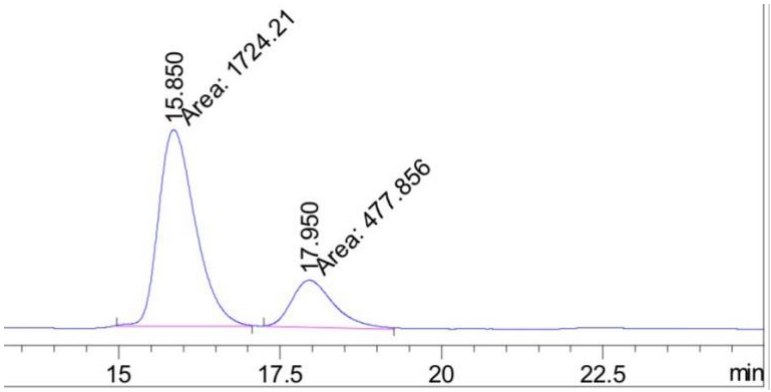

Peak #	RetTime [min]	Type	Width [min]	Area [mAU*s]	Height [mAU]	Area %
1	15.850	MM	0.6625	1724.20923	43.37505	78.2996
2	17.950	MM	0.7647	477.85596	10.41496	21.7004

21A

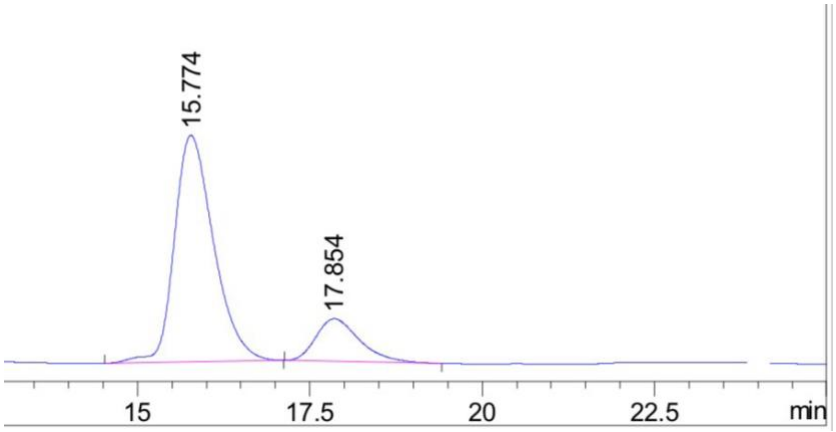

Peak #	RetTime [min]	Type	Width [min]	Area [mAU*s]	Height [mAU]	Area %
1	15.774	BB	0.6069	1584.61877	39.94205	82.6842
2	17.854	BB	0.6687	331.85162	7.52157	17.3158

21B

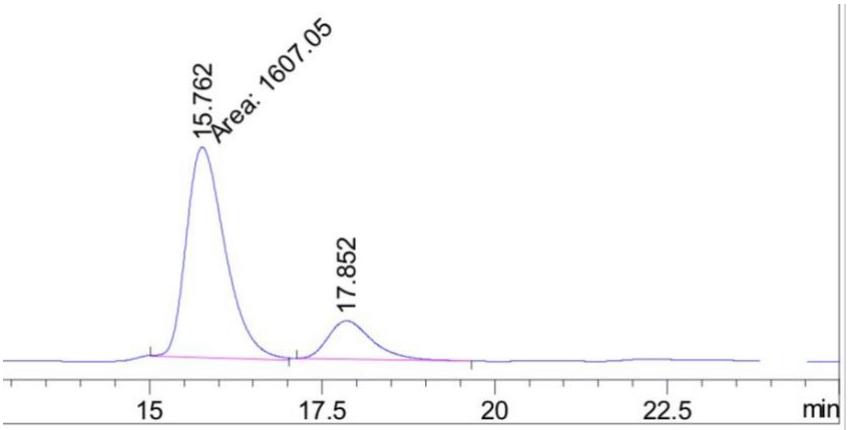

Peak #	RetTime [min]	Type	Width [min]	Area [mAU*s]	Height [mAU]	Area %
1	15.762	MM	0.6521	1607.04932	41.07294	82.8320
2	17.852	BB	0.6787	333.08249	7.49163	17.1680

Racemate - 20% IPA in hexanes, 45 min, AS-H, 1.0 mL/min HPLC

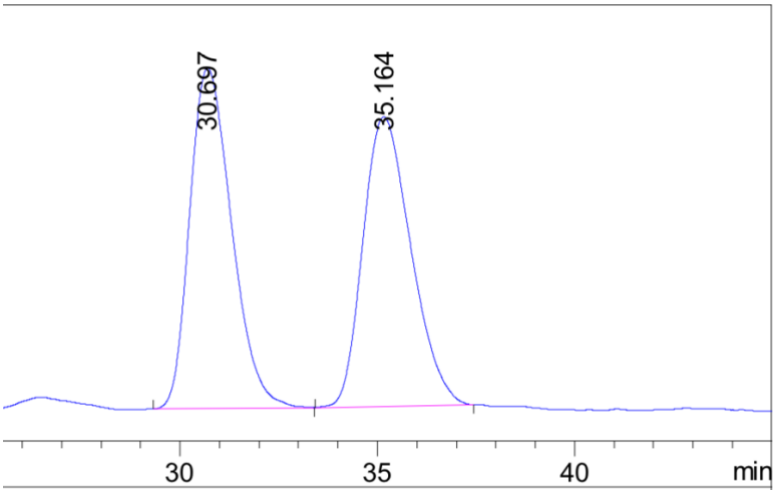

Peak #	RetTime [min]	Type	Width [min]	Area [mAU*s]	Height [mAU]	Area %
1	30.696	BB	1.1160	1021.40881	13.85574	50.3578
2	35.163	BB	1.2516	1006.89520	11.82272	49.6422

20A

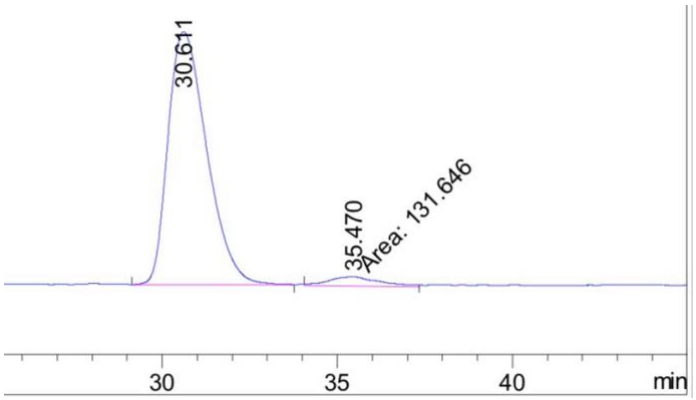

Peak #	RetTime [min]	Type	Width [min]	Area [mAU*s]	Height [mAU]	Area %
1	30.611	BB	1.2025	2727.80933	35.49994	95.3961
2	35.470	MM	1.7078	131.64574	1.28473	4.6039

20B

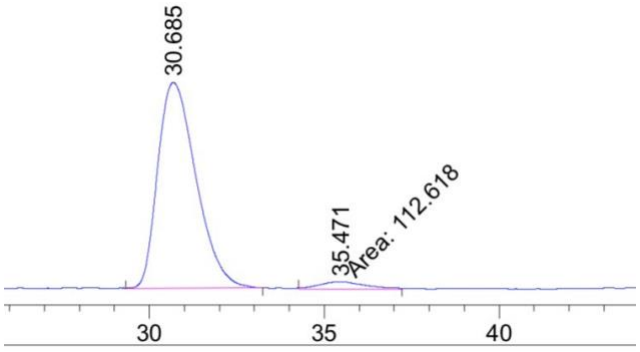

Peak #	RetTime [min]	Type	Width [min]	Area [mAU*s]	Height [mAU]	Area %
1	30.685	BB	1.1843	2365.33936	31.06634	95.4552
2	35.471	MM	1.6118	112.61768	1.16448	4.5448

22A

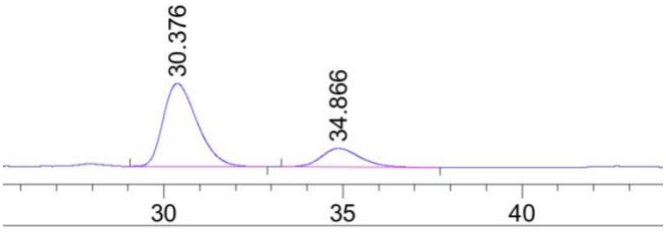

Peak #	RetTime [min]	Type	Width [min]	Area [mAU*s]	Height [mAU]	Area %
1	30.376	BB	1.0145	1532.36572	23.26165	79.2628
2	34.866	BB	1.0516	400.90558	5.22270	20.7372

22B

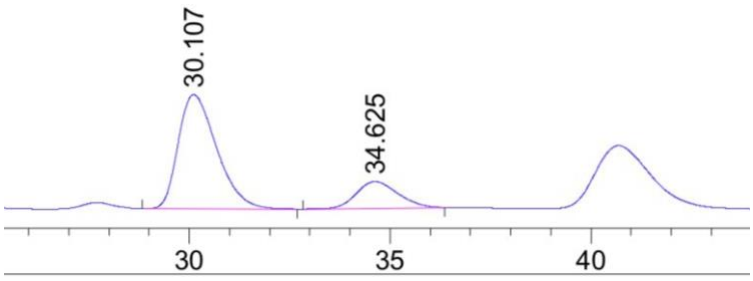

Peak #	RetTime [min]	Type	Width [min]	Area [mAU*s]	Height [mAU]	Area %
1	30.107	BB	1.0310	2178.57715	32.71055	79.9220
2	34.625	BB	1.0114	547.30341	7.62498	20.0780

23A

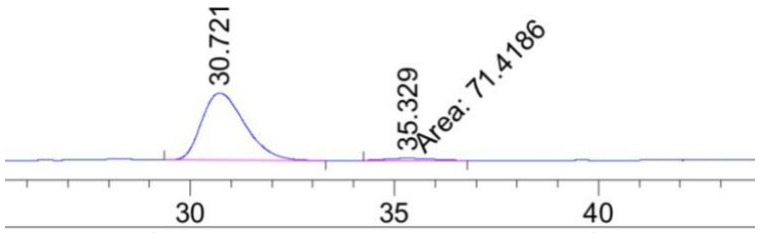

Peak #	RetTime [min]	Type	Width [min]	Area [mAU*s]	Height [mAU]	Area %
1	30.807	BB	1.1362	1392.25256	18.70895	95.4797
2	35.508	MM	1.6086	65.91336	6.82943e-1	4.5203

23B

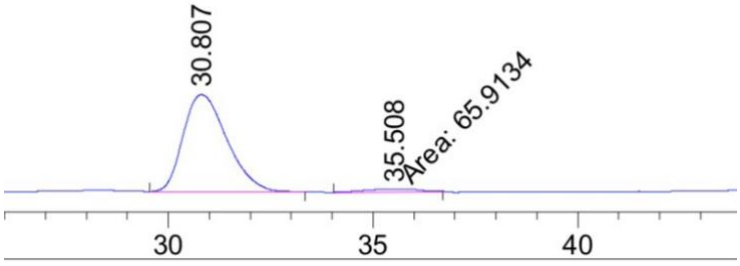

Peak #	RetTime [min]	Type	Width [min]	Area [mAU*s]	Height [mAU]	Area %
1	30.721	BB	1.1322	1408.08179	19.14140	95.1728
2	35.329	MM	1.5016	71.41861	7.92710e-1	4.8272

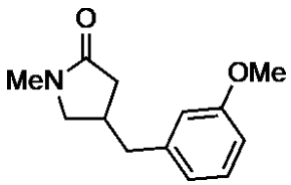

3b

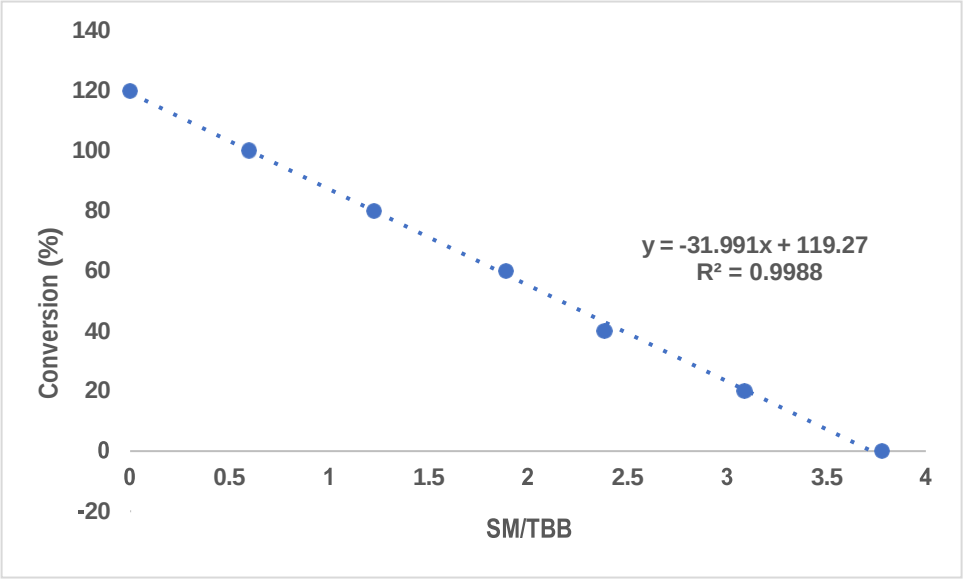

LCMS Method: MeCN-30-95, 8 min-1mL per min; 1 uL injection

	Variant	Conversion	ER
0-A	T36A	92.5265603	92.4:7.6
0-B		94.4798626	92.8:7.2
1-A	T36A W66A	50.4499035	
1-B		37.4445222	
2-A	T36A W66D	25.412827	
2-B		3.35189138	
3-A	T36A W66F	38.7839204	
3-B		28.9104325	
4-A	T36A W66L	34.7380804	76.3:23.7
4-B		40.1238724	76.8:23.2
5-A	T36A Y177A	27.4692836	
5-B		18.7152664	
6-A	T36A Y177D	40.2836619	58.2:41.8
6-B		33.226661	57.6:42.4
7-A	T36A Y177F	52.4927052	79.2:20.8
7-B		37.7309861	82.3:17.7
8-A	T36A Y177L	32.7285656	
8-B		26.9155291	

9-A	T36A Y177W	85.7108705	88.3:11.7
9-B		77.7545965	88.7:11.3
12-A	T36A Q232F	90.4976789	90.4:9.6
12-B		89.1712865	90.3:9.7
15-A	T36A F269A	64.4068258	85.4:14.6
15-B		58.5062757	85.0:15.0
16-A	T36A F269D	61.0553007	80.5:19.5
16-B		53.6434073	80.3:19.7
17-A	T36A F269L	86.4266058	87.7:12.3
17-B		66.1199896	87.2:12.8
18-A	T36A F269W	98.0066982	95.2:4.8
18-B		82.6309317	94.7:5.3
19-A	T36A Y343A	81.2806895	85.4:14.6
19-B		66.0772875	85.5:14.5
20-A	T36A Y343F	89.1977597	97.2:2.8
20-B		89.533922	96.7:3.3
21-A	T36A Y343D	84.1271038	88.4:11.6
21-B		70.0774117	88.3:11.7
22-A	T36A Y343L	88.0385051	89.6:10.4
22-B		85.5485112	89.7:10.3
23-A	T36A Y343W	62.8041243	94.1:5.9
23-B		59.7425481	94.4:5.6

Racemate: 40% IPA in hexanes, 30 min, AS-H, 1.0 mL/min HPLC.

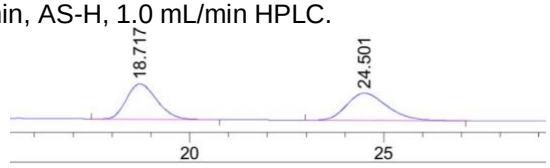

Peak #	RetTime [min]	Type	Width [min]	Area [mAU*s]	Height [mAU]	Area %
1	18.717	BB	0.8507	920.69238	16.92402	49.4418
2	24.501	BB	1.0656	941.48169	13.02067	50.5582

0A

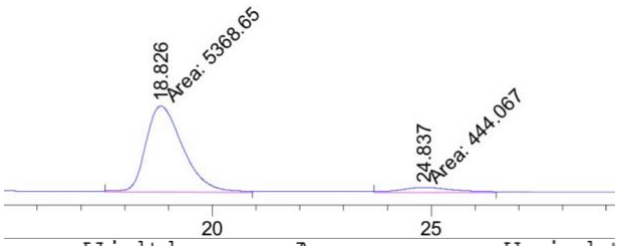

Peak #	RetTime [min]	Type	Width [min]	Area [mAU*s]	Height [mAU]	Area %
1	18.826	MM	0.9825	5368.64893	91.07092	92.3604
2	24.837	MM	1.4107	444.06702	5.24640	7.6396

0B

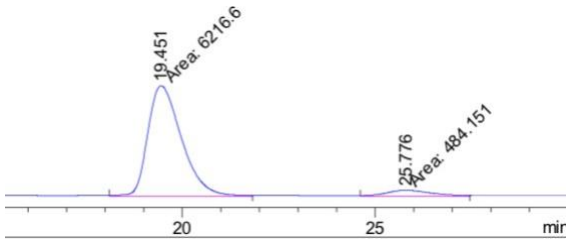

Peak #	RetTime [min]	Type	Width [min]	Area [mAU*s]	Height [mAU]	Area %
1	19.451	MM	1.0204	6216.59717	101.53646	92.7747
2	25.776	MM	1.4567	484.15134	5.53918	7.2253

4A

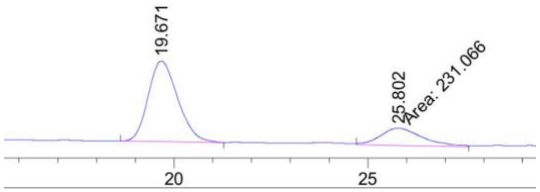

Peak #	RetTime [min]	Type	Width [min]	Area [mAU*s]	Height [mAU]	Area %
1	19.671	BB	0.8199	743.21851	13.98645	76.2835
2	25.802	MM	1.2654	231.06573	3.04328	23.7165

4B

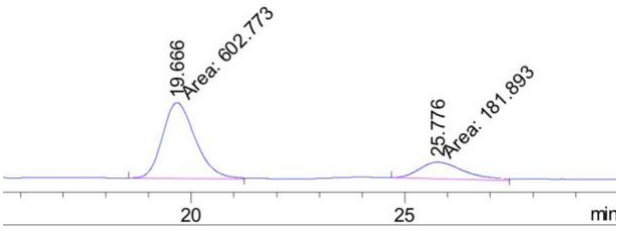

Peak #	RetTime [min]	Type	Width [min]	Area [mAU*s]	Height [mAU]	Area %
1	19.666	MF	0.8881	602.77313	11.31251	76.8190
2	25.776	MM	1.2111	181.89325	2.50306	23.1810

6A

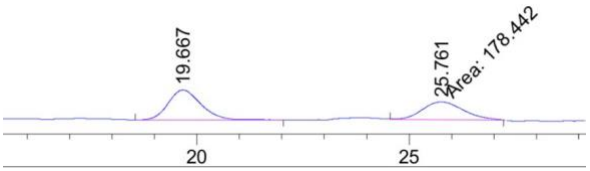

Peak #	RetTime [min]	Type	Width [min]	Area [mAU*s]	Height [mAU]	Area %
1	4.499	BB	0.1174	36.87138	4.81392	51.6868
2	5.374	BB	0.1545	34.46476	3.39179	48.3132

6B

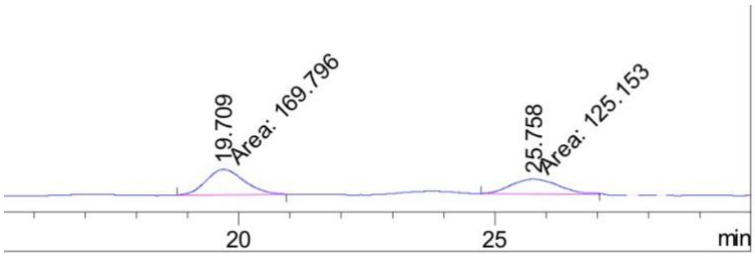

Peak #	RetTime [min]	Type	Width [min]	Area [mAU*s]	Height [mAU]	Area %
1	19.709	MM	0.8793	169.79616	3.21842	57.5679
2	25.758	MM	1.1060	125.15338	1.88596	42.4321

7A

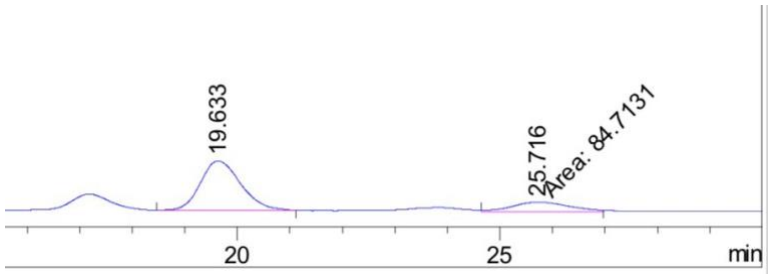

Peak #	RetTime [min]	Type	Width [min]	Area [mAU*s]	Height [mAU]	Area %
1	19.633	BB	0.8161	323.17661	6.08017	79.2314
2	25.716	MM	1.2414	84.71307	1.13736	20.7686

7B

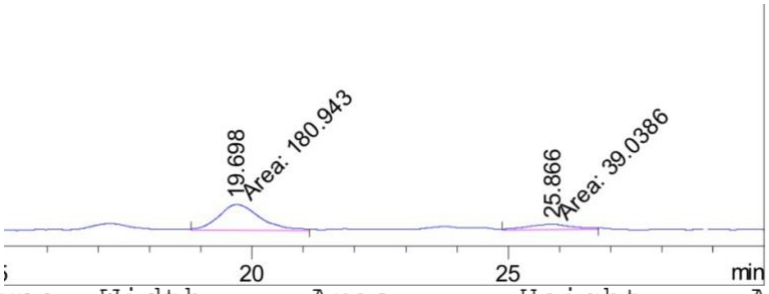

Peak #	RetTime [min]	Type	Width [min]	Area [mAU*s]	Height [mAU]	Area %
1	19.698	MM	0.9289	180.94321	3.24647	82.2537
2	25.866	MM	0.9834	39.03864	6.61615e-1	17.7463

9A

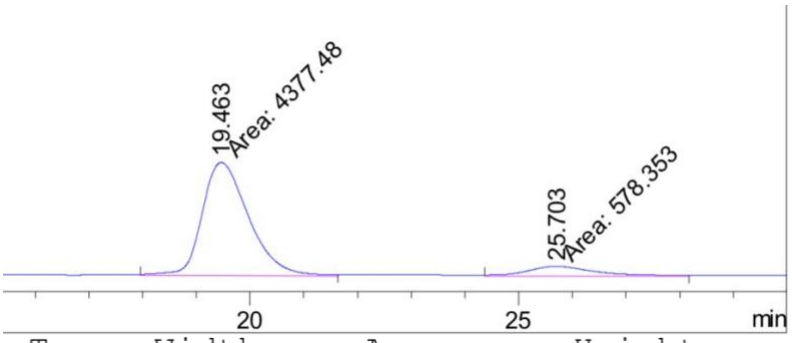

Peak #	RetTime [min]	Type	Width [min]	Area [mAU*s]	Height [mAU]	Area %
1	19.463	MM	1.0063	4377.48438	72.50117	88.3299
2	25.703	MM	1.5375	578.35315	6.26956	11.6701

9B

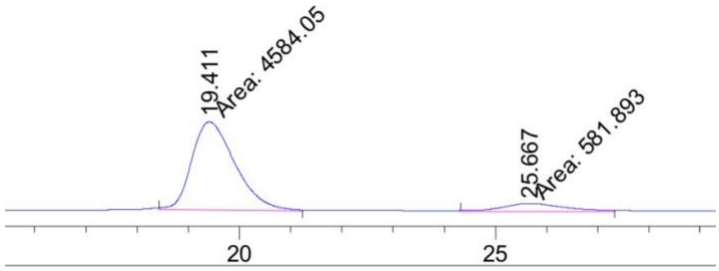

Peak #	RetTime [min]	Type	Width [min]	Area [mAU*s]	Height [mAU]	Area %
1	19.411	FM	0.9833	4584.04785	77.69775	88.7360
2	25.667	MM	1.4171	581.89252	6.84389	11.2640

12A

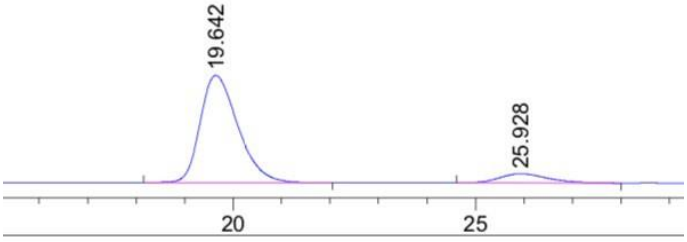

Peak #	RetTime [min]	Type	Width [min]	Area [mAU*s]	Height [mAU]	Area %
1	19.642	BB	0.8408	3555.88843	65.55466	90.3532
2	25.928	BB	0.9813	379.65359	5.59774	9.6468

12B

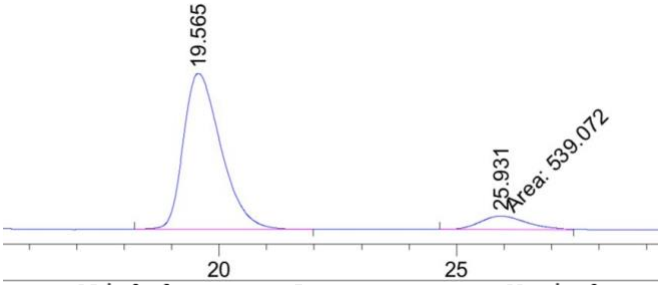

Peak #	RetTime [min]	Type	Width [min]	Area [mAU*s]	Height [mAU]	Area %
1	19.565	BB	0.8504	5018.67432	91.43363	90.3005
2	25.931	MF	1.1344	539.07227	7.91987	9.6995

15A

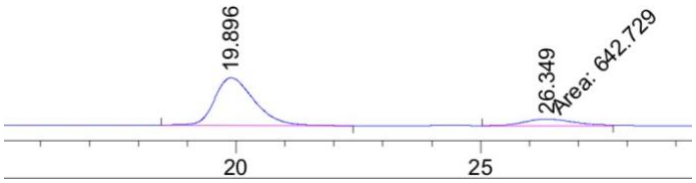

Peak #	RetTime [min]	Type	Width [min]	Area [mAU*s]	Height [mAU]	Area %
1	19.896	BB	0.8589	3756.08887	66.91380	85.3886
2	26.349	MF	1.1529	642.72870	9.29185	14.6114

15B

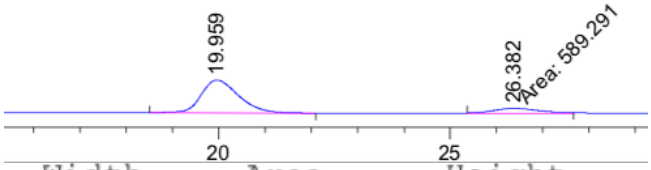

Peak #	RetTime [min]	Type	Width [min]	Area [mAU*s]	Height [mAU]	Area %
1	19.959	BB	0.8595	3330.19751	59.26749	84.9651
2	26.382	FM	1.1377	589.29138	8.63247	15.0349

16A

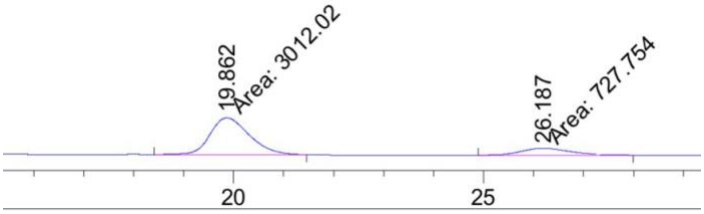

Peak #	RetTime [min]	Type	Width [min]	Area [mAU*s]	Height [mAU]	Area %
1	19.862	MF	0.9187	3012.01807	54.64400	80.5401
2	26.187	MM	1.1771	727.75439	10.30455	19.4599

17A

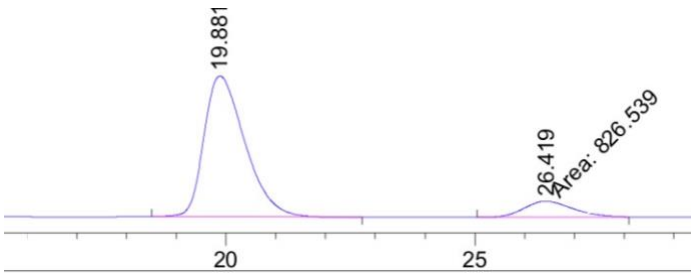

Peak #	RetTime [min]	Type	Width [min]	Area [mAU*s]	Height [mAU]	Area %
1	19.881	BB	0.8845	5917.35107	103.26502	87.7439
2	26.419	MF	1.1644	826.53925	11.83037	12.2561

17B

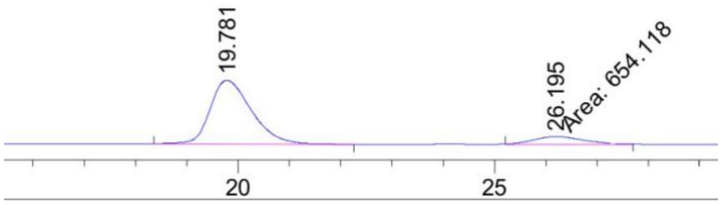

Peak #	RetTime [min]	Type	Width [min]	Area [mAU*s]	Height [mAU]	Area %
1	19.781	BB	0.8538	4436.39648	79.64844	87.1503
2	26.195	FM	1.1405	654.11780	9.55855	12.8497

18A

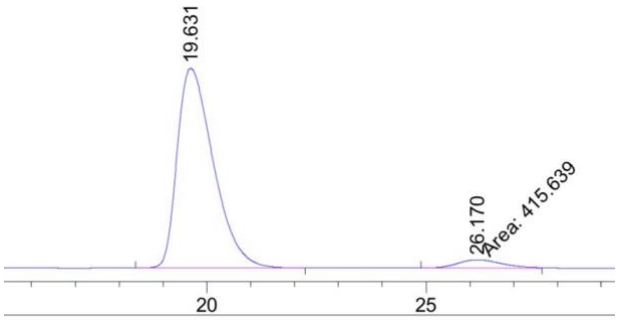

Peak #	RetTime [min]	Type	Width [min]	Area [mAU*s]	Height [mAU]	Area %
1	19.631	BB	0.8891	8268.94727	144.17519	95.2141
2	26.170	MF	1.1547	415.63895	5.99943	4.7859

18B

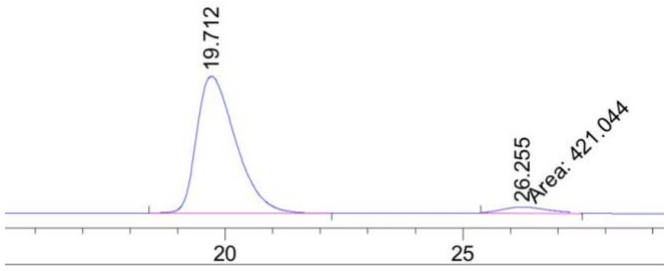

Peak #	RetTime [min]	Type	Width [min]	Area [mAU*s]	Height [mAU]	Area %
1	19.712	BB	0.8897	7571.31934	132.30164	94.7319
2	26.255	MF	1.1485	421.04358	6.11013	5.2681

19A

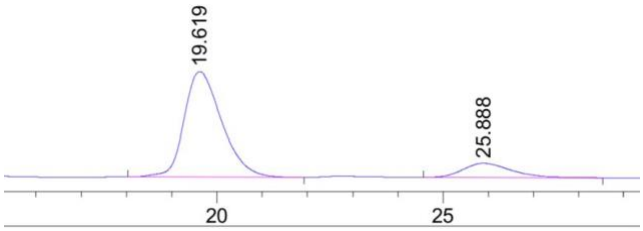

Peak #	RetTime [min]	Type	Width [min]	Area [mAU*s]	Height [mAU]	Area %
1	19.619	BB	0.8884	4455.91797	76.85581	85.3837
2	25.888	BB	1.0850	762.78143	10.36024	14.6163

19B

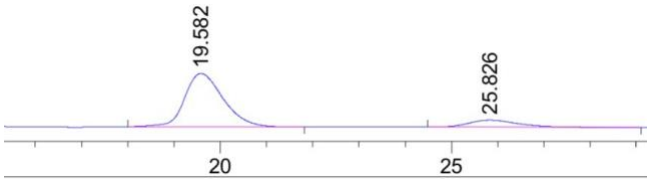

Peak #	RetTime [min]	Type	Width [min]	Area [mAU*s]	Height [mAU]	Area %
1	19.582	BB	0.8913	4153.05322	71.54024	85.7091
2	25.826	BB	1.1067	692.46613	9.40792	14.2909

21A

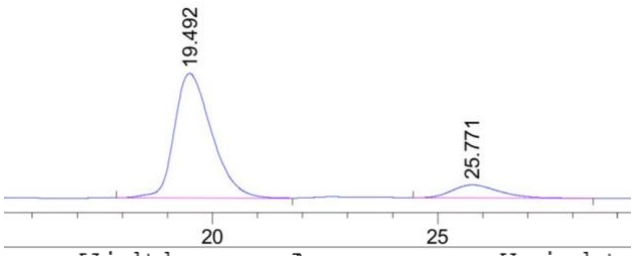

Peak #	RetTime [min]	Type	Width [min]	Area [mAU*s]	Height [mAU]	Area %
1	19.492	BB	0.8896	4641.53174	80.62835	88.3826
2	25.771	BB	1.0853	610.10443	8.44041	11.6174

21B

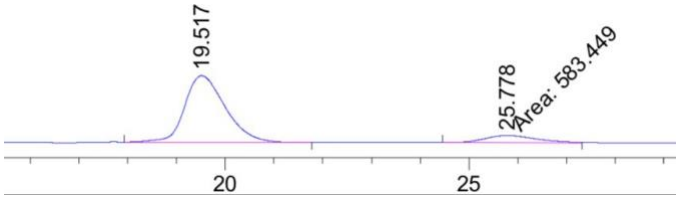

Peak #	RetTime [min]	Type	Width [min]	Area [mAU*s]	Height [mAU]	Area %
1	19.517	BB	0.8856	4395.04980	76.11992	88.2806
2	25.778	MF	1.2037	583.44879	8.07841	11.7194

22A

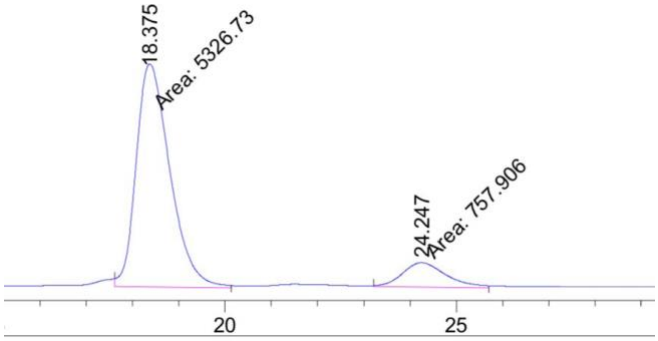

Peak #	RetTime [min]	Type	Width [min]	Area [mAU*s]	Height [mAU]	Area %
1	18.375	FM	0.8471	5326.72656	104.79765	87.5439
2	24.247	MM	1.1038	757.90576	11.44392	12.4561

22B

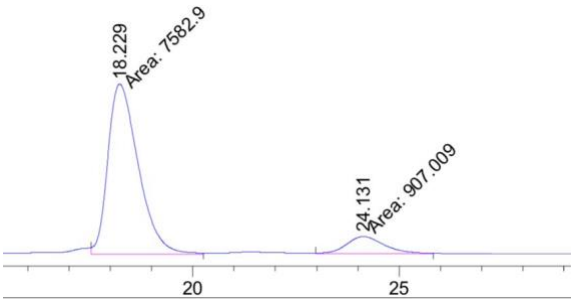

Peak #	RetTime [min]	Type	Width [min]	Area [mAU*s]	Height [mAU]	Area %
1	18.229	FM	0.8554	7582.89893	147.74095	89.3166
2	24.131	MM	1.0354	907.00922	14.59989	10.6834

Racemate: 20% IPA in hexanes, 60 min, AS-H, 1.0 mL/min. HPLC

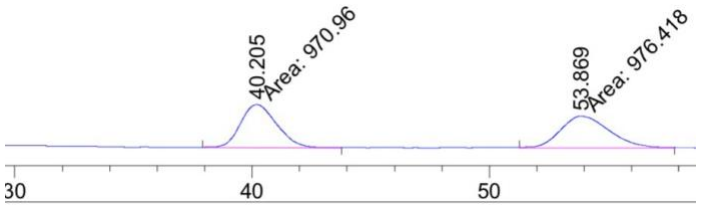

Peak #	RetTime [min]	Type	Width [min]	Area [mAU*s]	Height [mAU]	Area %
1	40.205	MM	1.8033	970.96027	8.97388	49.8599
2	53.869	MM	2.4461	976.41797	6.65286	50.1401

20A

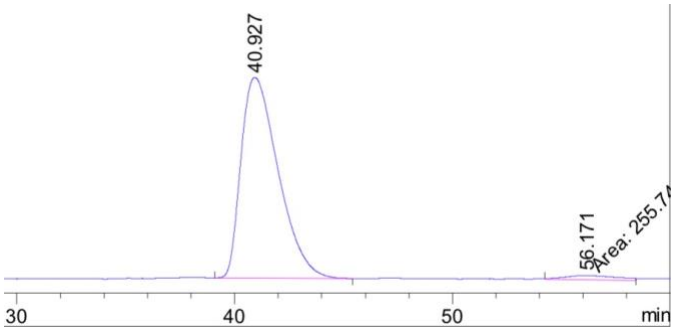

Peak #	RetTime [min]	Type	Width [min]	Area [mAU*s]	Height [mAU]	Area %
1	40.927	BB	1.8006	9031.57031	76.10278	97.2464
2	56.171	MM	2.7548	255.73964	1.54726	2.7536

20B

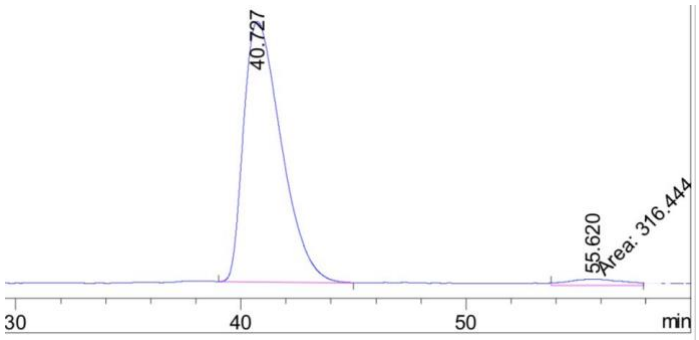

Peak #	RetTime [min]	Type	Width [min]	Area [mAU*s]	Height [mAU]	Area %
1	40.727	BB	1.7770	9383.75488	80.67696	96.7378
2	55.620	MM	2.8203	316.44418	1.87006	3.2622

23A

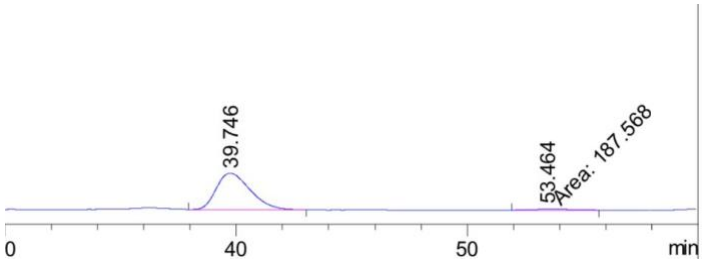

Peak #	RetTime [min]	Type	Width [min]	Area [mAU*s]	Height [mAU]	Area %
1	39.746	BB	1.5266	2988.06396	29.27956	94.0935
2	53.464	MM	2.5653	187.56813	1.21861	5.9065

23B

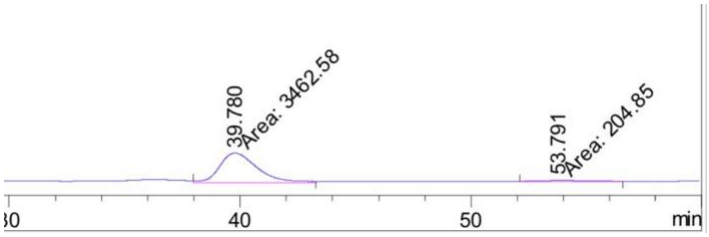

Peak #	RetTime [min]	Type	Width [min]	Area [mAU*s]	Height [mAU]	Area %
1	39.780	MM	1.9044	3462.57544	30.30389	94.4143
2	53.791	MM	2.8255	204.85025	1.20835	5.5857

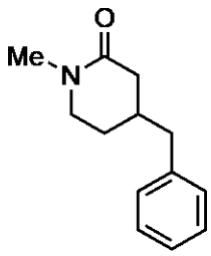

4b

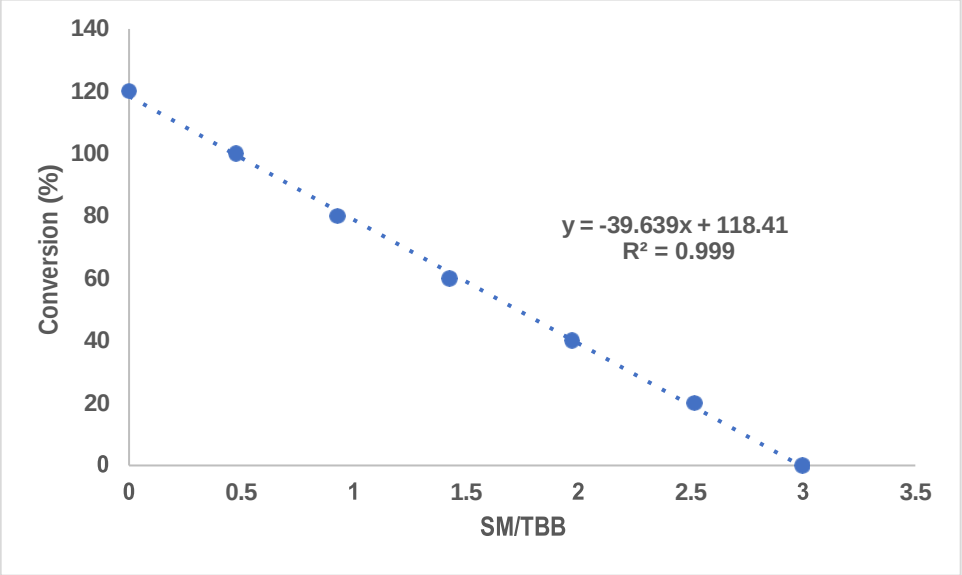

LCMS Method: MeCN-30-95, 8 min-1mL per min; 1 uL injection

	Variant	Conversion	ER
0-A	T36A	49.82500171	65.1:34.9
0-B		50.25766439	64.9:35.1
1-A	T36A W66A	92.92308287	63.2:36.8
1-B		89.90905131	62.9:37.1
2-A	T36A W66D	50.16324462	65.0:35.0
2-B		54.15055651	64.9:35.1
3-A	T36A W66F	70.36678152	69.6:30.4
3-B		71.973588	69.6:30.4
4-A	T36A W66L	93.70150831	64.5:35.5
4-B		92.86211473	65.2:34.8
5-A	T36A Y177A	27.0080463	nd
5-B		24.31667996	nd
6-A	T36A Y177D	27.69627192	nd
6-B		26.28446131	nd
7-A	T36A Y177F	43.97059489	57.1:42.9
7-B		51.23604947	57.4:42.6
8-A	T36A Y177L	25.6628206	nd
8-B		22.87048779	nd

9-A	T36A Y177W	37.16734647	nd
9-B		26.63588942	nd
12-A	T36A Q232F	51.84134103	73.7:26.3
12-B		51.10138363	73.9:26.1
15-A	T36A F269A	8.675438835	nd
15-B		8.654985896	nd
16-A	T36A F269D	26.67322327	nd
16-B		30.18883227	nd
17-A	T36A F269L	29.04498678	nd
17-B		30.03574781	nd
18-A	T36A F269W	29.3085012	75.3:24.7
18-B		35.54907368	74.7:25.3
19-A	T36A Y343A	87.88191327	71.8:28.2
19-B		90.10079597	72.1:27.9
20-A	T36A Y343F	26.65110853	nd
20-B		29.95355632	nd
21-A	T36A Y343D	81.4879875	65.9:34.1
21-B		78.91077004	65.4:34.6
22-A	T36A Y343L	51.19749905	nd
22-B		54.0722848	nd
23-A	T36A Y343W	31.111681	nd
23-B		37.07593234	nd

Racemate: IB-2IPA-80M-1mL. HPLC

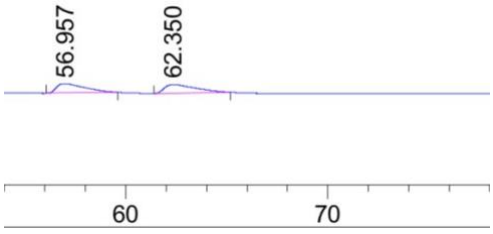

Peak #	RetTime [min]	Type	Width [min]	Area [mAU*s]	Area %
1	56.957	BB	1.3176	2343.77368	50.0188
2	62.350	BB	1.3500	2342.01587	49.9812

0A

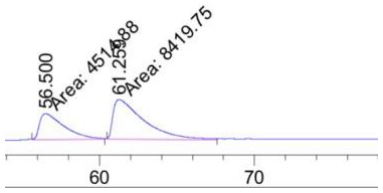

Peak #	RetTime [min]	Type	Width [min]	Area [mAU*s]	Area %
1	56.500	MM	1.8731	4514.87842	34.9054
2	61.259	MM	2.3093	8419.74512	65.0946

0B

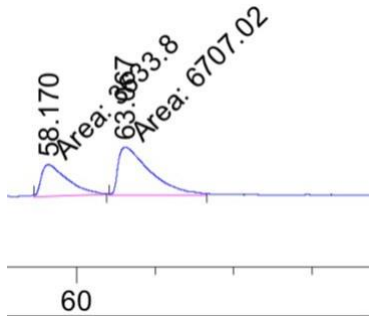

Peak #	RetTime [min]	Type	Width [min]	Area [mAU*s]	Area %
1	58.170	MM	1.9760	3633.79810	35.1403
2	63.067	MM	2.4116	6707.02197	64.8597

1A

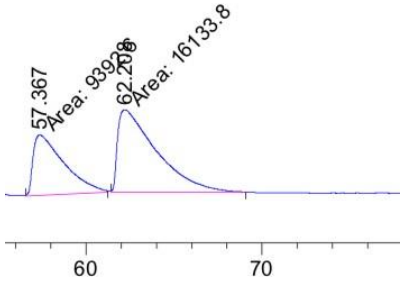

Peak #	RetTime [min]	Type	Width [min]	Area [mAU*s]	Area %
1	57.367	MM	2.0316	9392.59961	36.7957
2	62.208	MM	2.5567	1.61338e4	63.2043

1B

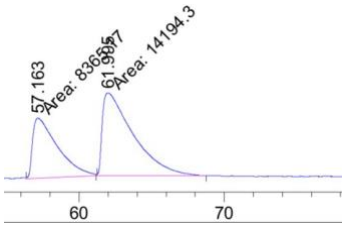

Peak #	RetTime [min]	Type	Width [min]	Area [mAU*s]	Area %
1	57.163	MM	1.9845	8365.17383	37.0806
2	61.995	MM	2.4530	1.41943e4	62.9194

2A

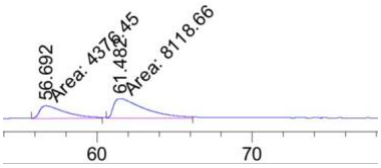

Peak #	RetTime [min]	Type	Width [min]	Area [mAU*s]	Area %
1	56.692	MM	1.8891	4376.45215	35.0253
2	61.482	MM	2.2693	8118.66113	64.9747

2B

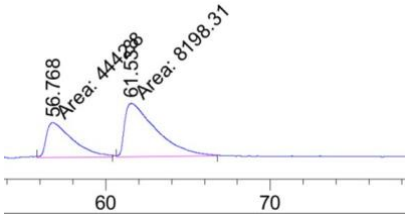

Peak #	RetTime [min]	Type	Width [min]	Area [mAU*s]	Area %
1	56.768	MM	1.8664	4442.80029	35.1456
2	61.538	MM	2.2371	8198.31250	64.8544

3A

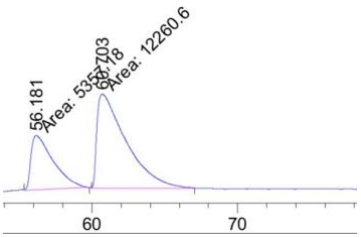

Peak #	RetTime [min]	Type	Width [min]	Area [mAU*s]	Area %
1	56.181	MM	1.7761	5357.17773	30.4078
2	60.703	MM	2.3381	1.22606e4	69.5922

3B

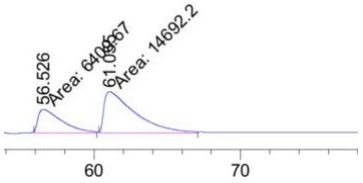

Peak #	RetTime [min]	Type	Width [min]	Area [mAU*s]	Area %
1	56.526	MM	1.8747	6409.67139	30.3749
2	61.055	MM	2.4334	1.46922e4	69.6251

4A

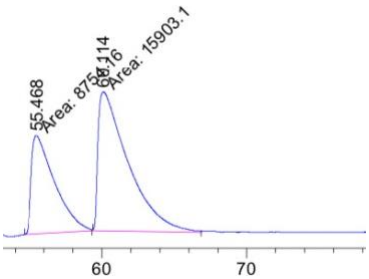

Peak #	RetTime [min]	Type	Width [min]	Area [mAU*s]	Area %
1	55.468	MM	1.8717	8754.16016	35.5034
2	60.114	MM	2.4127	1.59031e4	64.4966

4B

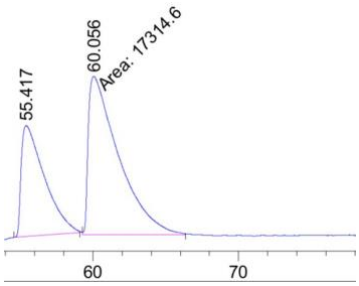

Peak #	RetTime [min]	Type	Width [min]	Area [mAU*s]	Area %
1	55.417	BB	1.4737	9249.59863	34.8198
2	60.056	MM	2.4184	1.73146e4	65.1802

7A

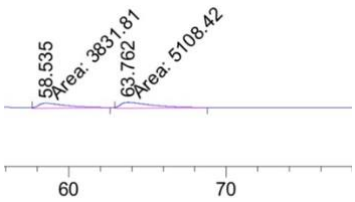

Peak #	RetTime [min]	Type	Width [min]	Area [mAU*s]	Area %
1	58.535	MM	2.0645	3831.81445	42.8603
2	63.762	MM	2.2872	5108.41699	57.1397

7B

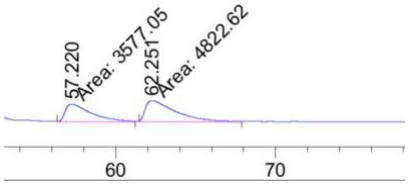

Peak #	RetTime [min]	Type	Width [min]	Area [mAU*s]	Area %
1	57.220	MM	1.9055	3577.05493	42.5857
2	62.251	MM	2.1749	4822.61523	57.4143

12A

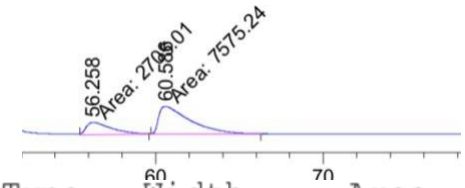

Peak #	RetTime [min]	Type	Width [min]	Area [mAU*s]	Area %
1	56.258	MM	1.7534	2705.01270	26.3127
2	60.586	MM	2.1989	7575.24463	73.6873

12B

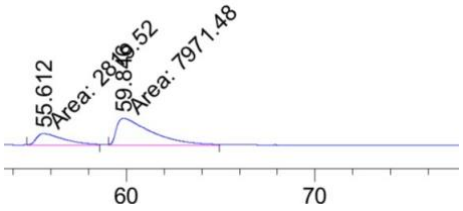

Peak #	RetTime [min]	Type	Width [min]	Area [mAU*s]	Area %
1	55.612	MM	1.7090	2819.51660	26.1284
2	59.846	MM	2.1381	7971.47559	73.8716

18A

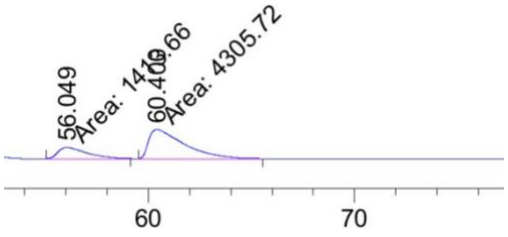

Peak #	RetTime [min]	Type	Width [min]	Area [mAU*s]	Area %
1	56.049	MM	1.7204	1413.66370	24.7171
2	60.400	MM	2.0568	4305.71729	75.2829

18B

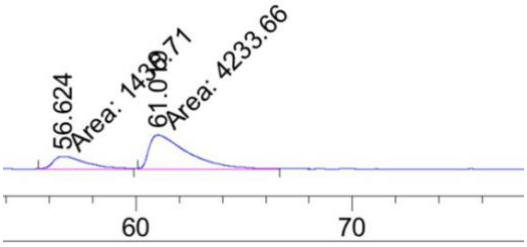

Peak #	RetTime [min]	Type	Width [min]	Area [mAU*s]	Area %
1	56.624	MM	1.8733	1436.71191	25.3372
2	61.019	MM	2.0813	4233.65820	74.6628

19A

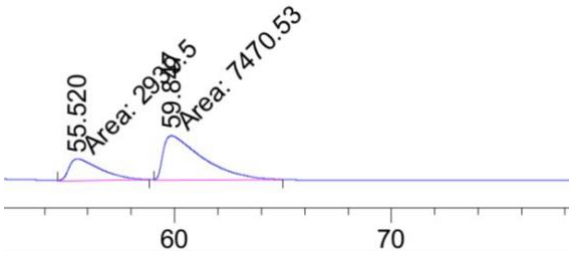

Peak #	RetTime [min]	Type	Width [min]	Area [mAU*s]	Area %
1	55.520	MM	1.6954	2939.49609	28.2372
2	59.847	MM	2.1218	7470.52588	71.7628

19B

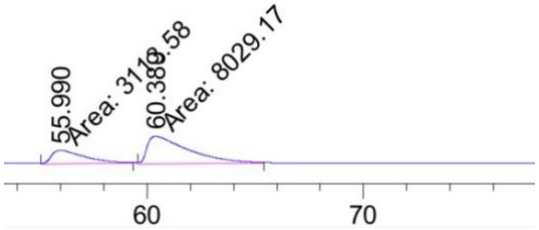

Peak #	RetTime [min]	Type	Width [min]	Area [mAU*s]	Area %
1	55.990	MM	1.7601	3113.57959	27.9427
2	60.389	MM	2.2221	8029.16602	72.0573

21A

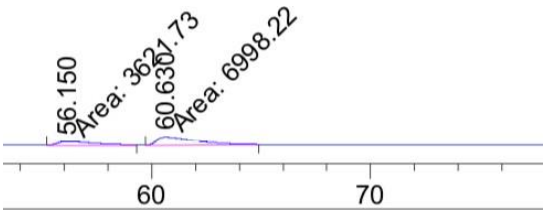

Peak #	RetTime [min]	Type	Width [min]	Area [mAU*s]	Area %
1	56.150	MM	2.2681	3621.73267	34.1031
2	60.630	MM	2.3012	6998.21875	65.8969

21B

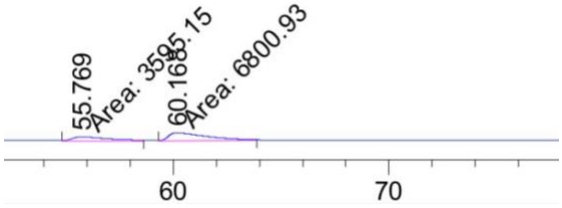

Peak #	RetTime [min]	Type	Width [min]	Area [mAU*s]	Area %
1	55.769	MM	2.1556	3595.15454	34.5818
2	60.168	MM	2.1866	6800.92725	65.4182

VALIDATION DATASET

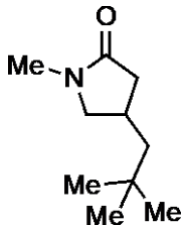

5b

Sample	Variant	Major	Minor
1	T36A-W66A	60.55	39.45
4	T36A-W66L	54.39	45.61
7	T36A-Y177F	67.99	32.01
12	T36A-Q232F	51.43	48.57
19	T36A-Y343A	64.55	35.45
20	T36A-Y343F	85.8	14.2
22	T36A-Y343W	68.9	31.1

Racemate : 20% IPA in hexanes, 45 min, AS-H, 1.0 mL/min. HPLC

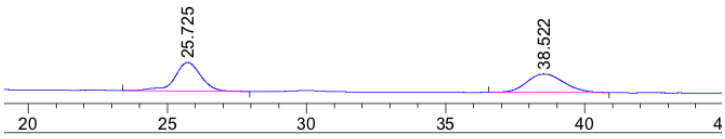

Peak #	RetTime [min]	Type	Width [min]	Area [mAU*s]	Height [mAU]	Area %
1	25.725	BB	0.9989	644.17432	9.90349	52.1086
2	38.522	BB	1.4326	592.04010	6.36860	47.8914

1-T36A-W66A

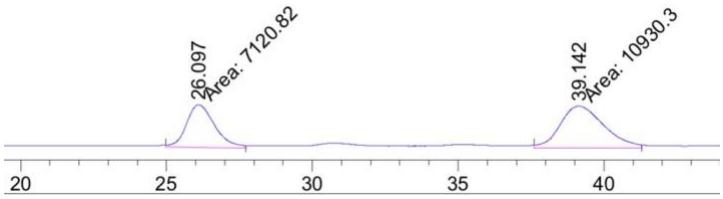

Peak #	RetTime [min]	Type	Width [min]	Area [mAU*s]	Height [mAU]	Area %
1	26.097	MM	1.1289	7120.81836	105.13045	39.4480
2	39.142	MM	1.7533	1.09303e4	103.90104	60.5520

4-T36A-W66L

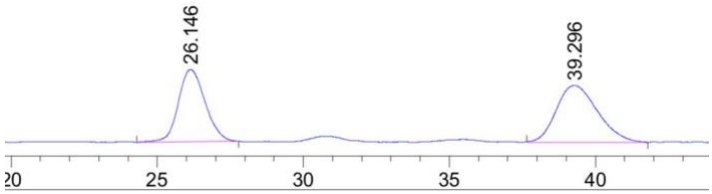

Peak #	RetTime [min]	Type	Width [min]	Area [mAU*s]	Height [mAU]	Area %
1	26.146	BB	0.8025	5743.94189	89.53410	45.6006
2	39.296	VB	1.1649	6852.26855	70.19315	54.3994

7-T36A-Y177F

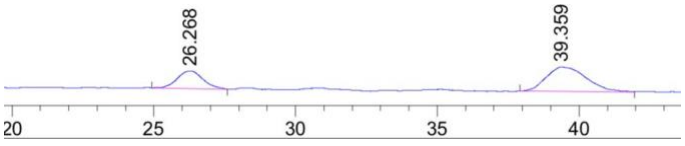

Peak #	RetTime [min]	Type	Width [min]	Area [mAU*s]	Height [mAU]	Area %
1	26.268	VB	0.7533	2647.34961	41.44339	32.0067
2	39.359	BV	1.1669	5623.88770	57.01008	67.9933

12-T36A-Q2323F

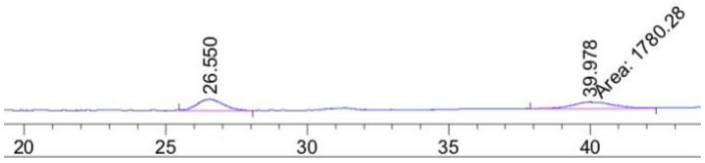

Peak #	RetTime [min]	Type	Width [min]	Area [mAU*s]	Height [mAU]	Area %
1	26.546	MM	1.1908	380.31668	5.32305	48.5684
2	40.046	MM	2.0992	402.73666	3.19752	51.4316

19-T36A-Y343A

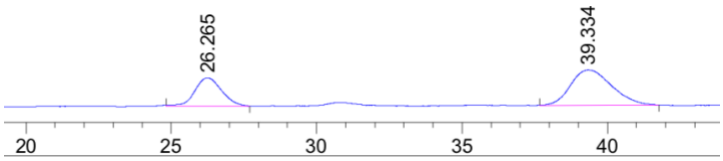

Peak #	RetTime [min]	Type	Width [min]	Area [mAU*s]	Height [mAU]	Area %
1	26.243	BB	1.0428	640.76624	9.42972	35.4417
2	39.345	BB	1.3306	1167.17932	11.87588	64.5583

20- T36A-Y343F

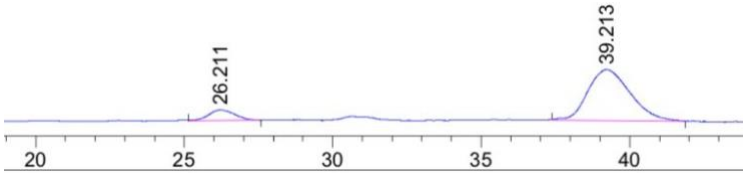

Peak #	RetTime [min]	Type	Width [min]	Area [mAU*s]	Height [mAU]	Area %
1	26.230	MM	1.2289	225.76825	3.06198	14.1544
2	39.212	BB	1.3858	1369.27124	13.94169	85.8456

22- T36A-Y343W

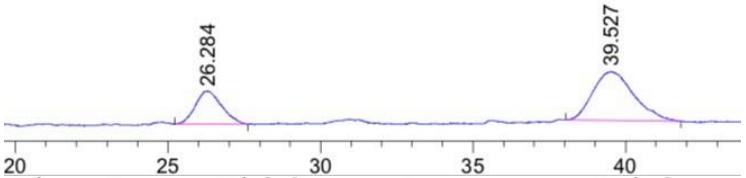

Peak #	RetTime [min]	Type	Width [min]	Area [mAU*s]	Height [mAU]	Area %
1	26.274	MM	1.1080	246.20857	3.70338	31.0758
2	39.512	MM	1.6506	546.07574	5.51393	68.9242

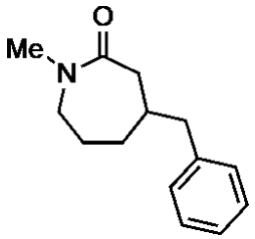

6b

Sample	Variant	Major	Minor
0	T36A-W66A	77.547	22.453
4	T36A-W66L	73.114	26.886
7	T36A-Y177F	77.285	22.715
12	T36A-Q232F	85.592	14.408
19	T36A-Y343A	79.125	20.875
20	T36A-Y343F	79.873	20.127
22	T36A-Y343W	83.241	16.759

Racemate: A5-5 (0.46 X 25 cm) 2.0 mL/min @ 20% MeOH (0.1% v/v DEA) / 80% CO2(100bar)(A5-5 is a ChiralTek phase, which is the CHIRALPAK AZ-H equivalent). SFC

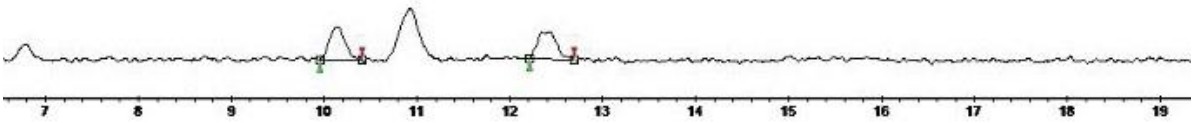

	time	area% (220 nm)
peak-1	10.15	49.52
peak-2	12.42	50.47
total		100.00

1-T36A-W66A

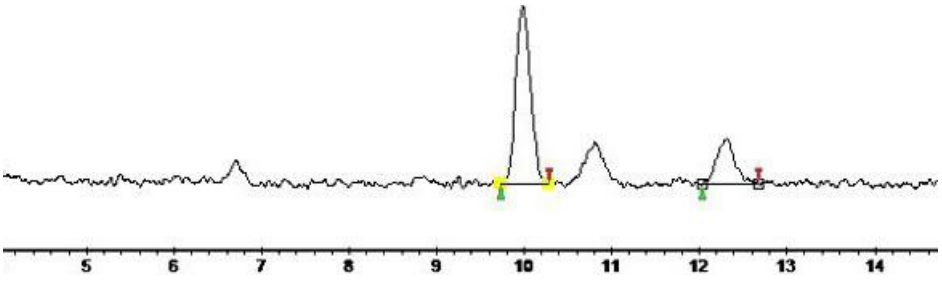

	time	area% (220 nm)
peak-1	9.93	77.547
peak-2	12.19	22.453
total		100.00

4-T36A-W66L

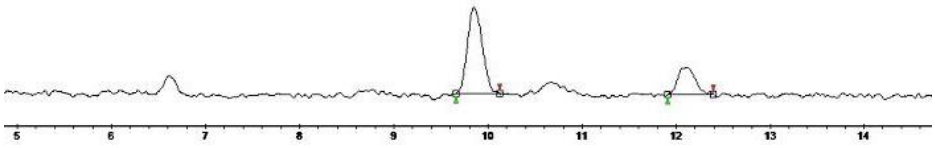

	time	area% (220 nm)
peak-1	9.85	73.114
peak-2	12.11	26.886
total		100.00

12-T36A-Q2323F

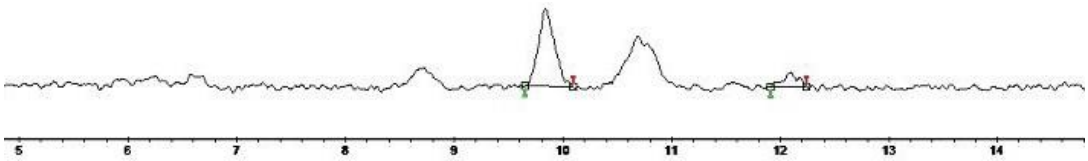

	time	area% (220 nm)
peak-1	9.84	85.592
peak-2	12.10	14.408
total		100.00

20- T36A-Y343F

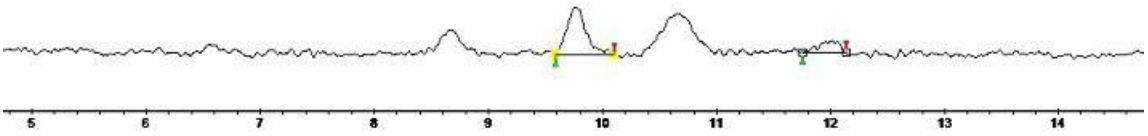

	time	area% (220 nm)
peak-1	9.76	79.873
peak-2	12.02	20.127
total		100.00

22- T36A-Y343W

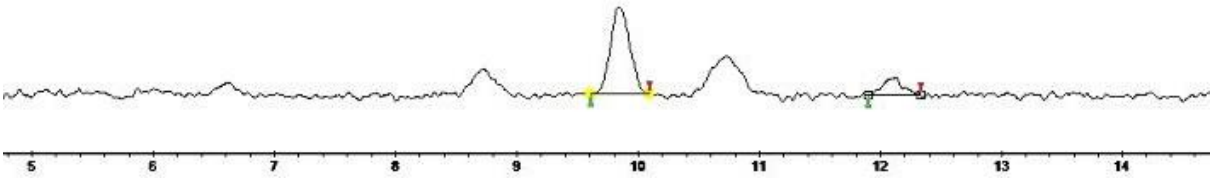

	time	area% (220 nm)
peak-1	9.83	83.241
peak-2	12.13	16.759
total		100.00

Racemate IC-5-IPA-1ML/MIN-180Min

#	Time	Type	Area	Height	Width	Area%	Symmetry
1	133.736	MM	3627.1	20.5	2.9559	52.696	1.145
2	151.499	MM	3256	17.4	3.1189	47.304	1.146

7-T36A-Y177F

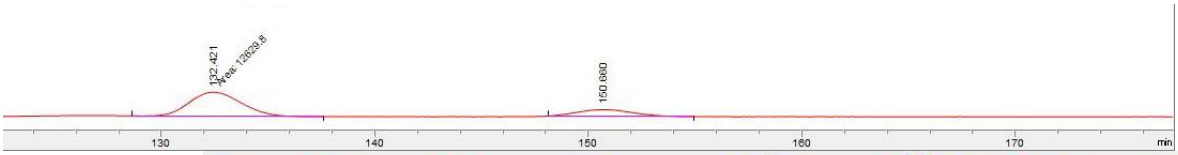

#	Time	Type	Area	Height	Width	Area%	Symmetry
1	132.421	MM	12629.8	71	2.9649	77.285	0.94
2	150.66	BV	3712	20	2.1679	22.715	0.92

19-T36A-Y343A

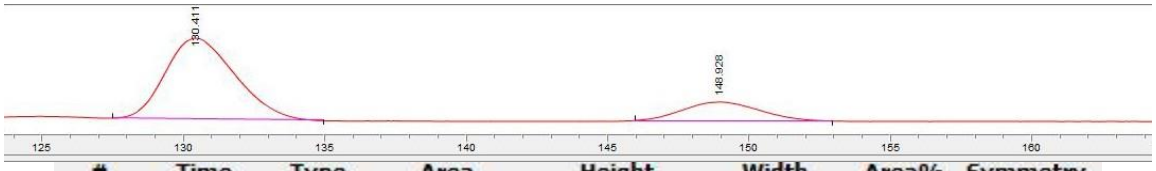

#	Time	Type	Area	Height	Width	Area%	Symmetry
1	130.411	VB	24730.4	143.9	2.0194	79.125	0.752
2	148.928	BV	6524.6	34.1	2.2407	20.875	0.908

Final external validation dataset: out-of-sample enzyme mutants

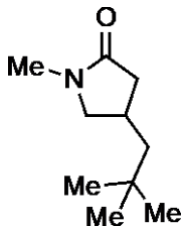

5b

Sample	Variant	e.r.
1	W66S	31:69
2	F269C	31:68
3	F269M	30:70
4	F269R	32:68
5	Y343C	32:68
5	Y343V	39:61
7	Y343M	22:78
8	F269Y	No product

Method – AS-20-IPA-45MIN

0-Rac

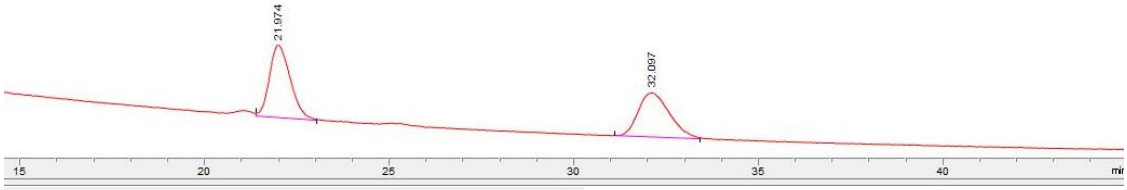

#	Time	Type	Area	Height	Width	Area%	Symmetry
1	21.974	VV	3252.3	83.1	0.5205	51.656	0.702
2	32.097	VV	3043.8	51.3	0.7066	48.344	0.79

1-W66S

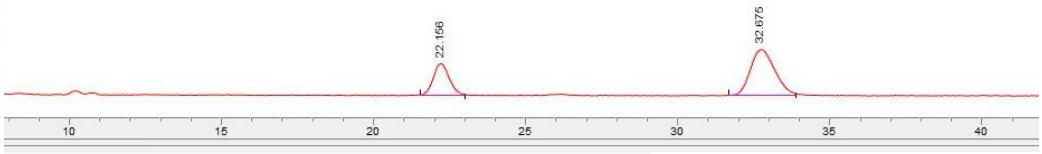

#	Time	Type	Area	Height	Width	Area%	Symmetry
1	22.156	VV	1531.1	40.8	0.4773	31.368	0.825
2	32.675	VV	3350.1	58.9	0.6817	68.632	0.723

2-F269C

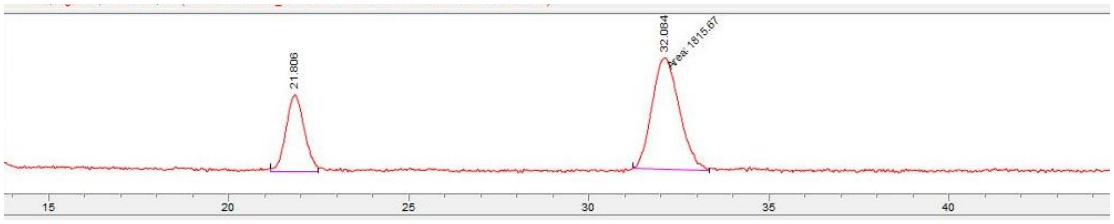

#	Time	Type	Area	Height	Width	Area%	Symmetry
1	21.806	VV	847.8	23.7	0.4253	31.831	0.917
2	32.084	MM	1815.7	34.3	0.8825	68.169	0.907

3-F269M

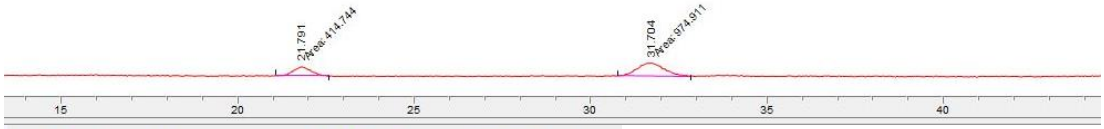

#	Time	Type	Area	Height	Width	Area%	Symmetry
1	21.791	MM	414.7	11.6	0.5947	29.845	0.847
2	31.704	MM	974.9	17.2	0.9443	70.155	1.003

4- F269R

#	Time	Type	Area	Height	Width	Area%	Symmetry
1	21.754	VV	540.2	14.2	0.4634	31.834	1.155
2	31.584	VV	1156.8	20.8	0.6622	68.166	0.94

5- Y343C

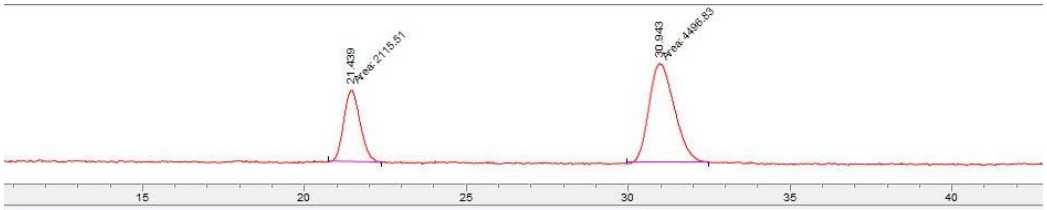

#	Time	Type	Area	Height	Width	Area%	Symmetry
1	21.439	MM	2115.5	59.5	0.5925	31.993	0.896
2	30.943	MM	4496.8	81.6	0.9187	68.007	0.689

6-Y343V

#	Time	Type	Area	Height	Width	Area%	Symmetry
1	21.368	VV	1820.2	50	0.4388	39.050	0.901
2	30.922	MM	2841	51.3	0.9227	60.950	0.755

7-Y343M

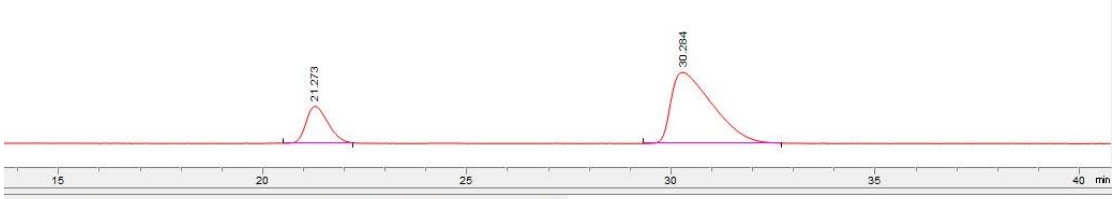

#	Time	Type	Area	Height	Width	Area%	Symmetry
1	21.273	VV	7543.4	197.3	0.5381	21.920	0.672
2	30.284	VV	26870.4	376.8	0.8619	78.080	0.371

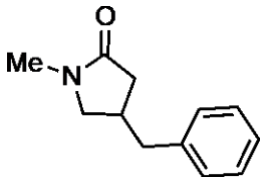

2b

Sample	Variant	e.r.
1	W66S	74:26
2	F269C	79:21
3	F269M	83:17
4	F269R	84:16
5	Y343C	83:17
5	Y343V	80:20
7	Y343M	No Reaction
8	F269Y	83:17

Method – AS-40-IPA-30MIN

0-Racemate

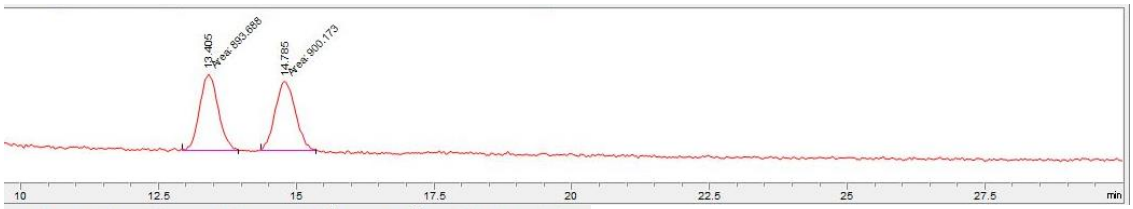

#	Time	Type	Area	Height	Width	Area%	Symmetry
1	13.405	MM	893.7	37.7	0.3953	49.819	0.946
2	14.785	MM	900.2	34.4	0.4368	50.181	0.89

1-W66S

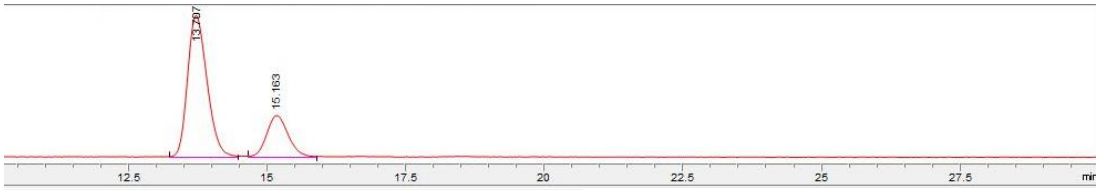

#	Time	Type	Area	Height	Width	Area%	Symmetry
1	13.707	VV	8534.8	341.1	0.3899	74.455	0.746
2	15.163	VV	2928.3	102.3	0.39	25.545	0.823

2-F269C

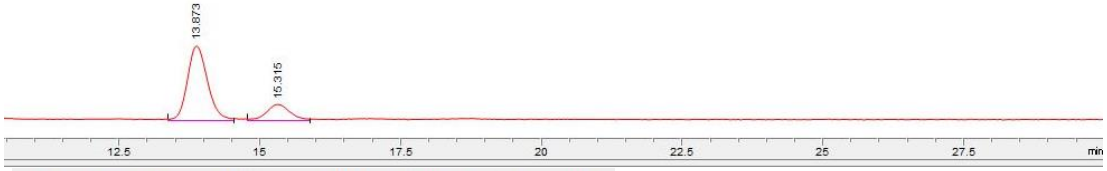

#	Time	Type	Area	Height	Width	Area%	Symmetry
1	13.873	VB	3377.7	133.4	0.3834	78.911	0.805
2	15.315	VV	902.7	29.4	0.396	21.089	0.881

3-F269M

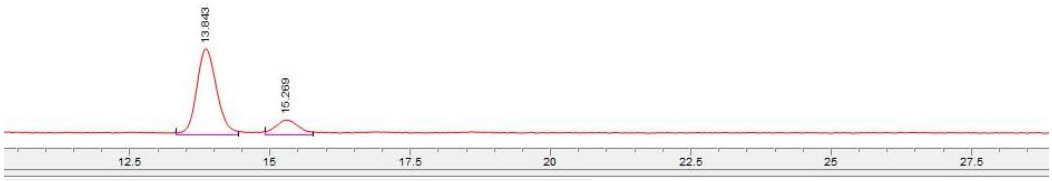

#	Time	Type	Area	Height	Width	Area%	Symmetry
1	13.843	VV	2654.7	105.3	0.3702	82.737	0.828
2	15.269	VV	553.9	18.6	0.3742	17.263	0.775

4- F269R

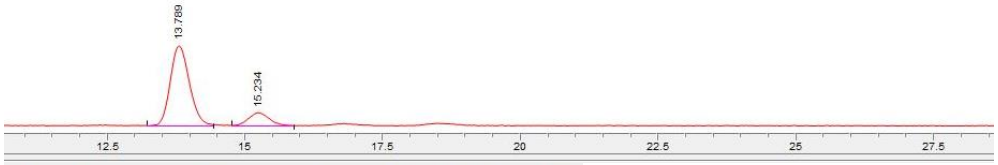

#	Time	Type	Area	Height	Width	Area%	Symmetry
1	13.789	VV	3567.3	144.6	0.3698	83.836	0.818
2	15.234	VV	687.8	24.6	0.3382	16.164	0.904

5- Y343C

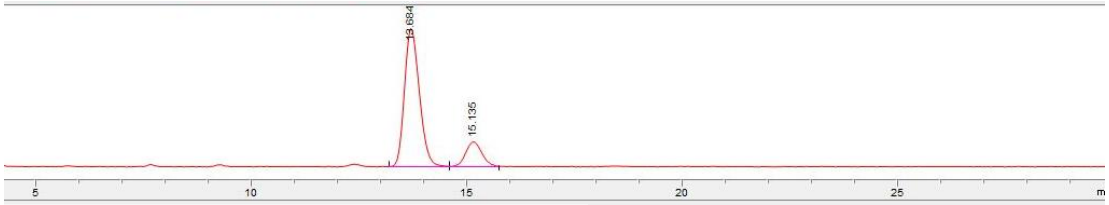

#	Time	Type	Area	Height	Width	Area%	Symmetry
1	13.684	VV	6347.3	259.7	0.3732	82.709	0.731
2	15.135	VV	1327	47.9	0.3411	17.291	0.876

6-Y343V

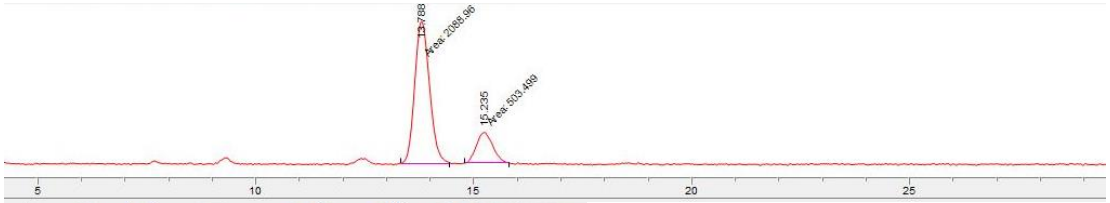

#	Time	Type	Area	Height	Width	Area%	Symmetry
1	13.788	MM	2089	87.6	0.3975	80.578	0.844
2	15.235	MM	503.5	18.9	0.443	19.422	0.967

8-F269Y

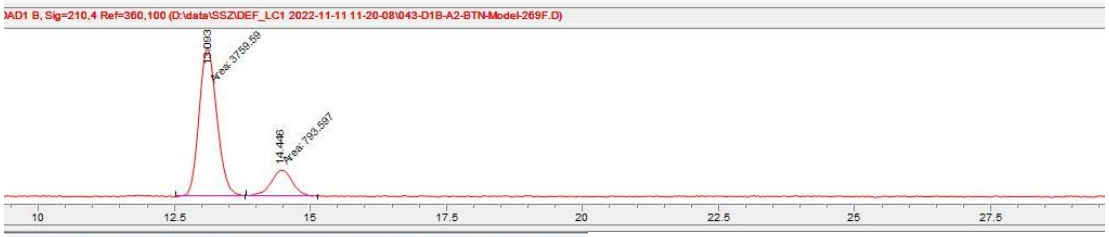

#	Time	Type	Area	Height	Width	Area%	Symmetry
1	13.093	MM	3759.6	163.9	0.3824	82.571	0.829
2	14.446	MM	793.6	28.5	0.4637	17.429	0.859

10. Characterization and NMR Spectra

SUBSTRATE CHARACTERIZATION

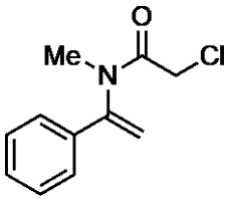

(1a) 2-chloro-N-methyl-N-(1-phenylvinyl)acetamide
(reported by Biegasiewicz *et al*.[11])

^{1}H-NMR (500 MHz, $CDCl_3$) δ 7.41 (m, 5H), 5.75 (s, 1H), 5.34 (s, 1H), 4.10 (s, 2H), 3.14 (s, 3H).

^{13}C-NMR (126 MHz; $CDCl_3$): δ 166.8, 147.7, 129.7, 129.2, 125.7, 113.1, 41.4, 36.1.

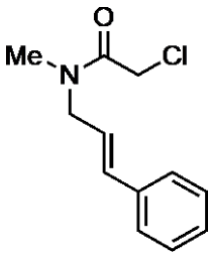

(2a) (*E*)- 2-chloro-N-cinnamyl-N-methylacetamide
(reported by Biegasiewicz *et al*.[11])

^{1}H-NMR (500 MHz, $CDCl_3$) δ 7.39 - 7.23 (m, 3H), 6.51 (t, J =15 Hz, 1H), 6.14 (m, 1H), 4.16 (m, 2H), 4.12 (s, 2H), 3.04 (d, J = 28Hz, 3H).

^{13}C-NMR (126 MHz, $CDCl_3$) δ 166.7, 136.4, 135.8, 134.0, 133.5, 132.6, 128.6, 128.2, 127.6, 126.5, 123.3, 52.2, 50.1, 41.4, 41.0, 35.0, 34.1.

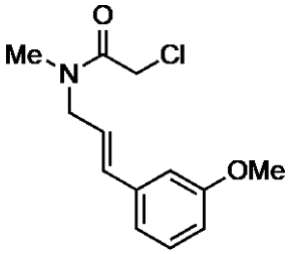

(3a) (*E*)-2-chloro-N-(3-(3-methoxyphenyl)allyl)-N-methylacetamide
(reported by Biegasiewicz *et al*.[11])

^{1}H-NMR (500 MHz, $CDCl_3$) δ 7.24 (m, 1H), 6.95 (t, J= 7 Hz, 1H), 6.90 (s, 1H), 6.81 (m, 1H), 6.48 (t, J= 15 Hz, 1H) 6.13 (m 1H) , 4.12 (m, J = 2.5 Hz, 4H), 3.80 (d, J = 6 Hz, 3H), 3.05 (d, J = 27.1 Hz, 3H).

^{13}C-NMR (126 MHz, $CDCl_3$) δ 167.0, 166.6, 159.8, 137.7, 137.2, 133.5, 132.6, 129.4, 123.6, 119.1, 113.9, 111.9, 111.6, 111.2, 55.2, 52.2, 50.2, 41.4, 41.3, 36.0, 35.0, 34.2, 33.2.

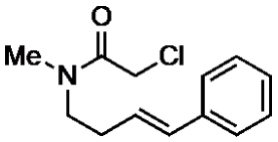

(4a) (*E*)-2-chloro-N-methyl-N-(4-phenylbut-3-en-1-yl)acetamide
(reported by Biegasiewicz *et al*.[11])

^{1}H-NMR 500 MHz, $CDCl_3$) δ 7.25 – 7.20 (m, 4H), 7.17 – 7.10 (m, 1H), 6.40 (t, J = 14 Hz 1H), 6.07 (m, 1H), 4.00 (d, J = 10 Hz, 2H), 3.46 (m, 2H), 2.99 (d, J = 34 Hz, 3H), 2.44 (m, 2H).

^{13}C-NMR (126 MHz, $CDCl_3$) δ 166.4, 137.3, 136.8, 133.3, 132.3, 128.6, 127.7, 127.0, 126.5, 126.1, 125.0, 50.3, 48.3, 41.5, 40.9, 36.2, 33.8, 32.1, 30.9.

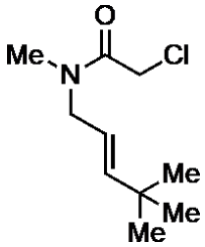

(5a). (*E*)-2-chloro-N-(4,4-dimethylpent-2-en-1-yl)-N-methylacetamide
(reported by Nicholls *et al*.[11])

^{1}H-NMR (500 MHz, $CDCl_3$) δ 5.63 (dd, J = 16, 7 Hz, 1H), 5.28 (m, 1H), 4.06 (d, J = 14 Hz, 2H), 3.94 (d, J = 20 Hz, 2H), 2.93 (d, J = 25 Hz, 3H), 1.01 (s, 9H)

^{13}C-NMR (500 MHz, $CDCl_3$) δ166.6, 166.2, 146.3, 145.5, 118.4, 52.2, 50.0, 41.5, 41.0, 34.5, 33.7, 33.1, 29.5.

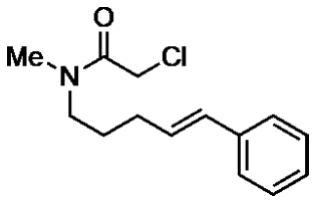

(6a). (*E*)-2-chloro-N-methyl-N-(5-phenylpent-4-en-1-yl)acetamide
(reported by Biegasiewicz *et al*.[11])

^{1}H-NMR 500 MHz, $CDCl_3$) δ 7.32 (m, 4H), 7.21(m, 1H), 6.42 (t, J = 14 Hz, 1H), 6.20 (m, 1H), 4.04 (d, J = 6.2 Hz, 2H), 3.44 (dt, J= 25, 6 Hz, 2H), 3.02 (d, J = 53 Hz, 3H), 2.24 (m, 2H), 1.79 (m, 2H).

^{13}C-NMR (126 MHz, $CDCl_3$) δ 166.4, 137.6, 137.2, 131.4, 130.6, 129.6, 128.5, 127.3, 126.0, 49.8, 48.0, 41.5, 40.9, 35.7, 33.7, 30.2, 29.9, 28.2, 26.6.

PRODUCT CHARACTERIZATION

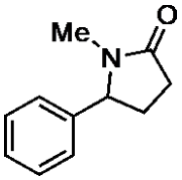

(1b). 1-methyl-5-phenylpyrrolidin-2-one (reported by Biegasiewicz *et al*.[11])

^{1}H-NMR 500 MHz, $CDCl_3$) δ 7.38 (m, 2H), 7.32 (m, 1H), 7.20 (m, 2H), 4.50 (t, J = 8 Hz, 1H), 2.67 (s, 3H), 2.56 (m, 1H), 2.47 (m, 2H), 1.87 (m, 1H).

^{13}C-NMR (126 MHz, $CDCl_3$) δ 175.6, 141.1, 129.0, 128.8, 128.1, 126.4, 64.6, 30.2, 28.6.

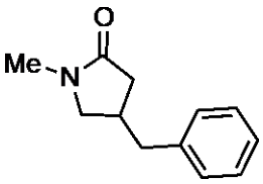

(2b). 4-benzyl-1-methylpyrrolidin-2-one
(reported by Biegasiewicz *et al*.[11])

^{1}H-NMR 500 MHz, $CDCl_3$) δ 7.30 (t, J= 7 Hz, 2H), 7.23 (t, J= 8 Hz, 1H), 7.15 (d, J= 7 Hz, 2H), 3.36 (dd, J= 9, 8 Hz, 1H), 3.08 (dd, J = 9, 6 Hz, 1H), 2.78 (s, 3H), 2.68 (m, 4H), 2.5 (dd, J = 17, 8 Hz, 1H), 2.16 (dd, J = 18, 5 Hz, 1H).

^{13}C-NMR (500 MHz, $CDCl_3$) δ 174.2, 139.3, 128.9, 126.4, 54.7, 40.7, 37.2, 33.2, 29.6.

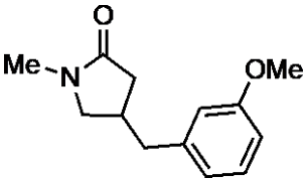

(3b). 4-(3-methoxybenzyl)-1-methylpyrrolidin-2-one
(reported by Biegasiewicz *et al*.[11])

^{1}H-NMR 500 MHz, $CDCl_3$) δ 7.22 (t, J = 8 Hz, 1H), 6.75 (m, 2H), 6.70 (t, J =2 Hz, 1H), 3.80 (s, 3H), 3.36 (dd, J = 10, 8 Hz, 1H), 3.08 (dd, J = 10, 6 Hz, 1H), 2.82 (s, 3H), 2.77 (m, 1H), 2.64 (m, 2H), 2.50 (dd, J = 17, 7.9 Hz, 1H), 2.16 (dd, J = 16, 6 Hz, 1H).

^{13}C-NMR (126 MHz, $CDCl_3$) δ 174.2, 159.8, 140.9, 129.6, 121.1, 114.7, 111.5, 55.2, 54.7, 40.7, 37.3, 33.0, 29.6.

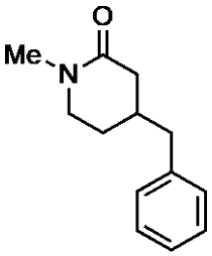

(4b). 4-benzyl-1-methylpiperidin-2-one
(reported by Biegasiewicz *et al*.[11])

^{1}H-NMR 500 MHz, $CDCl_3$) δ 7.28 (t, J=7 Hz, 2H), 7.20 (t, J=8 Hz, 1H), 7.12 (d, 2H), 3.24 (m, 2H), 2.92 (s, 3H), 2.59 (m, 2H), 2.47 (m, 1H), 2.07 (m, 2H), 1.85 (m, 1H), 1.48 (m, 1H).

^{13}C-NMR (126 MHz, $CDCl_3$) δ 169.6, 139.2, 129.1, 128.4, 126.5, 49.1, 42.0, 38.5, 35.1, 34.4, 28.6.

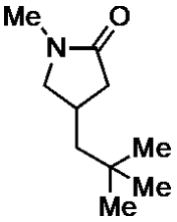

(5b). 1-methyl-4-neopentylpyrrolidin-2-one
(reported by Nicholls *et al*.[12])

^{1}H-NMR 500 MHz, $CDCl_3$) δ 3.45 (d, J = 1.5 Hz, 1H), 3.01(t, J= 8 Hz, 2.81 (s, 3H), 2.54 (dd, J = 16, 8 Hz, 1H), 2.42 (m, 1H), (2.07 (dd, J = 16, 10 Hz, 1H), 1.39 (d, J = 1.5 Hz, 1H), 0.91 (s, 9H)

^{13}C-NMR (126 MHz, $CDCl_3$) δ 174.6, 57.0, 49.3, 39.6, 30.9, 29.9, 29.5, 28.9.

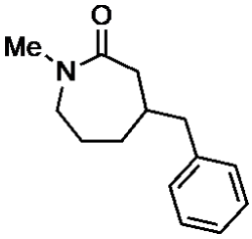

(6b) 4-benzyl-1-methylazepan-2-one
(reported by Biegasiewicz *et al.*[11])

^{1}H-NMR 500 MHz, $CDCl_3$) δ 7.27 (t, J=7 Hz, 2H), 7.19 (t, J= 7 Hz, 1H), 7.14 (d, J= 7 Hz, 2H), 3.46 (dd, J = 14, 11 Hz, 1H), 3.19 (dd, J = 15, 6 Hz, 1H), 2.97 (s, 3H), 2.71 (dd, J = 13, 5 Hz, 1H), 2.52 (m, 3H), 1.93 (m, 1H), 1.77 (m, 2H), 1.46 (m, 1H), 1.26 (m, 1H).

^{13}C-NMR (126 MHz, $CDCl_3$) δ174.4, 139.9, 129.2, 128.5, 126.1, 51.2, 42.8, 35.8, 35.1, 26.9.

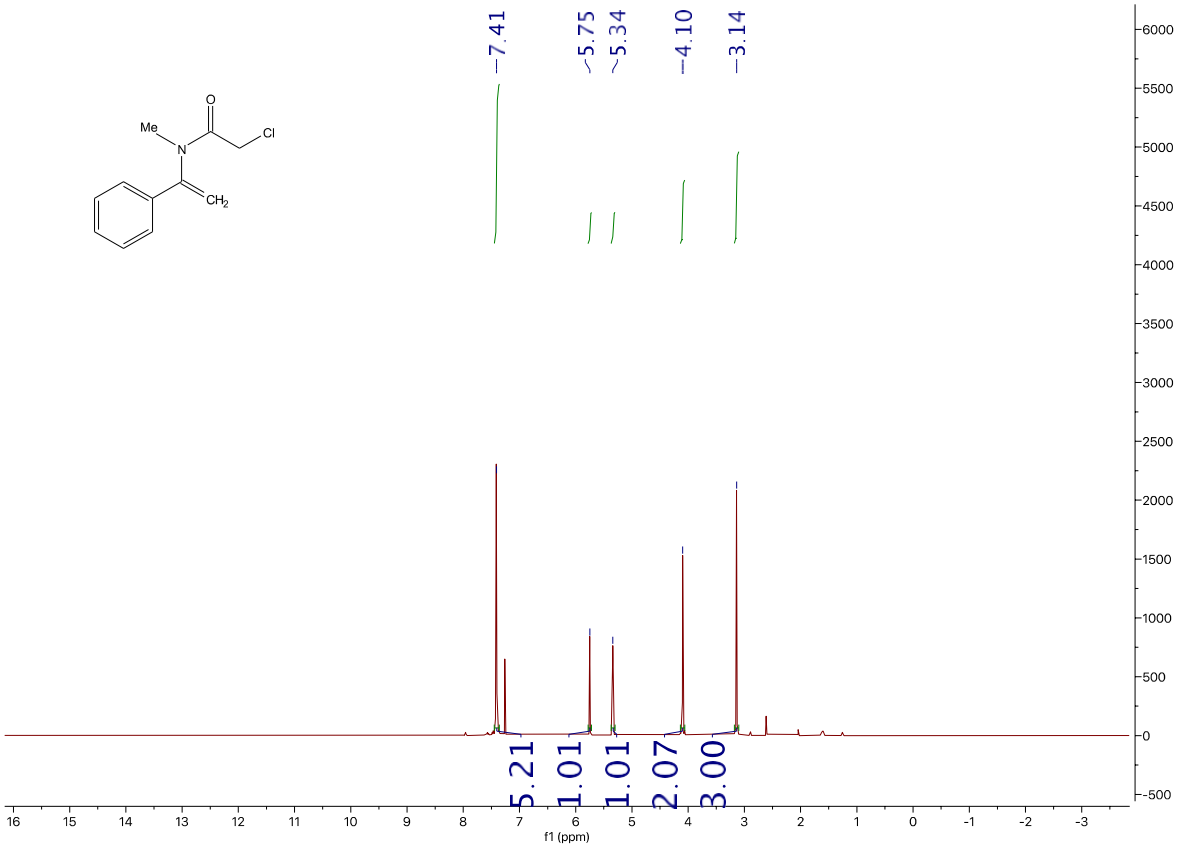
7.41
5.75
5.34
4.10
3.14
Me
N
O
Cl
CH2
5.21
1.01
1.01
2.07
3.00
f1 (ppm)

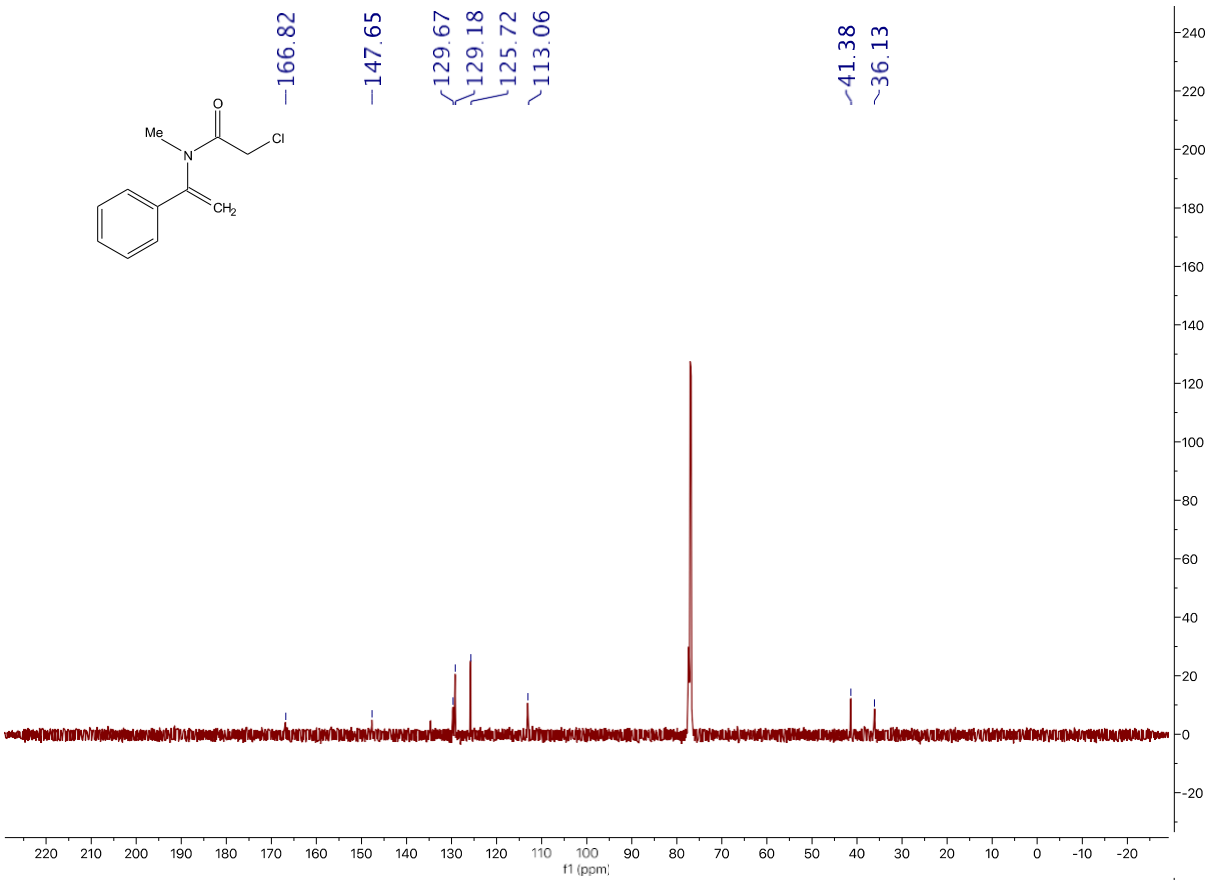
166.82
147.65
129.67
129.18
125.72
113.06
41.38
36.13
Me
N
O
Cl
CH2
f1 (ppm)

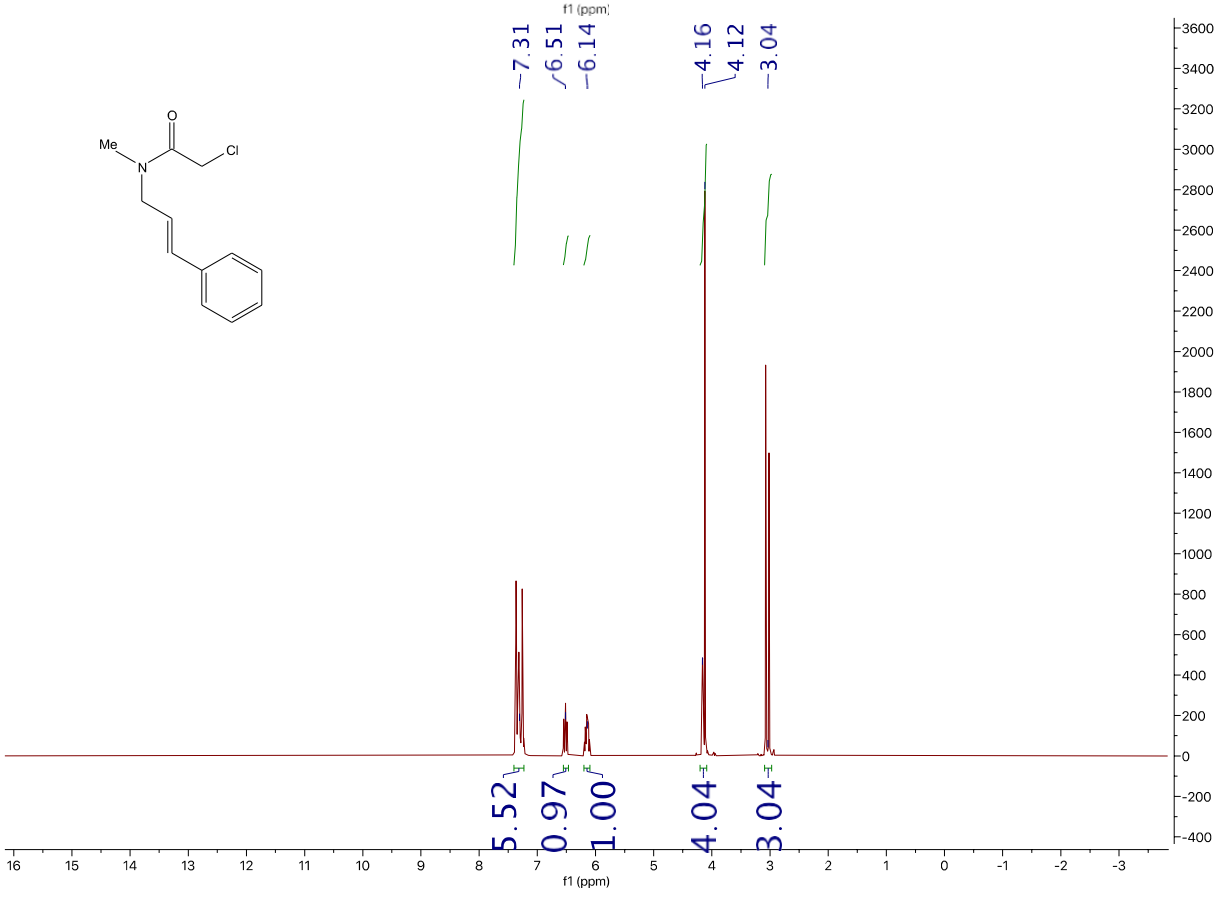
7.31
6.51
6.14
4.16
4.12
3.04
5.52
0.97
1.00
4.04
3.04
Me
N
O
Cl
f1 (ppm)

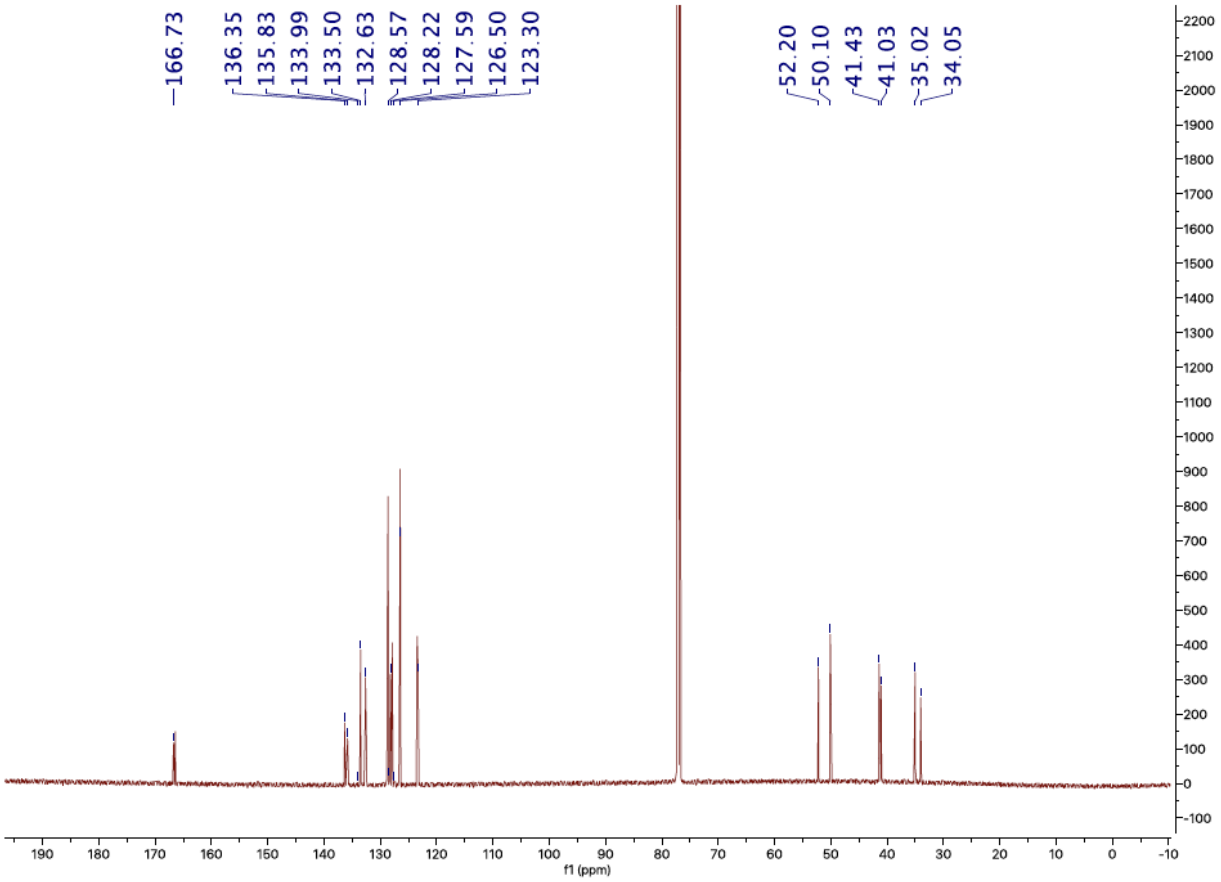
166.73
136.35
135.83
133.99
133.50
132.63
128.57
128.22
127.59
126.50
123.30
52.20
50.10
41.43
41.03
35.02
34.05
f1 (ppm)

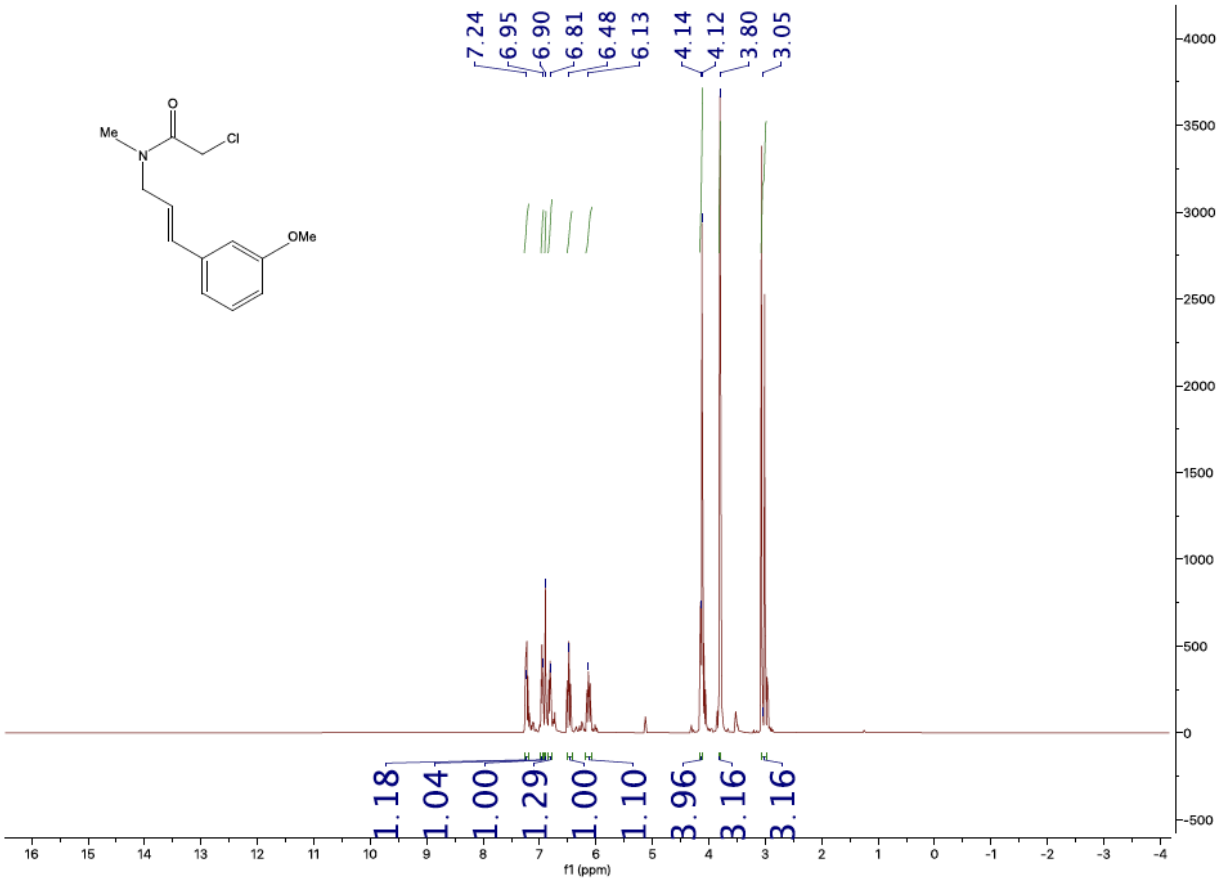
7.24
6.95
6.90
6.81
6.48
6.13
4.14
4.12
3.80
3.05
1.18
1.04
1.00
1.29
1.00
1.10
3.96
3.16
3.16
Me
N
O
Cl
OMe
f1 (ppm)

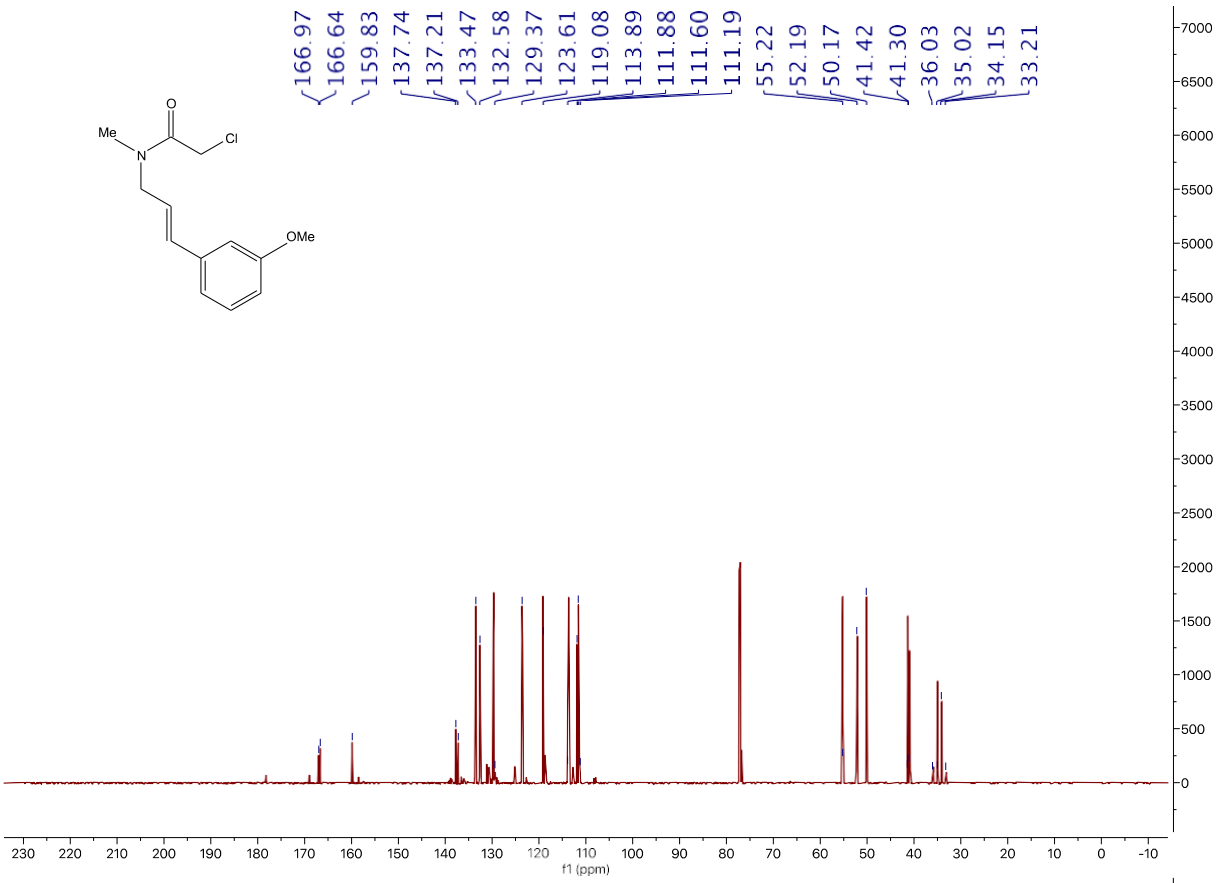
166.97
166.64
159.83
137.74
137.21
133.47
132.58
129.37
123.61
119.08
113.89
111.88
111.60
111.19
55.22
52.19
50.17
41.42
41.30
36.03
35.02
34.15
33.21
Me
N
O
Cl
OMe
f1 (ppm)

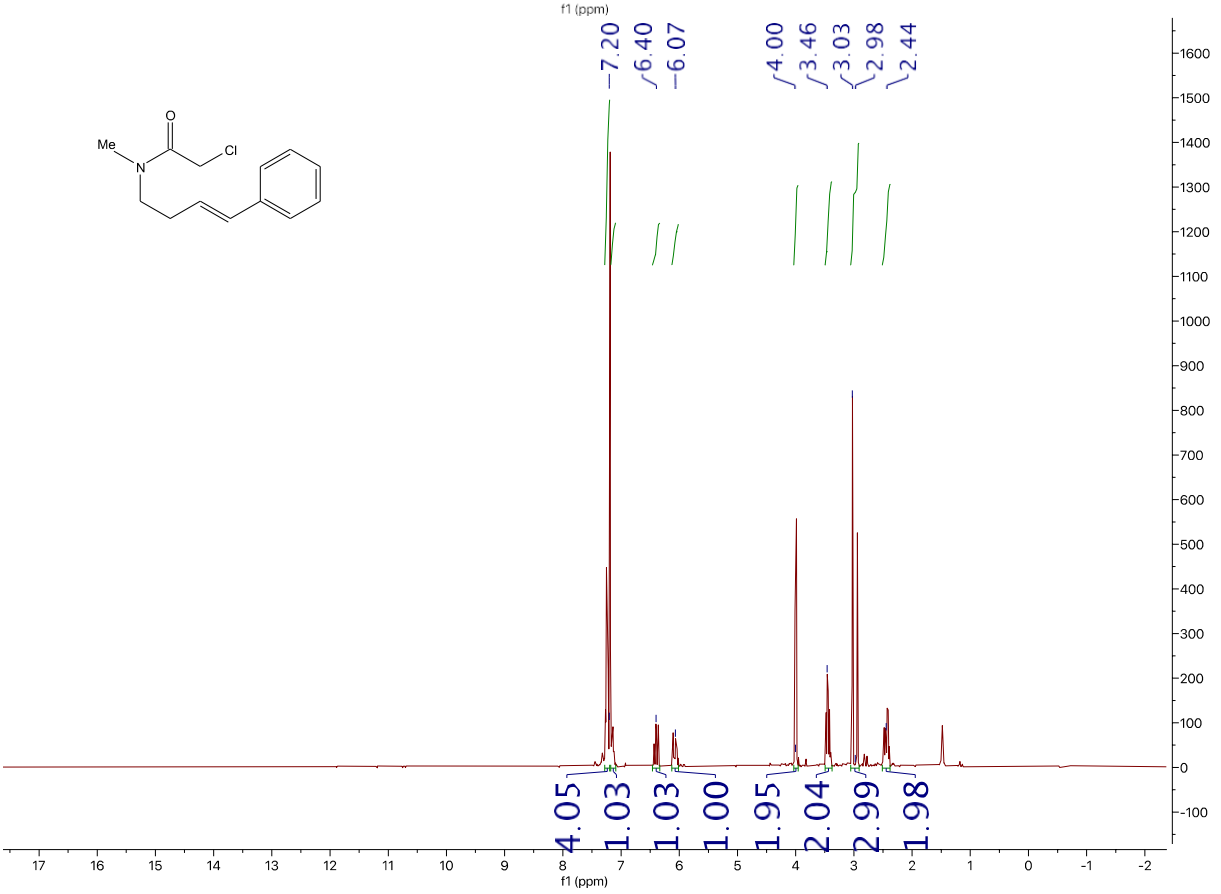
7.20
6.40
6.07
4.00
3.46
3.03
2.98
2.44
4.05
1.03
1.03
1.00
1.95
2.04
2.99
1.98
Me
N
O
Cl
f1 (ppm)

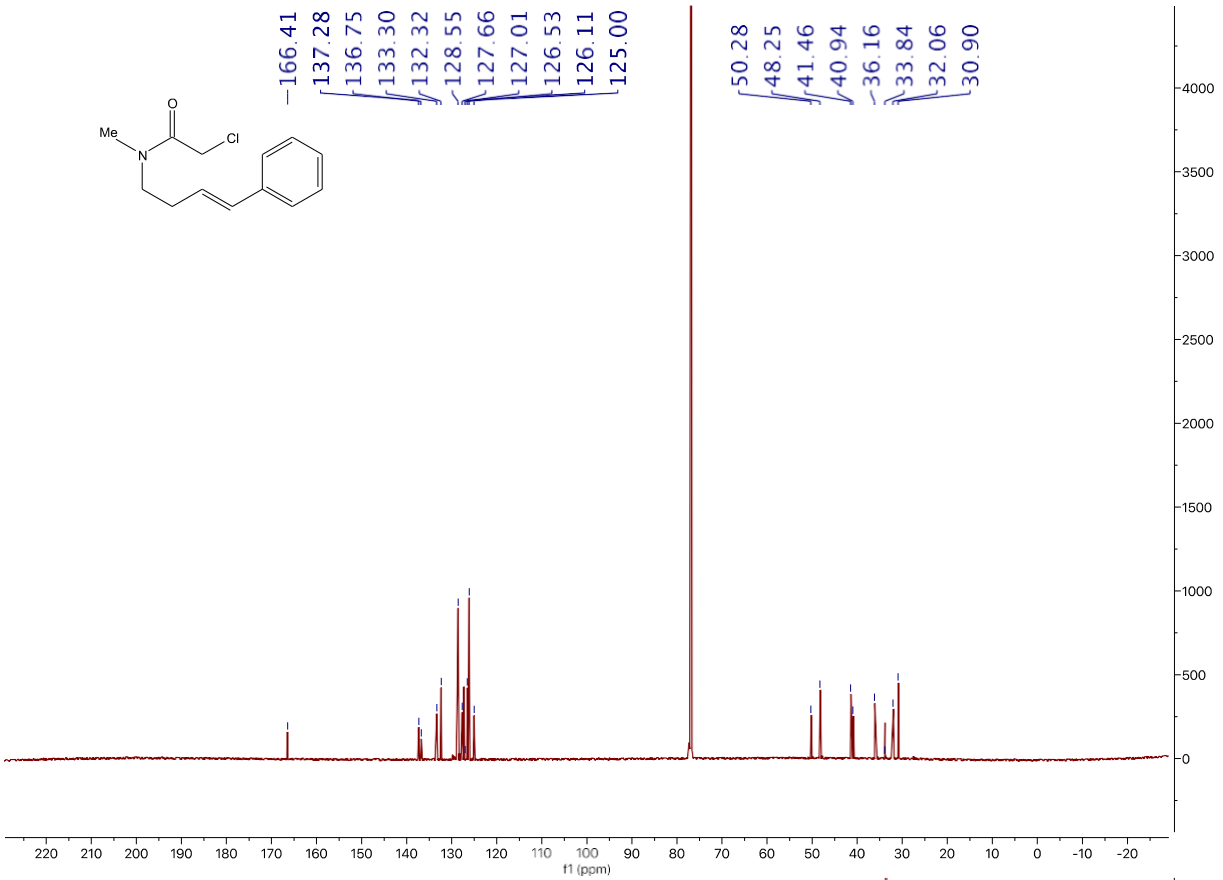
166.41
137.28
136.75
133.30
132.32
128.55
127.66
127.01
126.53
126.11
125.00
50.28
48.25
41.46
40.94
36.16
33.84
32.06
30.90
Me
N
O
Cl
f1 (ppm)

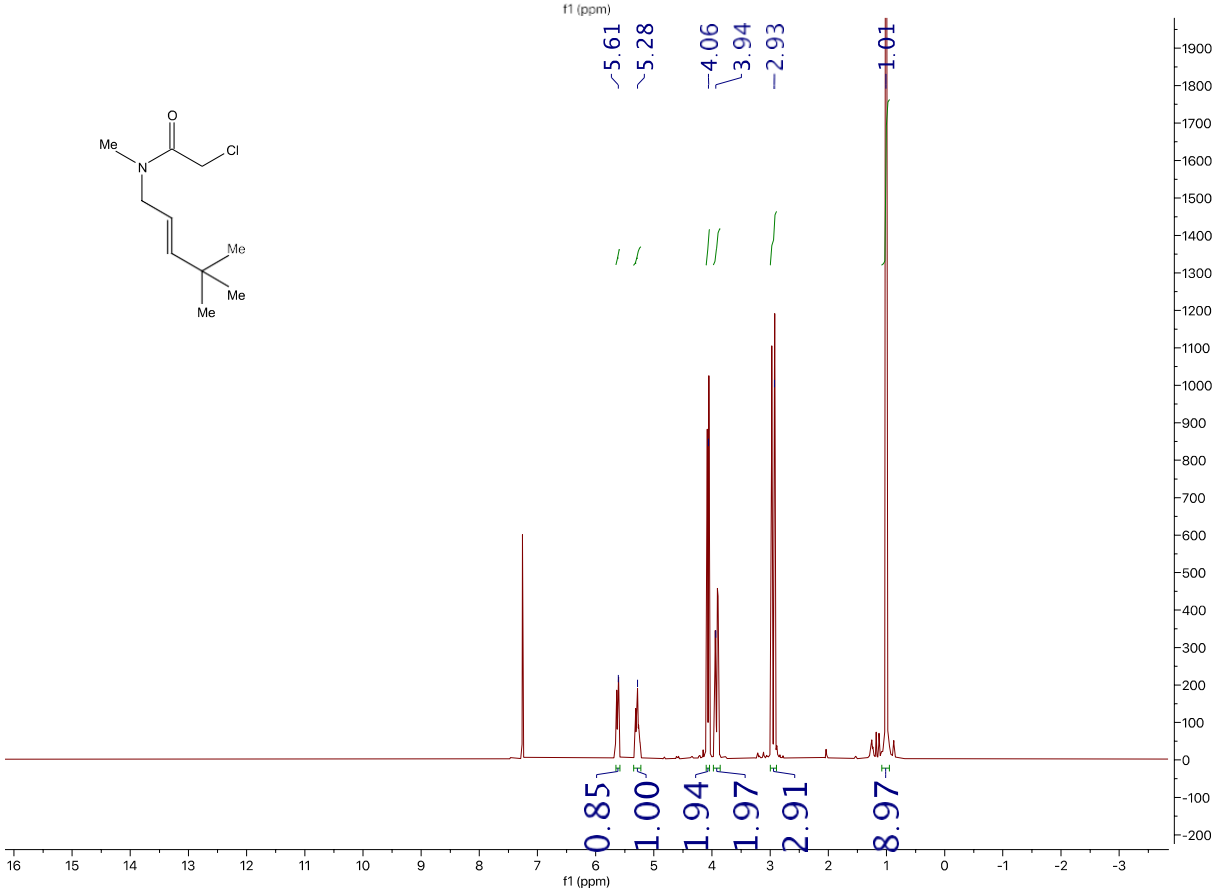
5.61
5.28
4.06
3.94
2.93
1.01
Me
N
O
Cl
Me
Me
Me
0.85
1.00
1.94
1.97
2.91
8.97
f1 (ppm)

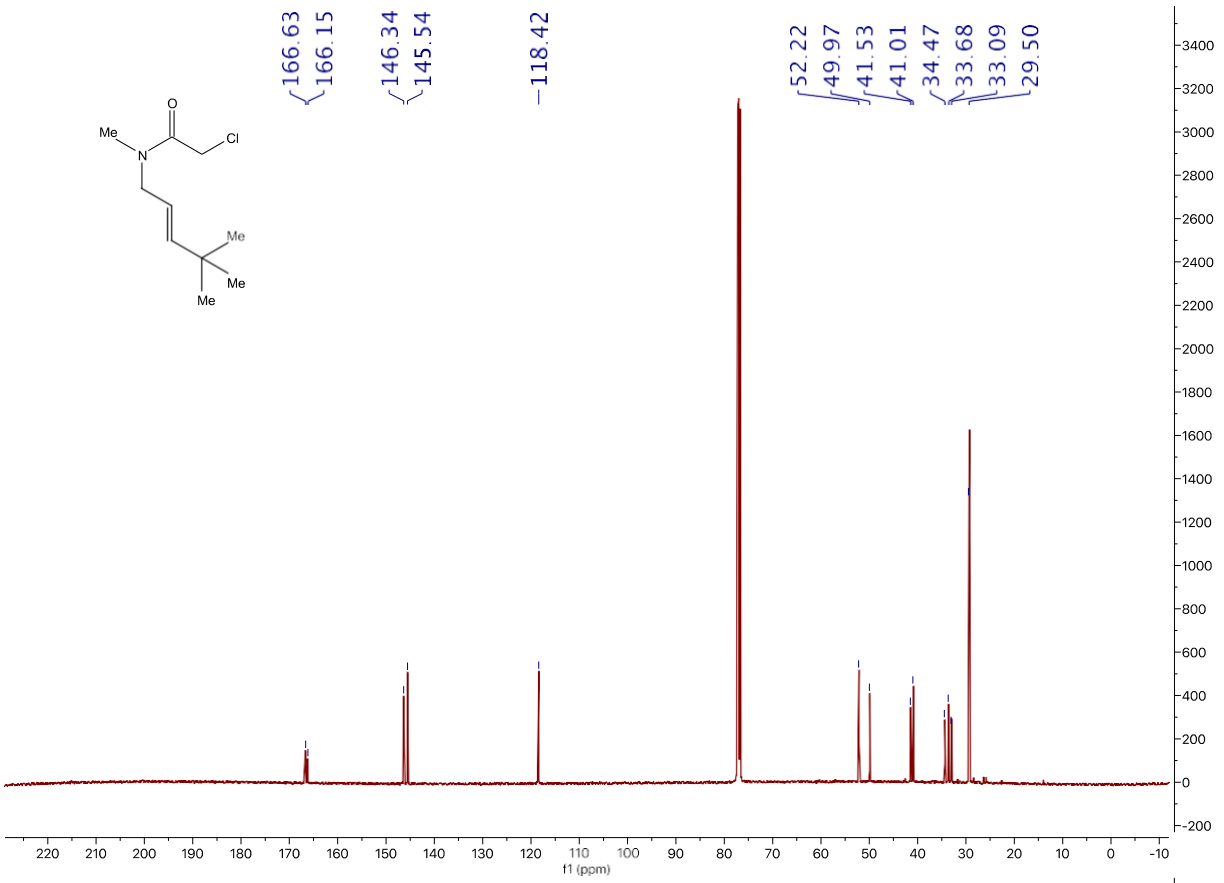
166.63
166.15
146.34
145.54
118.42
52.22
49.97
41.53
41.01
34.47
33.68
33.09
29.50
Me
N
O
Cl
Me
Me
Me
f1 (ppm)

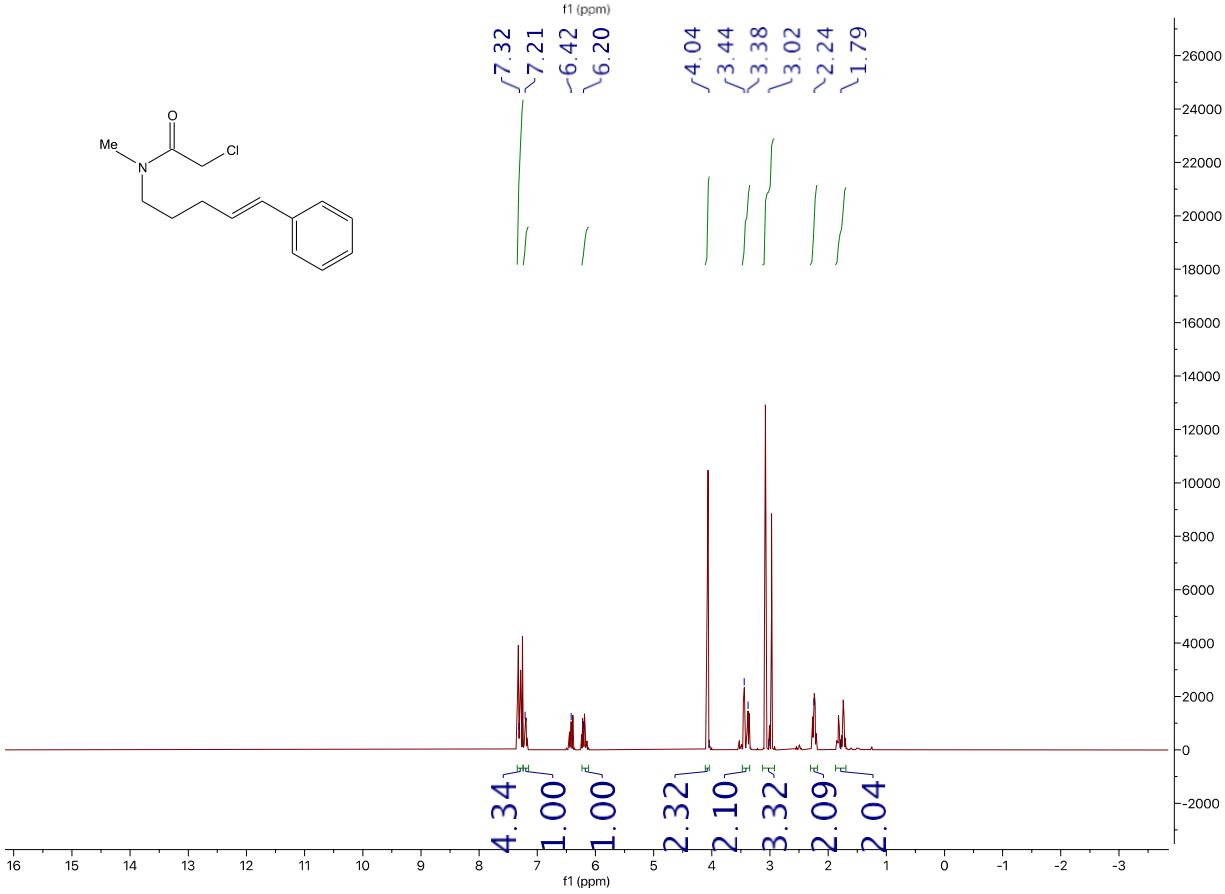
7.32
7.21
6.42
6.20
4.04
3.44
3.38
3.02
2.24
1.79
4.34
1.00
1.00
2.32
2.10
3.32
2.09
2.04
Me
N
O
Cl
f1 (ppm)

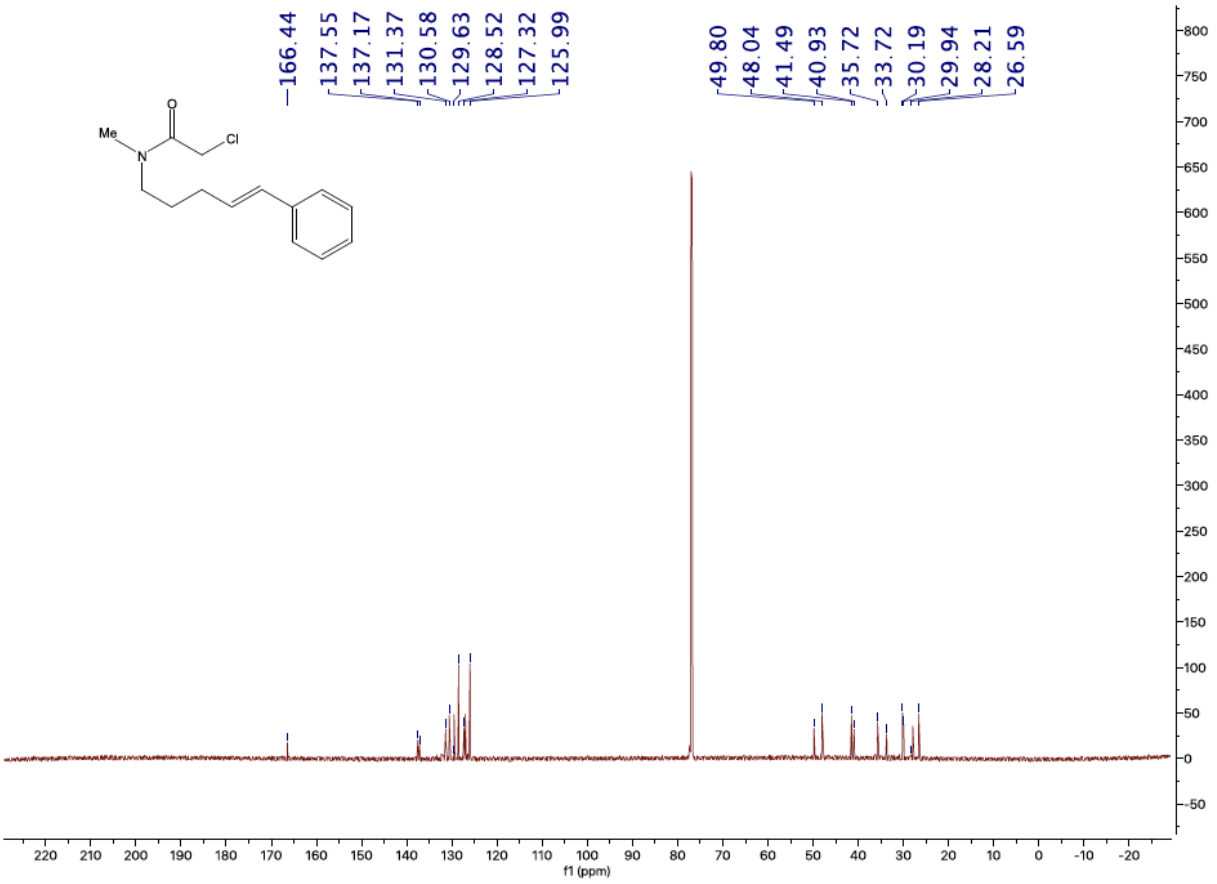
166.44
137.55
137.17
131.37
130.58
129.63
128.52
127.32
125.99
49.80
48.04
41.49
40.93
35.72
33.72
30.19
29.94
28.21
26.59
Me
N
O
Cl
f1 (ppm)

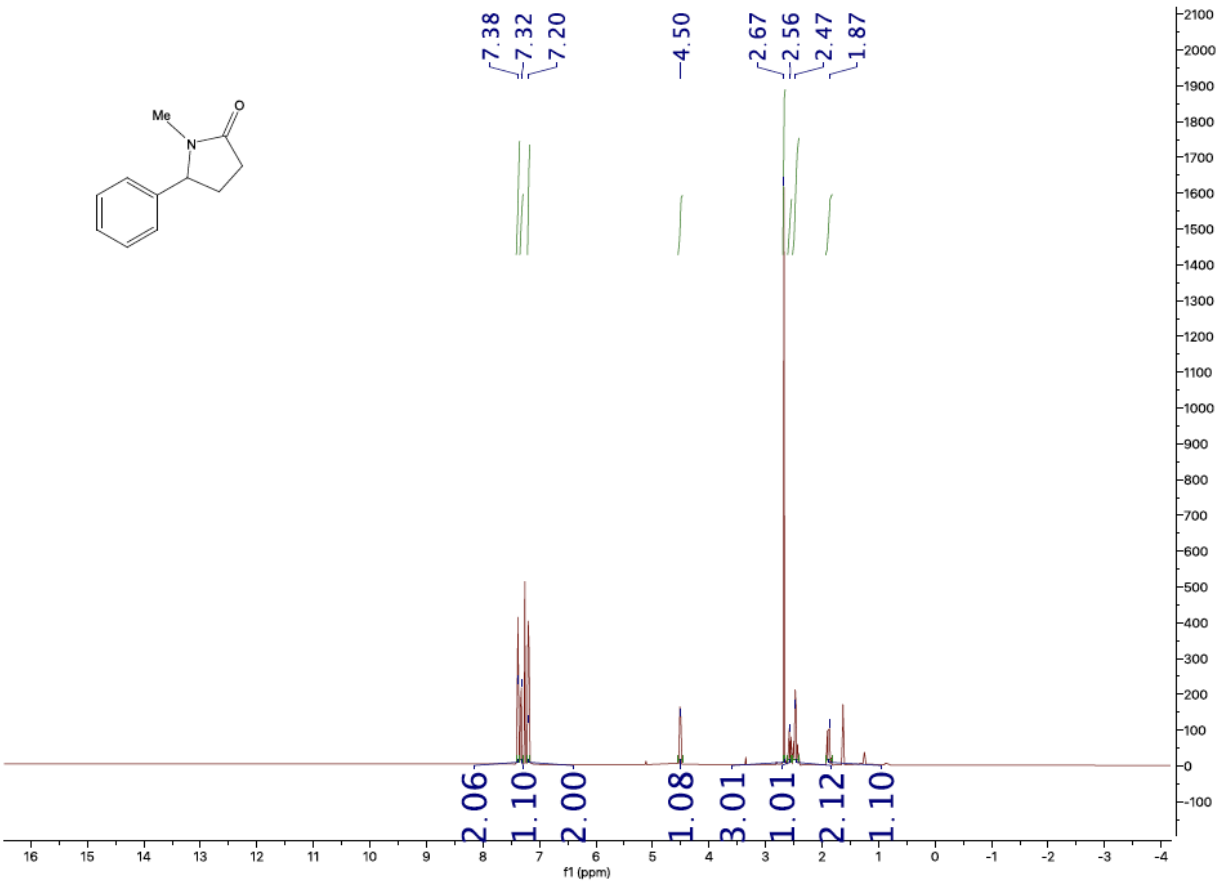
7.38
7.32
7.20
4.50
2.67
2.56
2.47
1.87
Me
N
O
2.06
1.10
2.00
1.08
3.01
1.01
2.12
1.10
f1 (ppm)

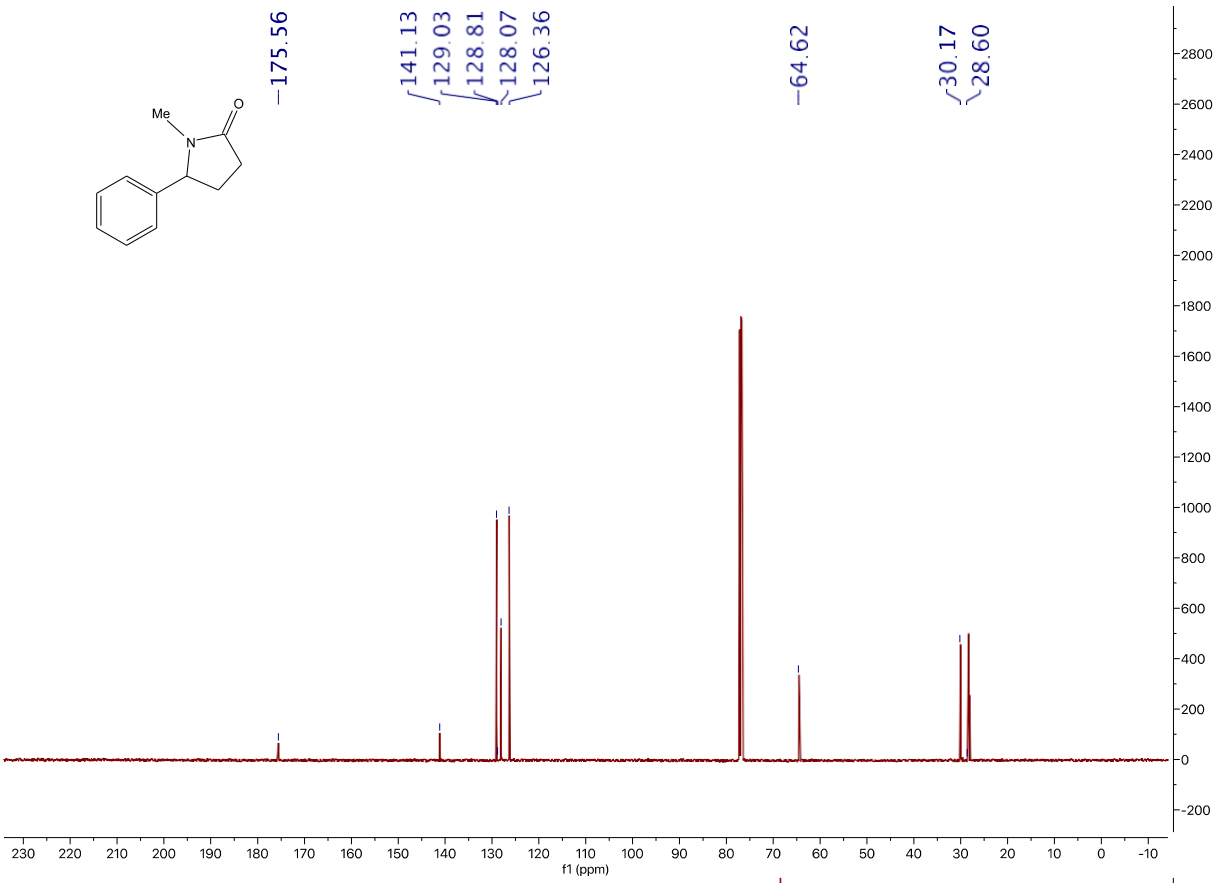
175.56
141.13
129.03
128.81
128.07
126.36
64.62
30.17
28.60
Me
N
O
f1 (ppm)

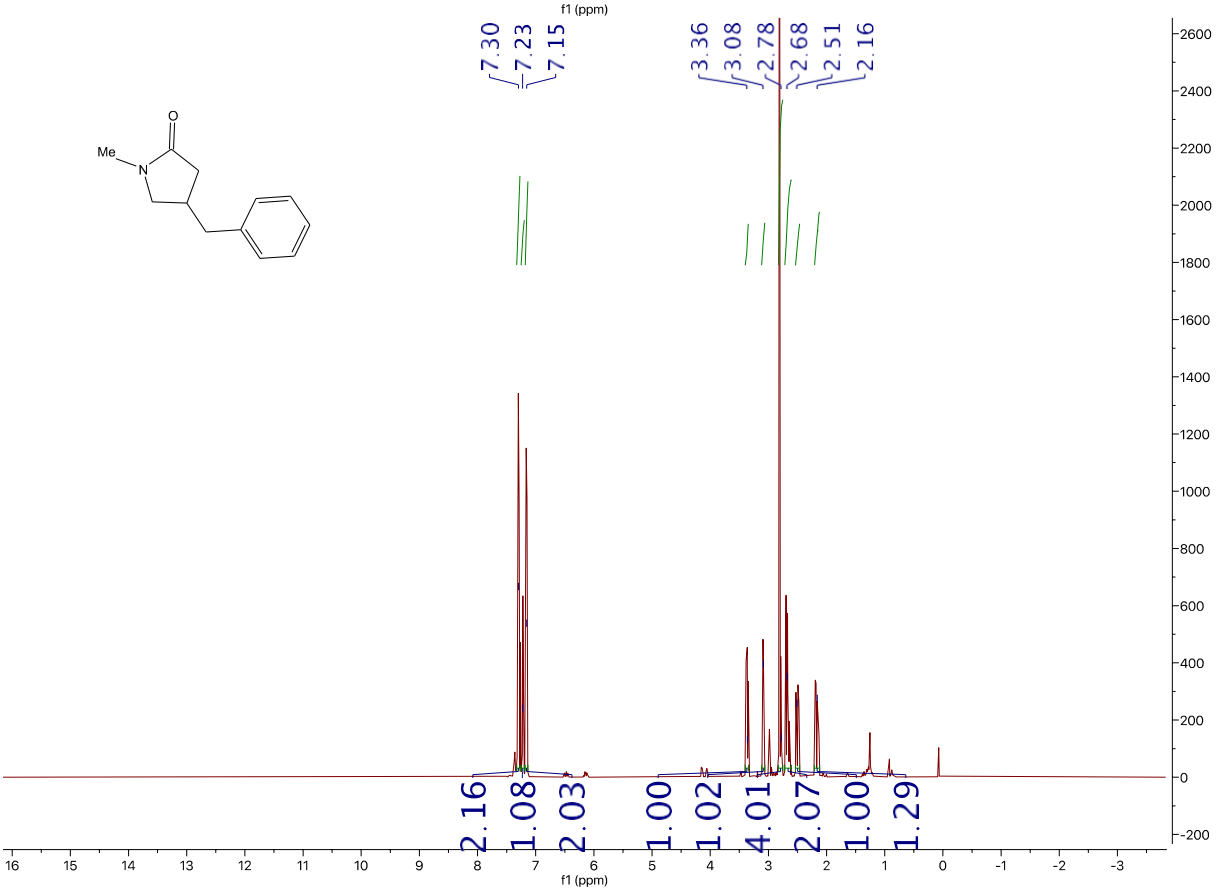
7.30
7.23
7.15
3.36
3.08
2.78
2.68
2.51
2.16
Me
N
O
2.16
1.08
2.03
1.00
1.02
4.01
2.07
1.00
1.29
f1 (ppm)

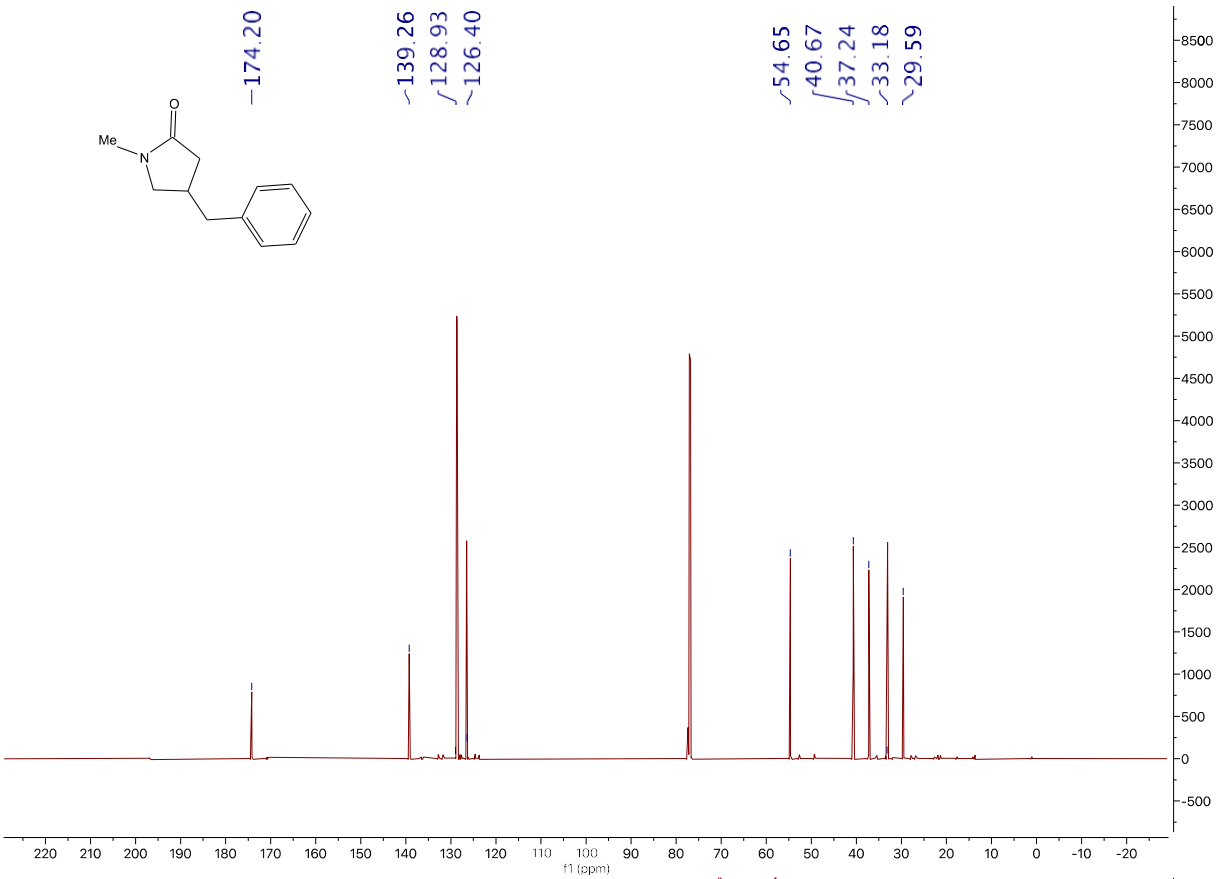
174.20
139.26
128.93
126.40
54.65
40.67
37.24
33.18
29.59
Me
N
O
f1 (ppm)

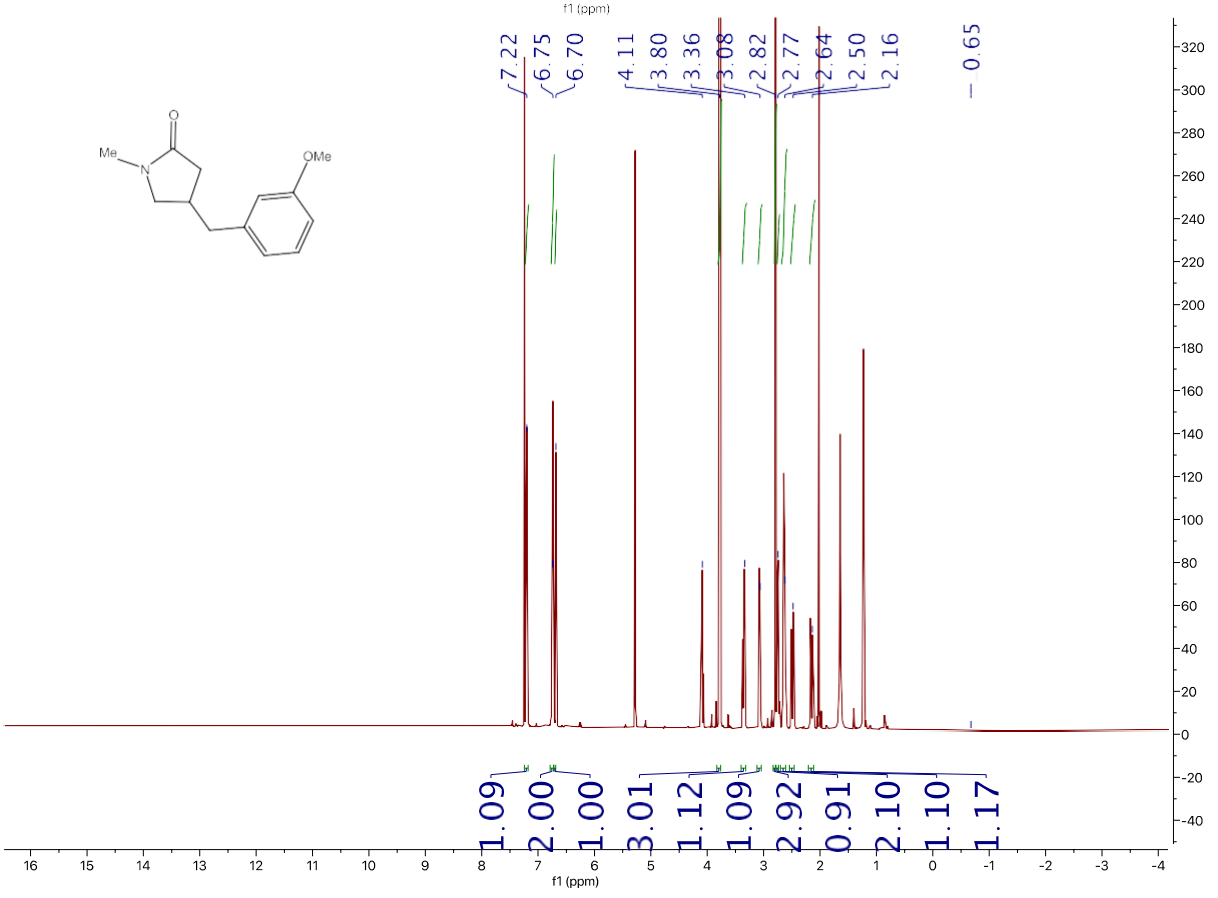
7.22
6.75
6.70
4.11
3.80
3.36
3.08
2.82
2.77
2.64
2.50
2.16
0.65
1.09
2.00
1.00
3.01
1.12
1.09
2.92
0.91
2.10
1.10
1.17
Me
N
O
OMe
f1 (ppm)

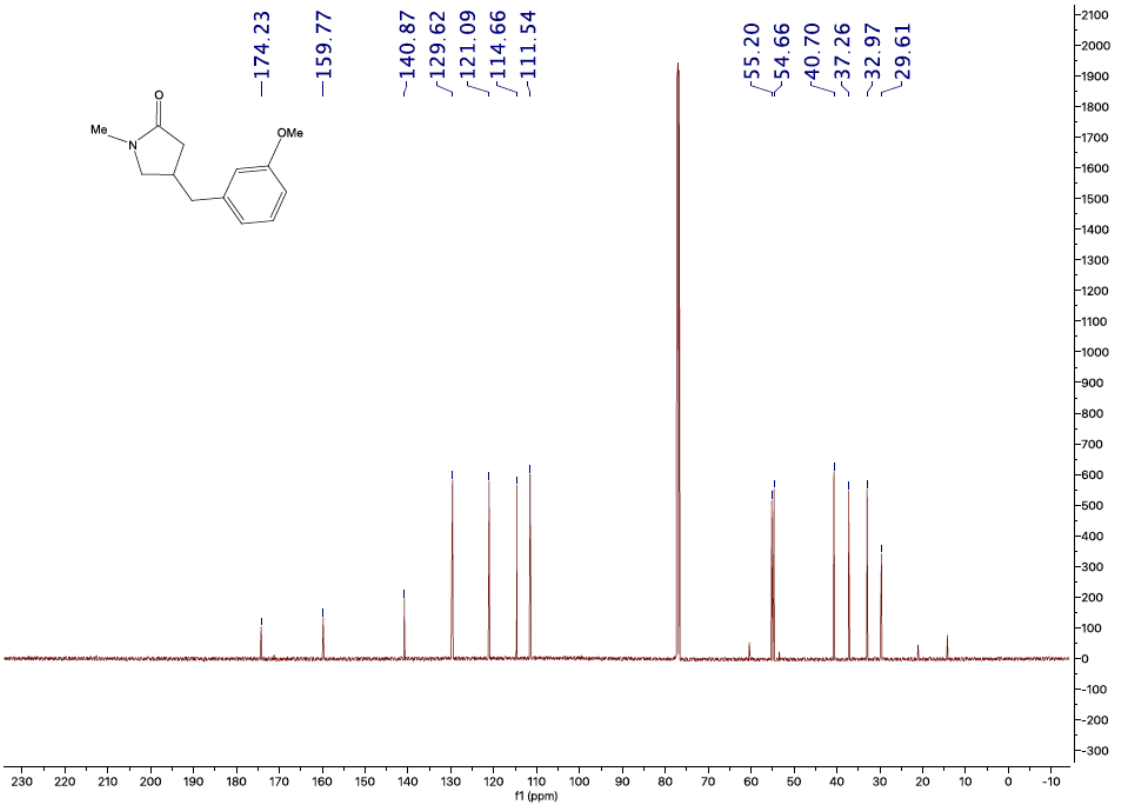
174.23
159.77
140.87
129.62
121.09
114.66
111.54
55.20
54.66
40.70
37.26
32.97
29.61
Me
N
O
OMe
f1 (ppm)

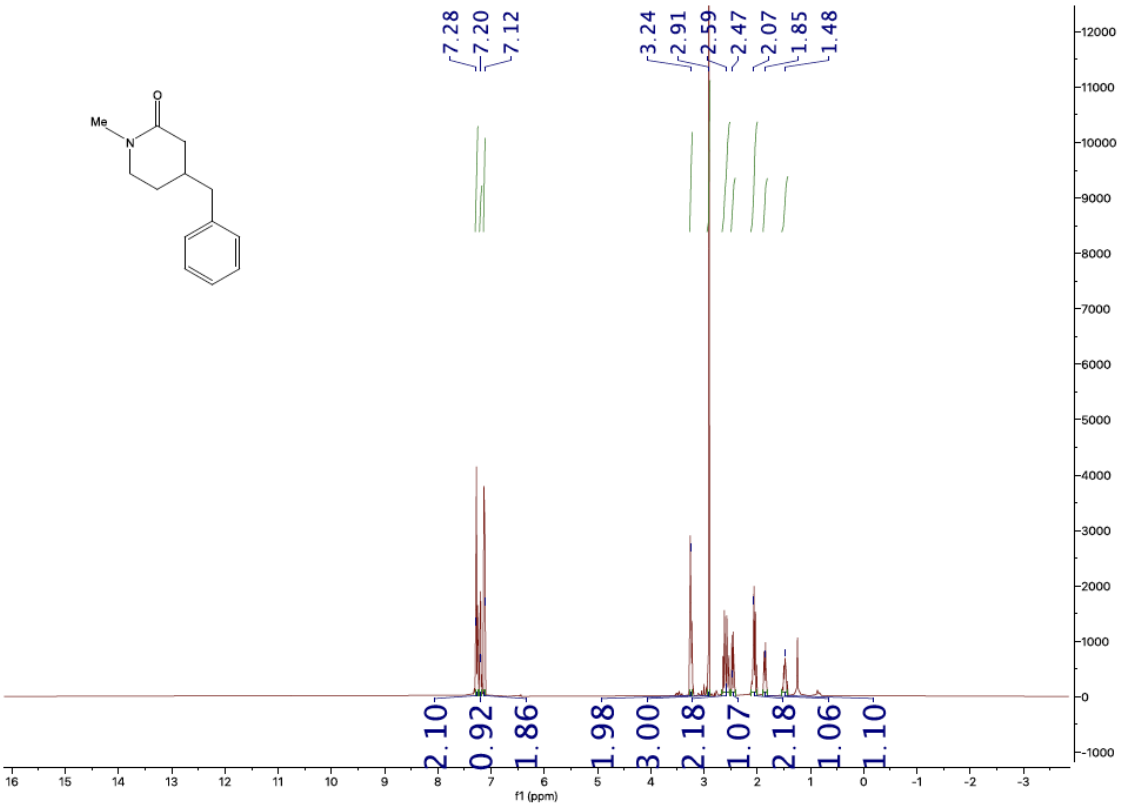
7.28
7.20
7.12
3.24
2.91
2.59
2.47
2.07
1.85
1.48
2.10
0.92
1.86
1.98
3.00
2.18
1.07
2.18
1.06
1.10
Me
N
O
f1 (ppm)

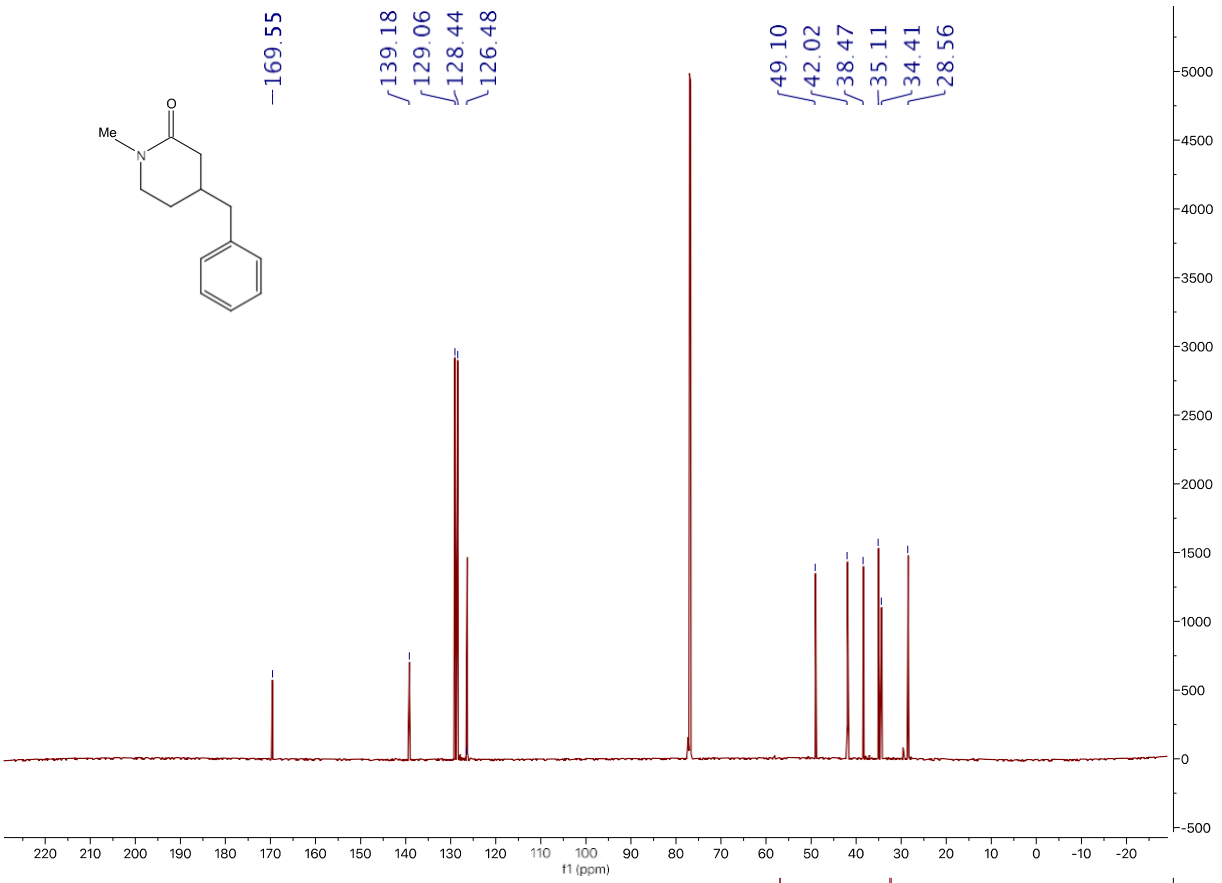
169.55
139.18
129.06
128.44
126.48
49.10
42.02
38.47
35.11
34.41
28.56
Me
N
O
f1 (ppm)

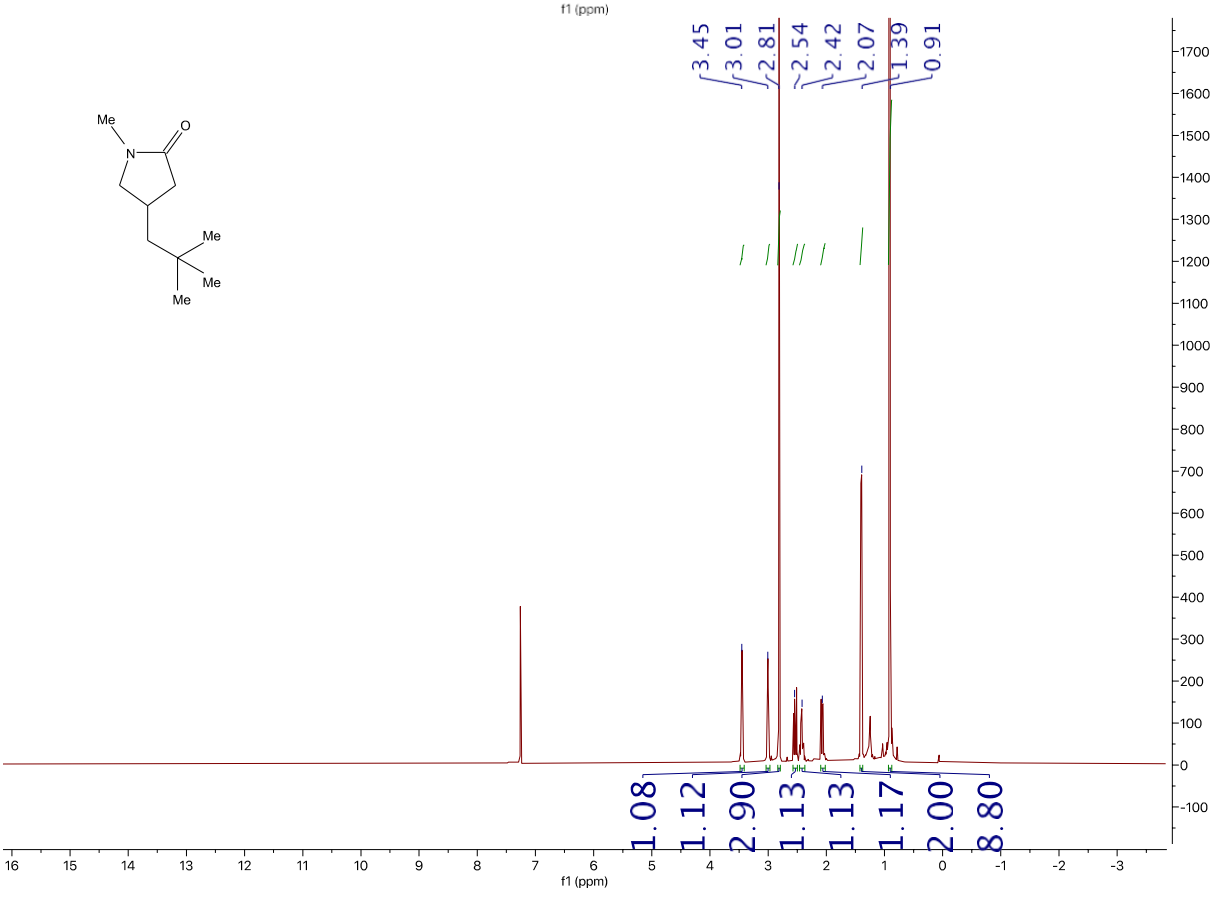
3.45
3.01
2.81
2.54
2.42
2.07
1.39
0.91
1.08
1.12
2.90
1.13
1.13
1.17
2.00
8.80
Me
N
O
Me
Me
Me
f1 (ppm)

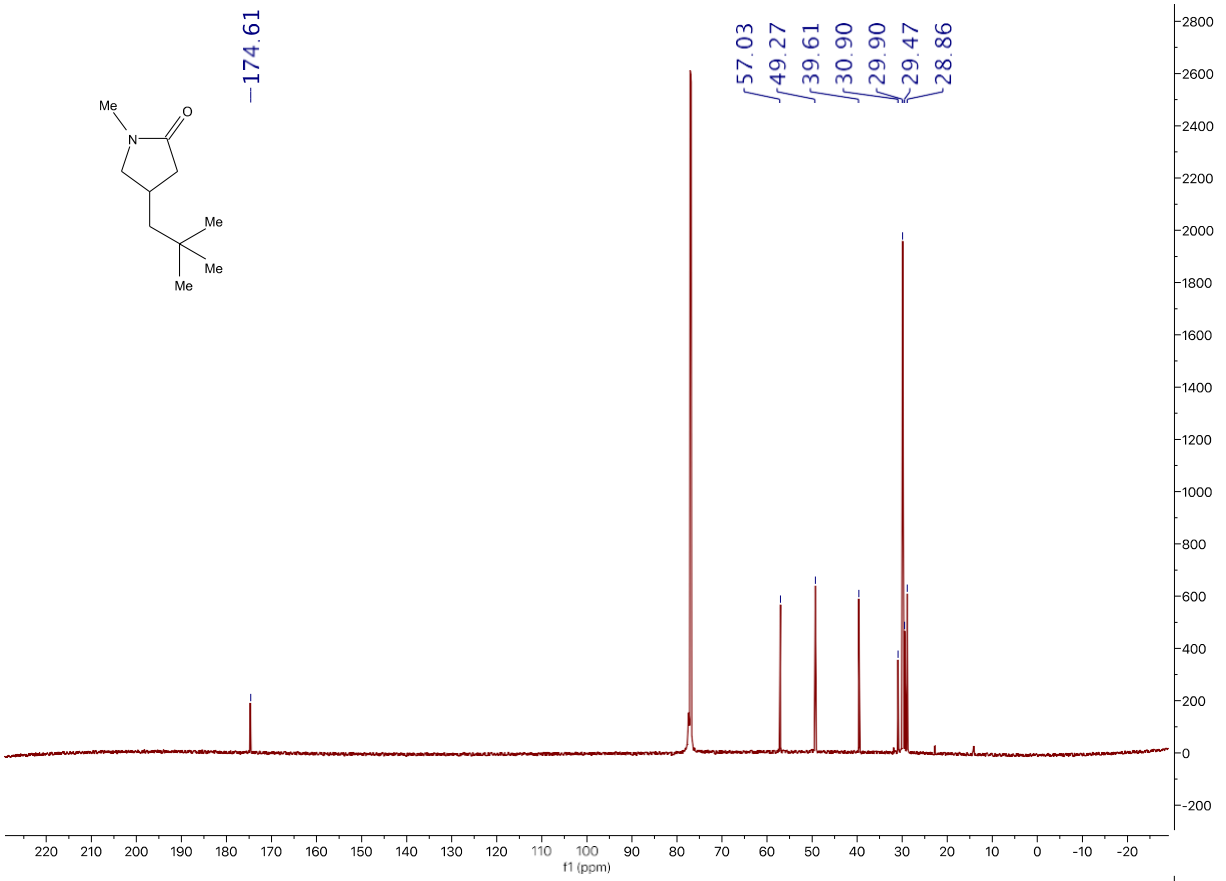
174.61
57.03
49.27
39.61
30.90
29.90
29.47
28.86
Me
N
O
Me
Me
Me
f1 (ppm)

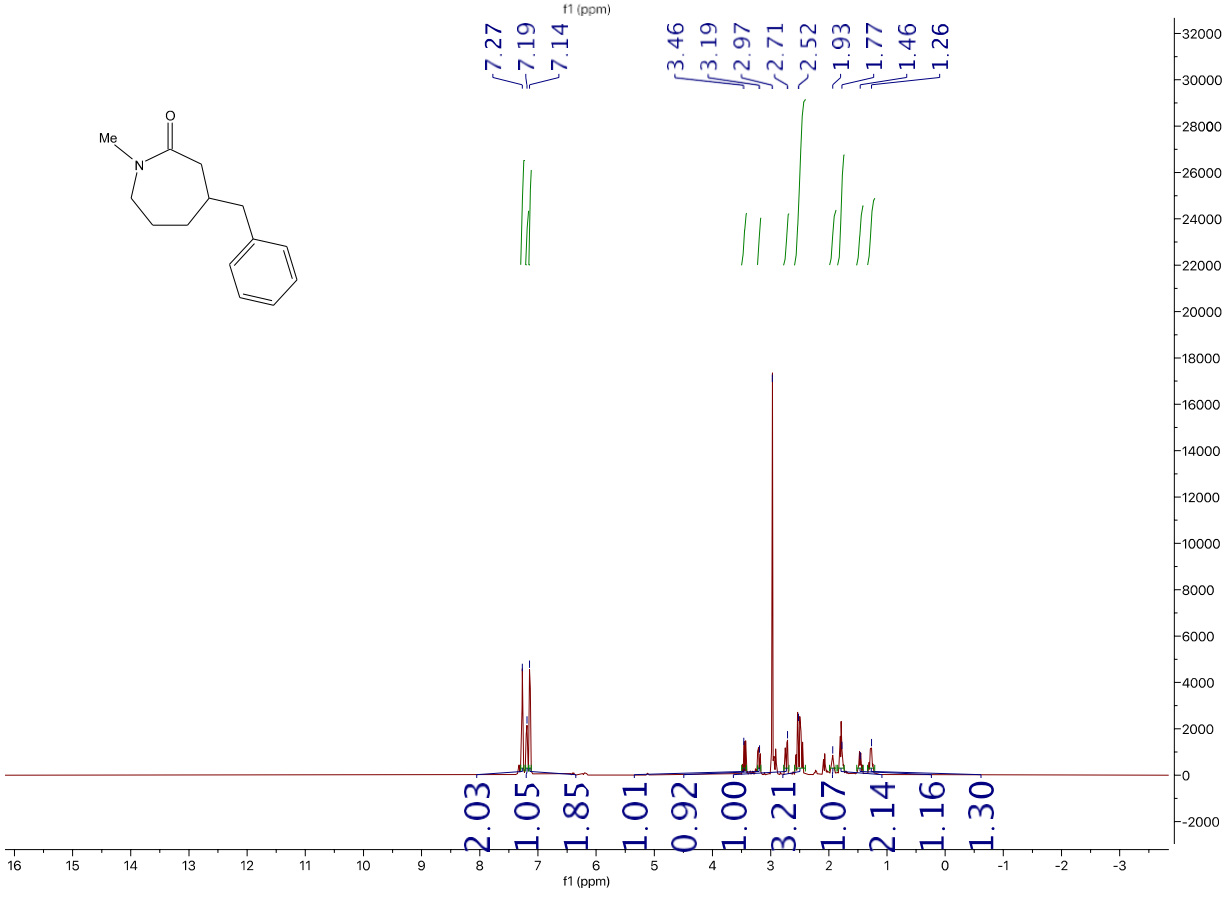
7.27
7.19
7.14
3.46
3.19
2.97
2.71
2.52
1.93
1.77
1.46
1.26
Me
N
O
2.03
1.05
1.85
1.01
0.92
1.00
3.21
1.07
2.14
1.16
1.30
f1 (ppm)

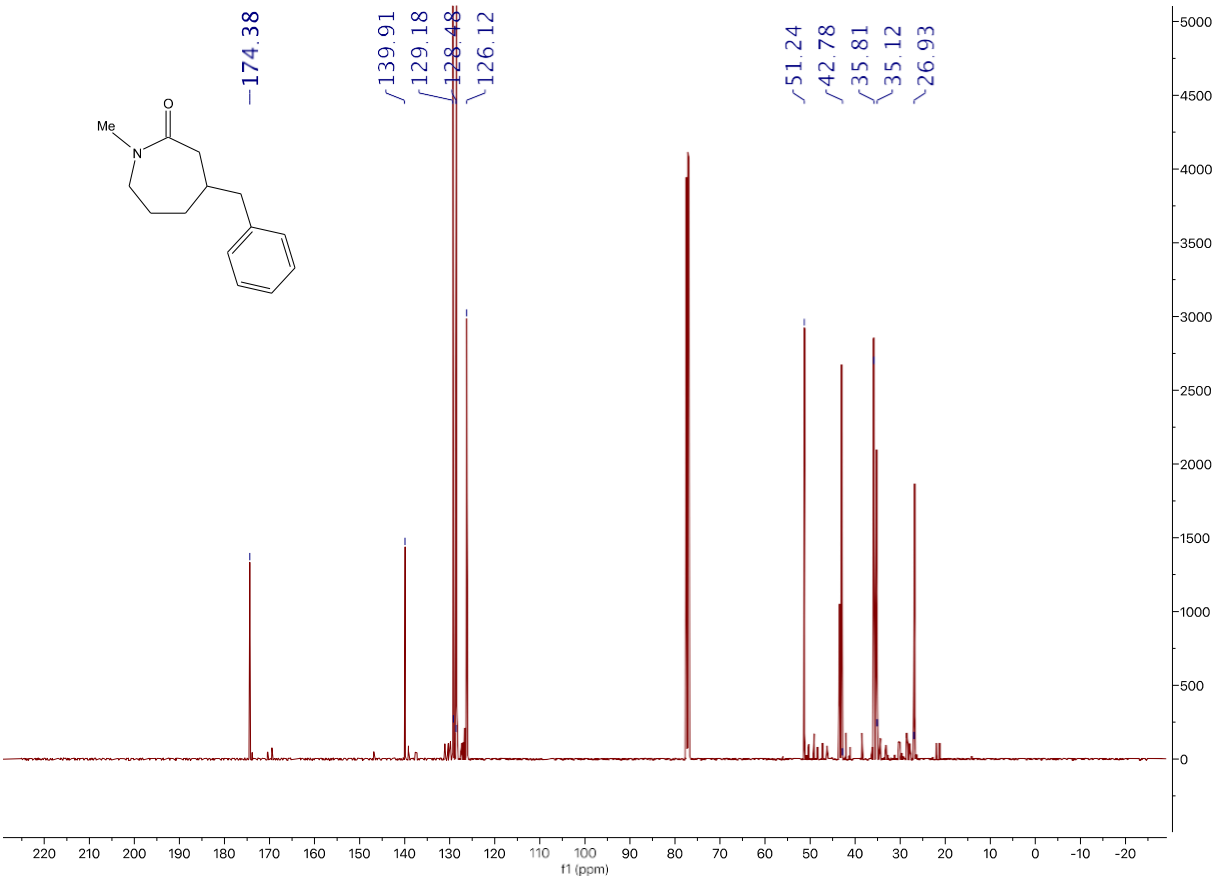
174.38
139.91
129.18
128.48
126.12
51.24
42.78
35.81
35.12
26.93
Me
N
O
5000
4500
4000
3500
3000
2500
2000
1500
1000
500
0
220 210 200 190 180 170 160 150 140 130 120 110 100 90 80 70 60 50 40 30 20 10 0 -10 -20
f1 (ppm)